UNIVERSITAT POLITÈCNICA DE VALÈNCIA

Universitat Politècnica de València

Doctoral Thesis

Doctoral Programme in Biotechnology

MONITORING OF THE PARAMETERS OF SYNTHESIS OF POLY(GLYCEROL SEBACATE) AND INFLUENCE ON THE PHYSICOCHEMICAL AND BIOLOGICAL PROPERTIES OF ITS ELASTOMER

Rubén Martín Cabezuelo

27th July, 2020

Supervised by:

Prof. Ana Vallés Lluch

Dr. Guillermo Vilariño Feltrer

ACKNOWLEDGMENTS

Para aquellos que siempre están
Incluso sin estar

INDEX

RESUMEN

El poli glycerol sebacato es un polímero que posee gran versatilidad gracias a sus propiedades mecánicas adaptables en función del proceso de síntesis que le preceda. Posee características tales como gran biocompatibilidad y buena biodegradabilidad que le confieren un gran atractivo en el ámbito de la ingeniería tisular y de diversas aplicaciones biomédicas como liberación de fármacos. Dichas propiedades son proporcionadas gracias a sus componentes principales, glicerol y ácido sebácico, ya que ambos poseen la aprobación de la “U.S. Food and Drug Administration”. Para sintetizar dicho polímero, se emplea un proceso de policondensación basado en dos etapas. La primera llamada prepolimerización, suele durar alrededor de 24h y se efectúa a altas temperaturas y bajo una atmósfera inerte de nitrógeno o argón. La siguiente etapa, la de polimerización, requiere de periodos más largos, alrededor de 48h, bajo las mismas condiciones de temperatura. En este proceso es cuando se suele emplear el uso de moldes para poder general el soporte material necesario para futuras aplicaciones biomédicas.

Como se mencionaba anteriormente, posee alta capacidad de adaptabilidad mecánica en función de qué parámetros de síntesis sean los empleados. Entre los parámetros que más afectan a las propiedades finales de la red polimérica de PGS se encuentran la temperatura, el tiempo de reacción y el ratio de sus componentes principales. A pesar de que la síntesis se realice del mismo modo en diferentes grupos de investigación, el material final que se obtiene puede variar mucho de uno a otro. Esto es debido a la inconsistencia en los procesos de síntesis y al desconocimiento de los efectos de los diferentes parámetros de síntesis. Por ello, un mayor entendimiento del proceso de síntesis es necesario, pudiendo reducir los costes de producción y permitir la producción a escala de este biomaterial.

En primer lugar, se estudió la etapa temprana de síntesis, la prepolimeración, mediante diversas técnicas de caracterización para determinar las propiedades fisicoquímicas del prepolímero durante los primeros momentos de su síntesis. Los resultaros mostraron la cinética de la reacción de policondensación entre los diferentes hidroxilos del glicerol y los carboxilos del ácido sebácico, formando en primer lugar cadenas largas mediante la reacción de los hidroxilos primarios, que luego, durante el proceso de polimerización entrecruzaban a través de la reacción de los remanentes hidroxilos secundarios.

Además de ello, se planteó una hipótesis acerca de uno de los parámetros de síntesis que no se habían estudiado anteriormente, la atmosfera aplicada. Este estudio reveló como las atmósferas inertes favorecen la generación de una red más ordenada, pero con menor grado de entrecruzamiento, mientras que atmósferas más oxidativas generaban una estructura menos organizada, pero con mayor entrecruzamiento de su red polimérica.

Para concluir, se empleó el PGS para poder resolver un problema de índole biológica. Se buscaba estudiar el efecto de la variación de la temperatura de curado del PGS mediante proteínas pertenecientes a la matriz extracelular (fibronectina y colágeno tipo I) en las etapas tempranas de adhesión de células

de cordón umbilical humano. Para ello fue necesario la optimización de la técnica de recubrimiento material llamada *spin coating* para lograr obtener recubrimientos lo suficientemente finos como para que su rugosidad no afecte al comportamiento de las proteínas y las células durante el estudio *in vitro* de los diferentes efectos de las diferentes redes poliméricas.

RESUM

El poli (glycerol sebacato) és un polímer que posseeix gran versatilitat gràcies a les seves propietats mecàniques adaptables en funció del procés de síntesi que el precedeixi. Posseeix característiques com ara gran biocompatibilitat i bona biodegradabilitat que li confereixen un gran atractiu en l'àmbit de l'enginyeria tissular i de diverses aplicacions biomèdiques com a alliberament de fàrmacs. Aquestes propietats són proporcionades gràcies als seus components principals, glicerol i àcid sebácico, ja que tots dos tenen l'aprovació de la "U.S. Aliments i medicaments ". Per sintetitzar dit polímer, s'empra un procés de policondensació basat en dues etapes. La primera, anomenada prepolimerització, sol durar al voltant de 24hores i s'efectua a altes temperatures i sota una atmosfera inert de nitrogen o argó. La següent etapa, la de polimerització, requereix de períodes més llargs, al voltant de 48 hores, sota les mateixes condicions de temperatura. En aquest procés és quan se sol emprar l'ús de motlles per a poder general el suport material necessari per a futures aplicacions biomèdiques.

Com s'esmentava anteriorment, posseeix alta capacitat d'adaptabilitat mecànica en funció de quins paràmetres de síntesi siguin els empleats. Entre els paràmetres que més afecten a les propietats finals de la xarxa polimèrica de PGS es troben la temperatura, el temps de reacció i la ràtio dels seus components principals. Tot i que la síntesi es faci de la mateixa manera en diferents grups de recerca, el material final que s'obté pot variar molt d'un a un altre. Això és a causa de la inconsistència en els processos de síntesi i a el desconeixement dels efectes dels diferents paràmetres de síntesi. Per això un major enteniment del procés de síntesi és necessari i pot reduir els costos de producció i permetre la producció a escala d'aquest biomaterial.

Per això en primer lloc es estudi l'etapa primerenca de síntesi, la prepolimerització, mitjançant diverses tècniques de caracterització per a determinar les propietats fisicoquímiques de l'prepolímer durant els primers moments de la seva síntesi. Els resultar-van mostrar la tendència cinètica de la reacció de policondensació entre els diferents hidroxils de l'glicerol i els carboxils de l'àcid sebácico. Formant en primer lloc cadenes llargues mitjançant la reacció dels hidroxils primaris, que després, durant el procés de polimerització s'entrecreuaven a través de la reacció dels romanents hidroxils secundaris.

A més d'això, es va plantejar una hipòtesi sobre un dels paràmetres de síntesi que no s'havien estudiat anteriorment, l'atmosfera aplicada. Aquest estudi va revelar com les atmosferes inerts afavoreixen la generació d'una xarxa més ordenada però amb menor grau d'entrecreuament, mentre que atmosferes més oxidatives generaven una estructura menys organitzada però amb major entrecreuament de la seva xarxa polimèrica.

Per concloure, es va emprar el PGS per poder resoldre un problema d'índole biològica. Es buscava estudiar l'efecte de la variació de la temperatura de curat de l'PGS mitjançant proteïnes pertanyents a la matriu extracel·lular (fibronectina i col·lagen tipus I) en les etapes primerenques d'adhesió de cèl·lules de cordó umbilical humà. Per això va ser necessari l'optimització de la tècnica de recobriment material anomenada *spin coating* per aconseguir obtenir

recobriments prou fins com perquè la seva rugositat no afecti el comportament de les proteïnes i les cèl·lules durant l'estudi in vitro dels diferents efectes de les diferents xarxes polimèriques.

SUMMARY

Poly (glycerol sebacate) is a polymer that has great versatility thanks to its adaptable mechanical properties depending on the synthesis process that precedes it. It has characteristics such as great biocompatibility and good biodegradability that make it highly attractive in the field of tissue engineering and biomedical applications such as drug delivery. These properties are provided thanks to its main components, glycerol and sebacic acid since both have the approval of the “U.S. Food and Drug Administration”. To synthesize the named polymer, a two-stage polycondensation process is used. The first called prepolymerization, usually lasts around 24 hours and is carried out at high temperatures and under inert atmosphere of nitrogen or argon. The next stage, the polymerization stage, requires longer periods, around 48 hours, under the same temperature conditions. To generate the material scaffold necessary for future biomedical applications moulds templates are usually used.

As mentioned previously, it has a high capacity for mechanical adaptability depending on which synthesis parameters are used. Among the parameters that most affect the final properties of the PGS polymer network are temperature, reaction time and the ratio of its main components. Although the synthesis is carried out in the same way in different research groups, the final material obtained can vary greatly from one to the other. This is due to the inconsistency in the synthesis processes and the lack of knowledge of the effects of the different synthesis parameters. Therefore, a better understanding of the synthesis process is necessary, being able to reduce production costs and allow the production of this biomaterial at scale.

Consequently, the early stage of synthesis (prepolymerization), was first studied by using various characterization techniques to determine its physicochemical properties during the first moments of its synthesis. The results showed the kinetic tendency of the polycondensation reaction between the different hydroxyls of glycerol and the carboxyls of sebacic acid. Firstly, linear chains are formed by the reaction of the primary hydroxyls, which then, during the polymerization process, cross-link through the reaction of the secondary hydroxyl remnants.

In addition to this, a hypothesis was raised about one of the synthesis parameters that had not been previously studied, the applied atmosphere. This study revealed how inert atmospheres favour the generation of a more ordered network but with a lesser degree of crosslinking, while more oxidative atmospheres generated a less organized structure but with greater crosslinking of its polymeric network.

To conclude, PGS was used to solve a biological problem. The aim was to study the effect of the variation of the PGS curing temperature using proteins belonging to the extracellular matrix (fibronectin and type I collagen) in the early stages of adhesion of human umbilical cord cells. For this, it was necessary to optimize the material coating technique called spin coating to obtain coatings thin enough so that their roughness does not affect the behaviour of proteins and cells during the in vitro study of the different effects of the different polymeric networks.

GLOSSARY

^{1}H-NMR	Proton nuclear magnetic resonance
3D	Three dimensional
AFM	Atomic force microscopy
ATR	Attenuated total reflection mode
Col I	Collagen type I
DA	Dry air (according to synthesis conditions)
DB	Degree of branching
DE	Degree of esterification
DMA	Dynamic Mechanical Analyser
DSC	Differential scanning calorimetry
E	Elastic modulus
E'	Storage modulus
ECM	Extracellular matrix
EEC	Equilibrium ethanol content
EtOH	Ethanol
EWC	Equilibrium water content
FA	Focal adhesion
FDA	Food and drug administration
Fn	Fibronectin
FTIR	Fourier-transform infrared spectroscopy
Gly	Glycerol
GPC	Gel permeation chromatography
HA	Humid air (according to synthesis conditions)
HBP	Hyperbranched polyester
HUVECs	Human umbilical vein endothelial cells

Mn	Average molecular weight
mPGS	Monomeric mixture of poly(glycerol sebacate)
mPPDS	Monomeric mixture of poly(propylenediol sebacate)
mPPGS	Monomeric mixture of poly(propylene glycol sebacate)
Mw	Molecular weight
PDI	Polydispersity index
PGS	Poly(glycerol sebacate)
pOH	Primary hydroxyl group
PPD	1,3-Propylenediol
PPG	Propylene glycol
pPGS	Prepolymer of poly(glycerol sebacate)
pPPDS	Prepolymer of poly(propylenediol sebacate)
pPPGS	Prepolymer of poly(propylene glycol sebacate)
SA	Sebacic Acid
sOH	Secondary hydroxyl group
T_d	Degradation temperature
TE	Tissue engineering
T_g	Glass transition temperature
TGA	Thermogravimetric analysis
t_{gel}	Gelification time
THF	Tetrahydrofuran
T_m	Melting temperature
t_{max}	Time of maximum viscosity

INTRODUCTION

Poly (glycerol sebacate) (PGS)

History of PGS

Mechanical and thermal properties of synthetic aliphatic polyesters are often inferior to the rest of its polymer family. This is the reason why Nagata *et al.* decided to design and build a polyester more suitable to the demand of the polymeric industry [1,2]. To do that, they incorporated a polyester network structure into the polymer backbone, to enhance its chemical and physical properties and control its degradation rate.

Then, a bunch of different methylene chain length aliphatic dicarboxylic acids (sebacic acid (10) , succinic acid (4), 1,12-dodecanedicarboxylic acid (14),1,18-octadecanedicarboxylic acid (20), and terephthalic acid (T)) were copolymerised with glycerol (Y), as a trifunctional alcohol, at high synthesis temperatures (around 200 ºC) for 4 h and under nitrogen environment. They concluded that all polyesters obtained had similar mechanical properties but the biological degradation rate presented wide disparities, particularly the polymer originated by the mixture of glycerol and sebacic acid (Y10), which was the only one that showed a significant loss of weight [1].

Soon after, in 2002, Wang *et al.*, in pursuit of a biodegradable elastomer for biomedical applications, decided to search for a polymer that took account of the fulfilment of some specific needs, such as [3]:

- The polymer degradation should be produced by hydrolysis to minimize individual differences in degradation characteristic rates, so polycondensation reaction was chosen as synthesis procedure. Thus, the resulting network would host hydrolysable ester bounds within its main polymer backbone and then avoid heterogeneous degradation.
- The polymeric network should be three-dimensional (3D) based on covalent crosslinking and hydrogen-bonding interactions to enhance mechanical properties with high elasticity. It should therefore have, at least, a trifunctional monomer to produce a 3D crosslinked network.
- It should have a low crosslinking degree since high degrees of crosslinking often lead to rigid and brittle polymers.
- The starting monomers had to be non-toxic.

Therefore, glycerol was chosen as the trifunctional monomer, which is the main compound for the formation of saponifiable lipids (triglycerides, phospholipids, etc). Sebacic acid, which is an intermediate in the ω-oxidation of fatty acids, was chosen as monomer with carboxyl functional groups, complementary to glycerol hydroxyl (a diacid in this case). Furthermore, it has an ideal chain length since short-chain dicarboxylic acids are more acidic and tend to form cyclic structures during the polymerization reaction, whereas long-chain dicarboxylic acids are more hydrophobic and immiscible with glycerol. Besides, glycerol and sebacic acid-containing polymers have the US Food and Drug Administration (FDA) approval for medical applications such as, cardiovascular, neurovascular,

orthopaedic, and soft tissue regeneration [3,4]. Hence, poly(glycerol sebacate) was firstly named as a potential polyester with further applications .

PGS synthesis and properties

As previously mentioned, PGS is synthesized by a two-step polycondensation reaction between glycerol and sebacic acid. At temperatures above 100 °C, the hydroxyl group of glycerol attacks the carboxyl group of sebacic acid to form a monoester, releasing a molecule of water as a subproduct of the reaction (Figure 1). In the early stages of the reaction, a viscous transparent liquid, with a waxy appearance and texture (at room temperature), is formed (the pre-polymer, hereafter named pPGS). If the reaction continues, a major crosslink process take place by increasing the interaction among the remaining free reactive groups leading to the final polymeric network. This final and completely cured PGS material becomes insoluble in any solvent and has an amber appearance.

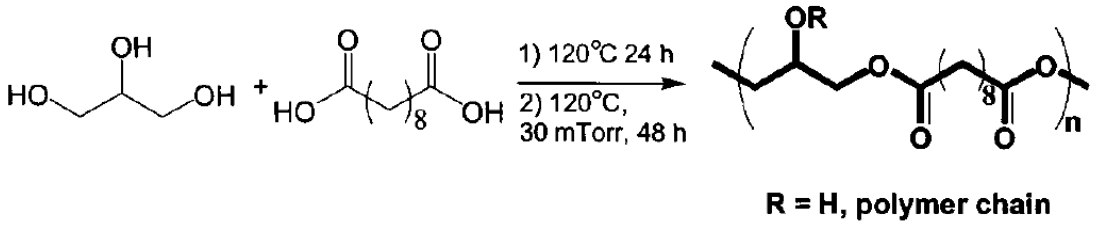

Figure 1. Chemical scheme of the poly(glycerol sebacate) synthesis. Extracted from [3].

What follows describes in detail the two steps in which PGS polymerisation is usually divided. The first step of the reaction is usually called pre-polymerisation. During this 24h step, a viscous pre-polymer is obtained by the formation of short linear segments from the condensation reaction between the monomers [5,6]. This short early macromers are formed mostly by the reaction between primary hydroxyls of glycerol and the carboxylic acid from sebacic acid, leading to a low degree of branching [7]. However, it was not been fully determined to date which is the chemical structure of the intermediate products formed during PGS pre-polymerization.

The next synthesis step is the curing, where polymerisation proceeds in the solid state after the macromers percolate yielding a cross-linked insoluble gelly structure. The prepolymer is conventionally cured for 48h at temperatures above 100 ºC to induce esterification between macromers and form a 3D- network in combination with random coil characteristics [8,9].

The formation of the network does not take place immediately, but rather gradually during both, the prepolymerization and the curing step. Proof of this is how the degree of esterification achieved during the reaction evolves progressively (Figure 2). Nevertheless, how the material structure evolves during its synthesis procedure remained still unknown.

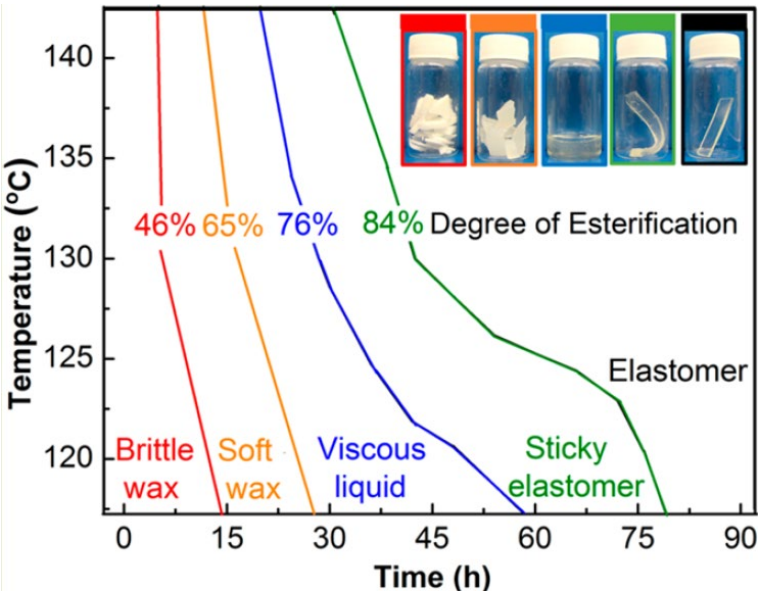

Figure 2. Map that describes the relationship between the esterification degree (DE) and specimen statuses. Filled squares in the figure denote the time and temperature values for thermal treatment where the measurement of DE and the observation of physical status were made for each specimen. Extracted from [5].

It has been shown recently how important a third step becomes, in order to achieve a better reproducibility of the material behaviour, which is the rinsing of unreacted monomers and oligo- or macromers not bonded to the main network [6]. This step is made gradually by washing the sample material starting with tetrahydrofuran (THF), to ethanol (EtOH) and finally, soaking it in water. In this way, PGS samples were more consistent and early release of degradation products, which can lead to dissimilar biological performances was avoided.

Some authors have studied an alternative synthesis path by using a microwave assisted synthesis because of the time- and energy-consuming conventional PGS synthesis. It increases the reactivity of each of the hydroxyl groups, producing polymers with a higher degree of esterification and in a reduced reaction time [10,11]. This study concludes that the only issue to be fixed is glycerol evaporation during the procedure, which alters the reproducibility of PGS synthesis [6,12].

PGS synthesis parameters and their influence on the final polymer characteristics

Pre-polymerization is usually carried out at temperatures around 120 ºC and 130 ºC for a time of 24 hours, under an inert atmosphere, commonly nitrogen (N_2). However, the conditions of the second stage of curing vary between published works, giving rise to materials with dissimilar outcomes, mainly mechanical properties, and biodegradability degrees. These known factors that influence the curing step are the temperature, the curing time, as well as the molar ratio of the monomers, and the atmospheric environment of the reaction [9]. The effect of curing temperature and curing time on the mass of PGS effectively crosslinked can be observed in Figure 3.

The curing temperature usually ranges between 110 ºC and 150 ºC [5,6,9]. It has been shown that at a higher curing temperature, the final mechanical properties

of the material increases, with Young's moduli ranging from 56 KPa at 110 ºC to 1200 KPa at 130 ºC, while decreasing the mass loss after the rinsing, because of a more crosslinked polymer [6]. Furthermore, the lower the curing temperature, the greater the degradation rate. It has been shown that PGS cured at 110 ºC loses around 20% of its mass in 15 days, while the PGS cured at 130 ºC does not reach 1% mass loss in 60 days [9], which highlights a direct relation between curing temperature and degree of crosslink of the final PGS structure. The more the curing temperature, the higher the mechanical properties due to an increase of its crosslink degree.

Regarding the curing time, several studies have been done on PGS synthesis conditions by using curing times from 24h to 114h. It has been shown that the curing time is directly correlated with the final mechanical properties of the material. That is, in accordance with the temperature parameter, the longer the curing time, the higher the degree of esterification of the polymer network obtained [13]. On the other hand, *in vitro* cytotoxic studies have proven that cytocompatibility of PGS improves with long curing times. This may be attributed to fewer soluble monomers and oligomers in the network when the PGS is more cured, which favours cell response and cell-material interaction [14].

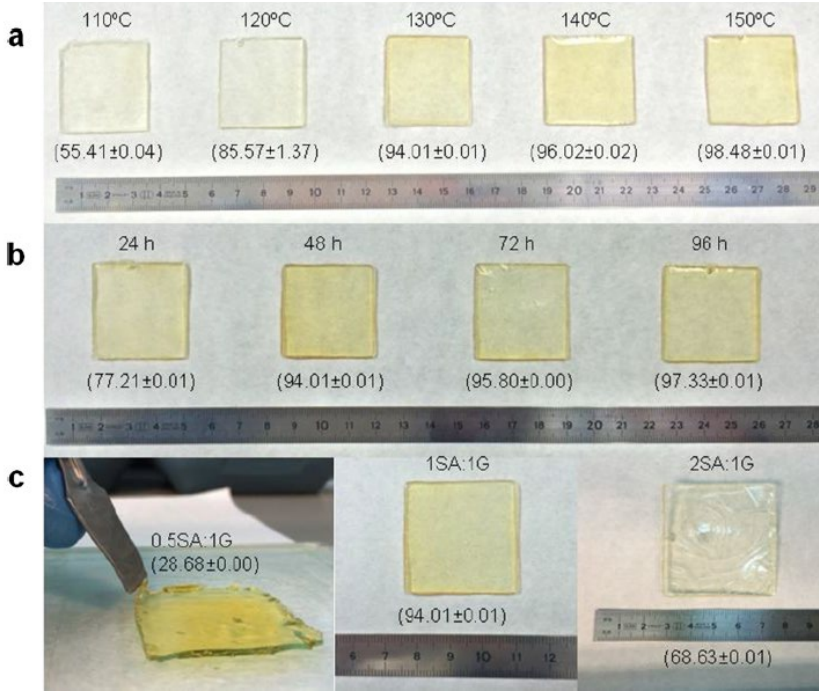

Figure 3. PGS films prepared from equimolar SA:G ratios and cured (a) at increasing temperatures (from left to right: 110 ºC, 120 ºC, 130 ºC, 140 ºC and 150 ºC) for 48h, and (b) for different times at 130 ºC (24, 48, 72 and 96 h). (c) PGS films prepared from 0.5:1, 1:1 and 2:1 sebacic acid:glycerol ratios and cured at 130 ºC/48h. The values between brackets are mass fractions (%) of efficiently crosslinked chains, *i.e.*, ratios of experimental mass after rinsing per reagents unit mass at different synthesis conditions. Extracted from [6].

The atmospheres applied during the pre-polymerization used to be argon (Ar), N_2, or alternatively vacuum was applied. The underlying explanation is to avoid uncontrolled reactions among monomers, as it was done the first time PGS was synthetized by Wang *et al.* in 2002 [3]. Although no reference has been found regarding the effect of different atmospheric conditions during pre-polymerization

on the final properties of the PGS, most of the studies seems to state that no differences appear to be found between the materials obtained at different atmospheres (Ar, and N_2).

The influence of the molar ratio of reagents determines the final PGS properties as well. The synthesis of PGS is usually carried out at an equimolar ratio of its monomers (SA:Gly; 1:1). Notwithstanding, a number of studies have carried out considering the stoichiometric ratio (3:2), or even at different proportions between reagents [5,6,15]. Some studies have shown that the higher the molar ratio of sebacic acid, the lower the resistance of the final material obtained. In particular, when the molar ratio is 2:1, a PGS with Young's modulus around 1 MPa is obtained, while at an equimolar ratio, this same mechanical parameter has a 4-fold increment [6]. Emphasising the fundamental effect the molar ratio and curing time have over PGS final characteristics, it can be observed n Figure 4 that it is possible to predict the PGS mechanical properties by knowing the starting molar ratio and curing time [15].

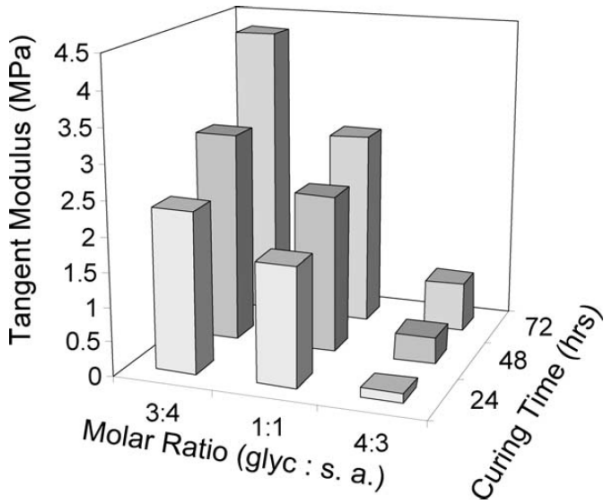

Figure 4. Tangent moduli (at 10% strain) for PGS cylinders synthesized at various processing parameters. Linear regression can be used to predict the modulus (70% power) from these two variables: Modulus (MPa) = 3.607– 1.410 * (ratio of glycerol:sebacic acid) + 0.60 * (vacuum curing time in hours). Extracted from [15].

Apart from that, it must be considered that most of the studies carried out with regard the PGS synthesis process have determined that loss of glycerol occurs by evaporation during the procedure, which alters the real ratio of monomers applied. This loss of glycerol has been followed by some groups, which have determined the evaporation as a function of the time and temperature of synthesis [5,14]. This is the main reason why an equimolar ratio of monomers is used instead of a stoichiometrically one. Thanks to the excess of glycerol provided by this ratio (1:1), the effect of glycerol evaporation is slightly compensated.

PGS applications

Biocompatible polymers, such as PGS, possess a wide range of tunable mechanical properties. This is the reason why it becomes interesting for its application in the field of tissue engineering. Thus, one of the most common applications of PGS in this field is the development of three-dimensional

scaffolds, which would serve as a support to house cells from a wide variety of tissues. Once the damaged tissue starts to regenerate, the supporting PGS scaffold should decompose by releasing non-toxic metabolizable degradation sub-products, avoiding a host response [3].

Some of the target tissues by PGS scaffolding techniques for regenerative medicine are:

- Myocardial tissue. The published studies focus mainly on the synthesis of cardiac patches for regeneration of the myocardial wall, thanks to the PGS adaptable stiffness range, from 0.004 to 1.2 MPa [9]. The synthesized scaffolds allowed the proper contraction amplitude which is mandatory for cardiac patches [16,17].
- Vascular tissue. It has been investigated he generation of tubular conducts based on PGS. The studies focused on PGS interactions with endothelial cells and smooth muscle cells and the evaluation of its hemocompatibility [18–20].
- Bone and articular cartilage. PGS scaffolds support the formation of matrix from cartilage *in vitro* [15,21]. Furthermore, PGS enhance bone regeneration, more specifically, it allows the repairment of critical size bone defects [22] by facilitating the connection among bone defects as shown in Figure 5.

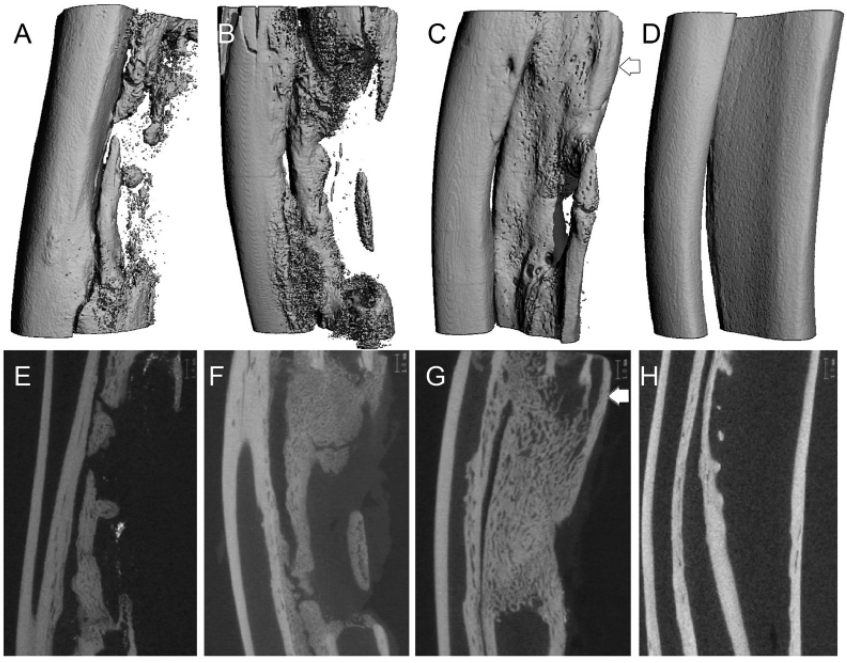

Figure 5. Rabbit ulna defect micro computed tomography 3D rendering after 4 week (B) (n = 2) and 8 week (C) (n = 5) retrieved ulna samples compared to an 8 week empty negative controls (A) (n = 5) and an intact ulna (D). (E–H) The corresponding midsection X-ray for control, 4 week, 8 week and intact ulna. Extracted from [22].

- Retinal tissue. PGS membranes have been developed of to induce selective photoreceptor elimination by creating a permissive environment since, in retinal implantation, the presence of donor cells and the host cells hinder the formation of functional tissue [23,24].

- Nervous tissue. The biocompatibility of PGS has been studied for the reconstruction of neural networks promoting spinal cord repair in rats [25]. *In vitro* studies with Schwann cells have shown that PGS has no detrimental effects on cell metabolic activity, adhesion or proliferation with no signal of apoptosis [26].

Thanks to PGS tailored biodegradability, studies have been carried out about the bioadsorption of PGS, for its use as a vehicle for drug release [27].

In addition, it is worth mentioning the application of PGS as a tissue adhesive since, due to its mechanical properties, biocompatibility and resorption [28]. The copolymerization of PGS and lactic acid (called P (GS-co-LA)) as a surgical sealant has also been investigated, since this material behaves as a liquid at 45 ºC, while it solidifies at body temperature and presents good biocompatibility. PGS films have been developed for the prevention of adhesions during surgery, which serves as an effective barrier in patients undergoing open surgery and laparoscopic (surgery to explore the abdominal cavity) [29].

OBJECTIVES

Poly(glycerol sebacate) (PGS) is a polyester whose synthesis is based on a two-step polymerization process. A wax-like material at room temperature (pPGS) is obtained during its prepolymerization step, which takes 24h under constant stirring. After 48h of curing step, the final PGS network is produced. The variation PGS synthesis parameters, such as, temperature, reaction time, ratio of monomers and atmospheric environment, can alter its chemical morphology. This fact highlights the versatility of PGS as a polymeric material while its synthesis variability becomes an issue. Therefore, the material morphology and properties during its pre- and polymerization remain unknown. The understanding of the effect each of the PGS synthesis parameters possess on its final PGS morphology and properties would be fundamental for modulating the elastomeric PGS networks obtained to suit the properties required in a particular application.

Thus, in order to understand and determine the PGS material morphology and properties the following objectives have been addressed in this thesis:

1. Determine and characterise the molecular mechanism of synthesis of poly(glycerol sebacate)
2. Study the effect of different atmospheric synthesis conditions on pPGS and PGS networks.
3. Analise and determine the effect of temperature on PGS coating substrates properties by biological characterisations.

CHAPTER 1: Unveiling the key synthesis mechanism for optimal poly(glycerol sebacate) hyperbranched polymer synthesis

ABSTRACT

Poly(glycerol sebacate (PGS) is an interesting option for glycerol (Gly) applications that can produce a wide range of industrial interesting products. PGS is part of the family of hyperbranched polyesters (HBP) which possesses an extensive variety of applications due to its tunable chemical and mechanical properties, together with its great biocompatibility and biodegradability. However, its low reproducibility synthesis becomes a challenge for its industrial scalability and development of replicable products of commercial interest. While the reaction is undoubtedly based on the polycondensation of glycerol hydroxyls with sebacic acid carboxyl groups, the exact polymer structure has not been established yet . Indeed, numerous synthesis variables come into play during PGS synthesis: temperature, time, ratio of monomers and atmosphere conditions. The understanding and monitoring of these parameters are fundamental to control PGS synthesis procedure allowing a scalable and reproducible final product.

To unveil the origin of scattering in PGS properties, the study of different PGS synthesis conditions was performed using Gly-like reagents. Furthermore, the prevention of water and Gly loss were achieved by modifying its PGS early prepolymerization synthesis conditions and parameters. Each reaction was monitored by titration, FTIR and ^{1}H-NMR techniques in other to understand the polymer chemical distribution. The characteristic HBP properties such as polydispersity (PDI), degree of esterification (DE) and branching (DB) were calculated together with the determination of hydroxyl affinity during PGS prepolymerization.

Keywords: Poly(glycerol sebacate), glycerol loss, hyperbranched polyesters, polycondensation and ^{1}H-NMR

INTRODUCTION

Poly(glycerol sebacate) (PGS) is one of the most studied hyperbranched polyesters thus far [4,5,29,30]. This is because PGS shows polyvalent properties for biomedical and tissue engineering (TE) applications, such as biodegradability and biocompatibility, thanks to its FDA-approved main monomers interaction, glycerol (Gly) and sebacic acid (SA) [31,32]. Conventionally, PGS synthesis begins with 24h pre-polymerization of an equimolar ratio of its reagents, glycerol (Gly) and sebacic acid (SA), under inert atmosphere flow, following by a 48h curing in an oven, both steps at 130 ºC [1,3,6]. Nevertheless, several studies have shown how the irreproducibility of PGS synthesis leads to a challenging industrial scalability for further commercialization, having different broad final properties with same synthesis conditions [5,6,15,33–37].

Now, at a time when the implementation of best practice and enhancement of the environmental population awareness are rising, bio-based monomers have gained important interest [38–40]. It is the case of the trifunctional alcohol Gly, typically found as one of the byproducts of biodiesel production [41]. It opens the possibility of achieving better and more sustainable outcomes when scalability and industrialization of PGS synthesis procedure are the primary target [42]. This fact highlights the necessity of fully understanding PGS synthesis, based on a typical hyperbranched polymers (HBP) synthesis methodology by A_2 + B_3 reaction, two-step polycondensation system [43–45].

HBP, studied for the first time by Young H. Kim and Owen W. Webster at early 1990s [46], as random branch-on-branch topology dendritic macromolecules, are nowadays one of the more promising alternatives to dendrimers [46]. HBP properties and characteristics stood out due to its versatility, which raises the possibility of its multipurpose applications in several fields, including drug delivery, biosensing and imaging, catalysis or nanoencapsulation, among others [47–57]. This is possible thanks to its characteristic properties, such as controlled molecular weight, wide range of polydispersity, which may be optimized up to values around 1.5, and degree of branching, up to 70%, unlike the 100% of most dendrimers [43,48].

Thus, the aim of this study is to shed light on PGS HBP synthesis parameters: Gly different hydroxyl functionality effect, polycondensation reaction kinetics, degree of branching and the loss of Gly and water during rection. This last factor may play a key role during early stages of PGS synthesis, and it has been overlooked on mainstream PGS synthesis protocols [5]. For that purpose, different synthesis scenarios were evaluated, using similar Gly alcohols and different environmental conditions in order to understand PGS key synthesis steps. To avoid water and Gly loss during prepolymerization, a sealed system that allows water and Gly recirculation was developed, achieving the expected reproducibility of the final product (Scheme 1).

Scheme 1 pPGS experimental setup

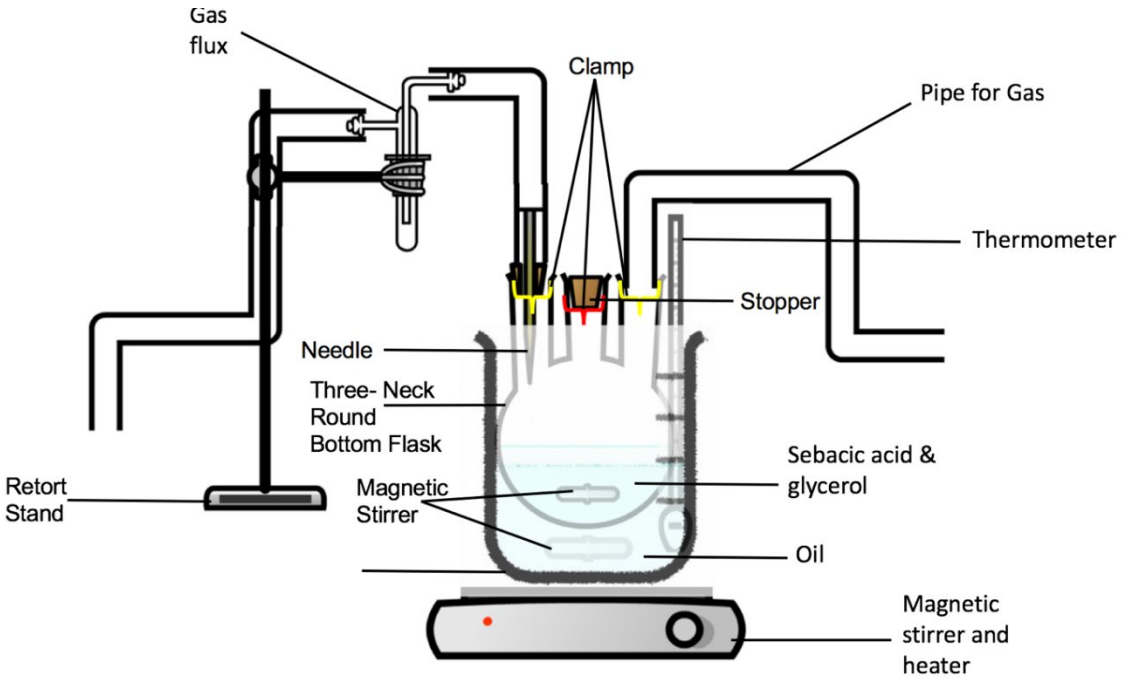

PGS HBP from Gly and SA was synthetized, and its polycondensation reaction was monitored by titration, FTIR and ^{1}H-NMR spectroscopy over reaction time. Others have studied glycerol-based hyperbranched polymers by nuclear magnetic resonances techniques and validated the chemical shift assignments, demonstrating how the technique was sensitive enough to determine the glycerol and its 5 possible derivatives resulting from its polycondensation with SA [7,14,45,58]. Complementary characterization techniques such as differential scanning calorimetry and thermogravimetry analysis were performed to support previous data results [59].

MATERIALS AND METHODS

General procedure for synthesis of Poly(glycerol sebacate) prepolymer and derivatives.

Equimolar (1:1) and stoichiometric (3:2) ratios of sebacic acid (SA) (>99%, Sigma Aldrich) and glycerol (Gly) (99%, Sigma Aldrich) were measured and mixed under nitrogen gas, in a round bottom flask at 130 ºC. The starting point of the prepolymerization reaction (t = 0h; mPGS) was determined once the mixture was homogenous. Then, samples at different time points (0h < t < 24h; pPGS) were collected and then cooled at room temperature.

Similar synthesis procedure was applied for 1,3-propanediol (PPD) (Sigma Aldrich) and propylene glycol (PPG) (Sigma Aldrich), at equimolar/stoichiometric ratio together with SA (PPDS and PPGS respectively), but only samples at t = 0h (mPPDS and mPPGS) and t = 24h (pPPDS and pPPGS) were collected.

Characterisations

Fourier Transform Infrared Spectroscopy

A Platinum ATR from ALPHA II spectrometer in attenuated total reflection mode (ATR) was used to confirm the chemical bonds in the frequency range of 400-4000 cm^{-1} at 4 cm^{-1} resolution.

Titration

The titration method used to determine the degree of esterification (DE), was adapted from [5]. For that purpose, a 250 mL Erlenmeyer flask with 50 mL of a 25:75 wt% ethanol:tetrahydrofuran solution (EtOH:THF) (absolute ethanol and tetrahydrofuran, Scharlau) was used to dilute 100 mg of each sample (monomers and prepolymers) while stirring. Once the sample was completely dissolved, 5 drops of phenol red solution (Sigma Aldrich) were mixed and a 0.1 M solution of potassium hydroxide (KOH); Sigma-Aldrich) was added dropwise to perform the titration by changing the solution colour from transparent to pinkish-purple when a pH of 10 was achieved. The following equation was used to calculate the DE, adapted from [5]:

$$DE = 1 - \frac{V_1 - V_0}{V_{mon} - V_0} \quad (1)$$

Were V_0 is the volume of KOH solution used for the blank test, V_{mon} is the volume used for the monomers (mPGS, mPPDS and mPPGS), and V_1 the volume used for each pPGS sample.

^{1}H-NMR spectroscopy

^{1}H-NMR was utilized to confirm chemical compositions of mPGS and pPGS samples and to determine its reaction degree and branching by mean of end-group analysis. Samples from 0h to 24h were dissolved in Acetone-d^6 (Sigma-Aldrich).

The spectra were acquired on a 400 MHz Varian Inova spectrometer and samples were reported in parts per million (ppm) relative to the acetone-d^6 solvent (δ_H = 2.05 ppm) as an internal reference. SA characteristic sharp peaks

are located between δ1-2.5 ppm. The data extracted was analysed using MestReNova Processor software.

Gel permeation chromatography

The weight average molecular weight (M_w), the number average molecular weight (M_n) and the polydispersity index (PDI), of the mPGS and pPGS samples were measured by gel permeation chromatography (GPC, OMNISEC System GPC(, using THF as the mobile phase and polystyrene standards for calibration.

Rheology measurements

In order to scan the viscosity of monomeric samples during gelation and curing until the break-up of the formed network, a Discovery HR-2 hybrid rheometer (TA Instruments) was used. Viscosity was monitored every 300s throughout the curing process at constant temperature (130 ºC) at 1.5 rad·s^{-1} of rotational speed. Samples were placed between disposable 25 mm-diameter parallel plates, separated by a gap of 1000 μm.

For mPPDS and mPPGS rheology analysis, all experimental parameters were set as mentioned but time, which was set based on PGS gelation point, in order to compare the results between all the samples.

Differential scanning calorimetry

Differential Scanning Calorimetry (DSC) measurements of mPGS and pPGS were performed in a Perkin Elmer DSC 8000 device. For each experiment around 3 mg of each sample were weighed in a standard aluminium pan and then, sealed. Pans were cooled to -80 ºC and scanned up to 60 ºC at 20 ºC·min^{-1} under a constant nitrogen flow of 50 ml·min^{-1}. The melting point temperature (T_m) was determined for each sample from its calorimetric curve.

RESULTS AND DISCUSSION

Effect of molecular configuration during prepolymerization

Viscosity of monomeric mixtures was monitored at constant temperature of 130 ºC, in order to understand the effect of different chemical distribution of primary (pOH) and secondary (sOH) hydroxyl groups , as represented in Scheme 1. An equimolar ratio of Gly and SA was used to determine the time conditions for the rest of the mixtures. Once the mixture was broken under the stress exerted during the rheometric procedure, the gel point record was achieved. Thus, the time for the following viscosity measurements (PPDS and PPGS) was set as the maximum time where the maximum viscosity (t_{max}) of pPGS was achieved (around 50h). Constant values of viscosity were obtained from the rheometry measurements of PPDS and PPGS.

Scheme 2. Representation of glycerol, propylene glycol and 1,3.propanediol together with sebacic acid.

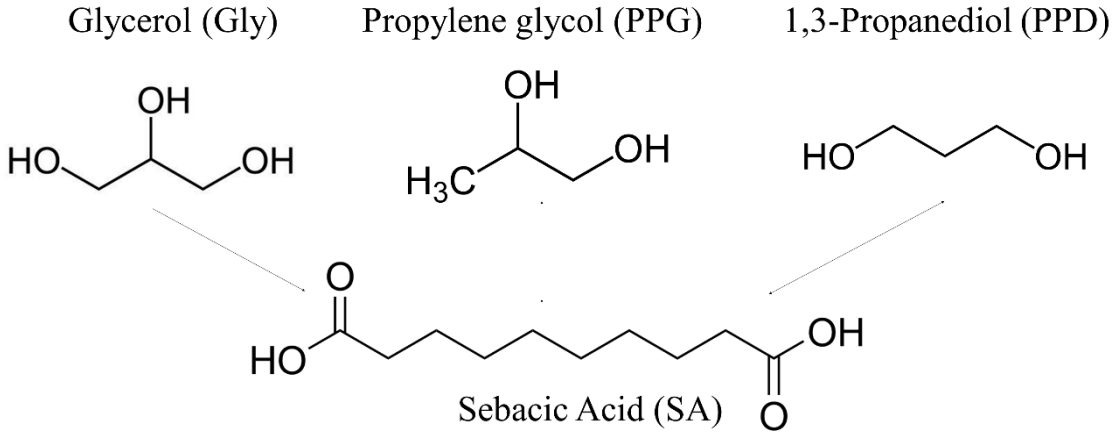

Polycondensation reaction of equimolar Gly and SA at 130 ºC after 24h leads to a wax-like prepolymer mixture (pPGS). The reaction is conducted thanks to the presence of pOH and sOH groups (Gly) and carboxyl groups (SA). Yet hydroxyl reactivity during the synthesis reaction remains unknown. The use of PPG and PPD, with same chemical composition but hydroxyl groups distribution, may be useful in order to understand the preference that follows the usual reaction among Gly and SA as to form PGS. PPG contains both, one pOH and one sOH group, while PPD have only two pOH groups.

From viscosity monitoring (Figure 6) can be determine how Gly + SA is the only monomeric mixture that produce crosslink reaction thanks to the presence of three hydroxyl groups, (two of them primary and the middle secondary one) which may react by mean of polycondensation with the two free carboxyl provided by SA.

PPG and PPD were not able to produce any crosslink because of its chemical distribution. The reaction among PPD or PPG, together with SA, produces linear macromers which maintain its viscosity value constant at logarithmic scale. This is because of the absence of a third hydroxyl which allows the macromers chains to crosslink. Thus, the only possible chain growth direction for these two different monomeric combinations, can be determined as a linear macromer distribution.

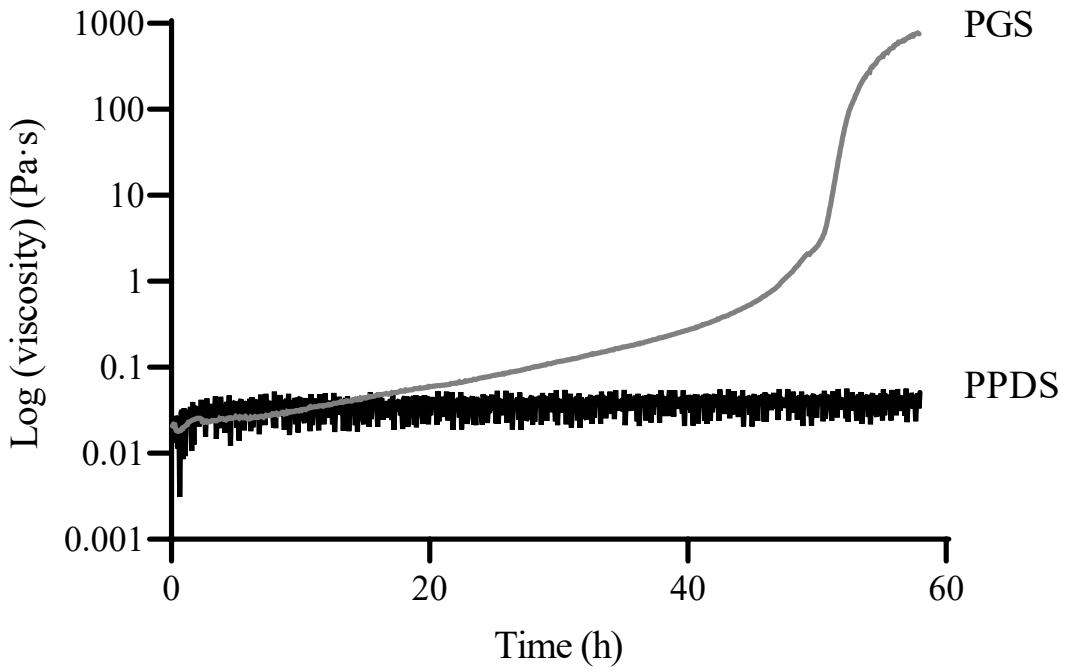

Figure 6 Viscosity monitoring of different monomeric mixtures as represented in Scheme 2(PGS, PPDS and PPGS), at 130 ºC.

For chemical bond identification of monomeric mixtures at the start (“m”; 0h) and the end (“p”, 24h) of its prepolymerization, FTIR characterization technique was performed. The obtained FTIR spectra (Figure 7a and b) have a broad band at 3300 cm^{-1} for hydroxyl groups (O-H stretching). More precisely, pOH and sOH saturated alcohol groups are present by two sharp peaks at 1030 cm^{-1} and 1100 cm^{-1} respectively. Aliphatic C-H absorption is displayed at 2850-2950 cm^{-1} together with the unreacted carboxyl carbonyl (-COOH) at 1700 cm^{-1}. After 24h of reaction the ester carbonyl ($-COO^-$) at 1730 cm^{-1} and C-O peak at 1168 cm^{-1} are present in Figure 7b.

All spectra from monomeric samples at 0h (Figure 7a) present its broad band of -OH groups around 3300 cm^{-1}, but there are some differences after 24h (Figure 7b) with prepolymers. Only pPGS keeps a hydroxyl broad peak. From Scheme 2 can be elucidated the theoretical stoichiometric ratio of pOH and sOH of mPPGS and mPGS as 1 and 2 respectively. Values extracted from Figure 7b are represented as the ratio of pPH/sOH in Figure 7c. The resulting hydroxyl ratio is reduced to the half of the previously calculated theoretical one, when compared with the empirical ratio for pPPGS and pPGS (0.5 and 1, respectively).

There is a common trend when free carboxyl carbonyl peak (-COOH) shifts from 1700 cm^{-1} to the reacted ester group ($-COO^-$) at 1730 cm^{-1} in each of the 24h FTIR spectra. The major peak from C-O bonding at 1168 cm^{-1}, is only present after 24h. Based on the alcoholic monomer used, there are distinct outcomes on polycondensation subsequent reaction.

If PPD is mixed and reacted with the SA, the resulting pPPDS has major signal at COO^- when compared with the free COOH groups. When PPG is the alcohol which react with the SA, the resulting spectra shows two peaks with similar

intensity at 1700 cm^{-1} and 1730 cm^{-1}. Finally, for pPGS, the peak around 1700-1730 cm^{-1} becomes more homogeneous, presenting both signals together but displaced to the 1730 cm^{-1} peak.

The resulting data present how during the 24h prepolymerization process, the priority chain growth trend is the polycondensation of the free carboxyl group with the primary alcohol by polycondensation, rather than the secondary one. This synthesis step reduces the presence of primary hydroxyl groups and increases the relative signal of the secondary hydroxyl groups, highlighting the tendency of chain growing of the macromers of the polyesters.

All three combinations of monomers result in a polyester, with different degrees of esterification. PPD, which is rich in pOH, leads to a higher degree of esterification when compared with the PPG, because of the presence of the sOH. This fact highlights how the presence of a secondary hydroxyl group and one primary, instead of two primaries in the case of pPPDS, alters the final prepolymer chemical structure. With the pPGS sample, the homogeneous peak around 1730 cm^{-1} suggest a higher degree of esterification of all the monomeric mixtures because of a higher amount of reacted ester groups than carboxyl carbonyl.

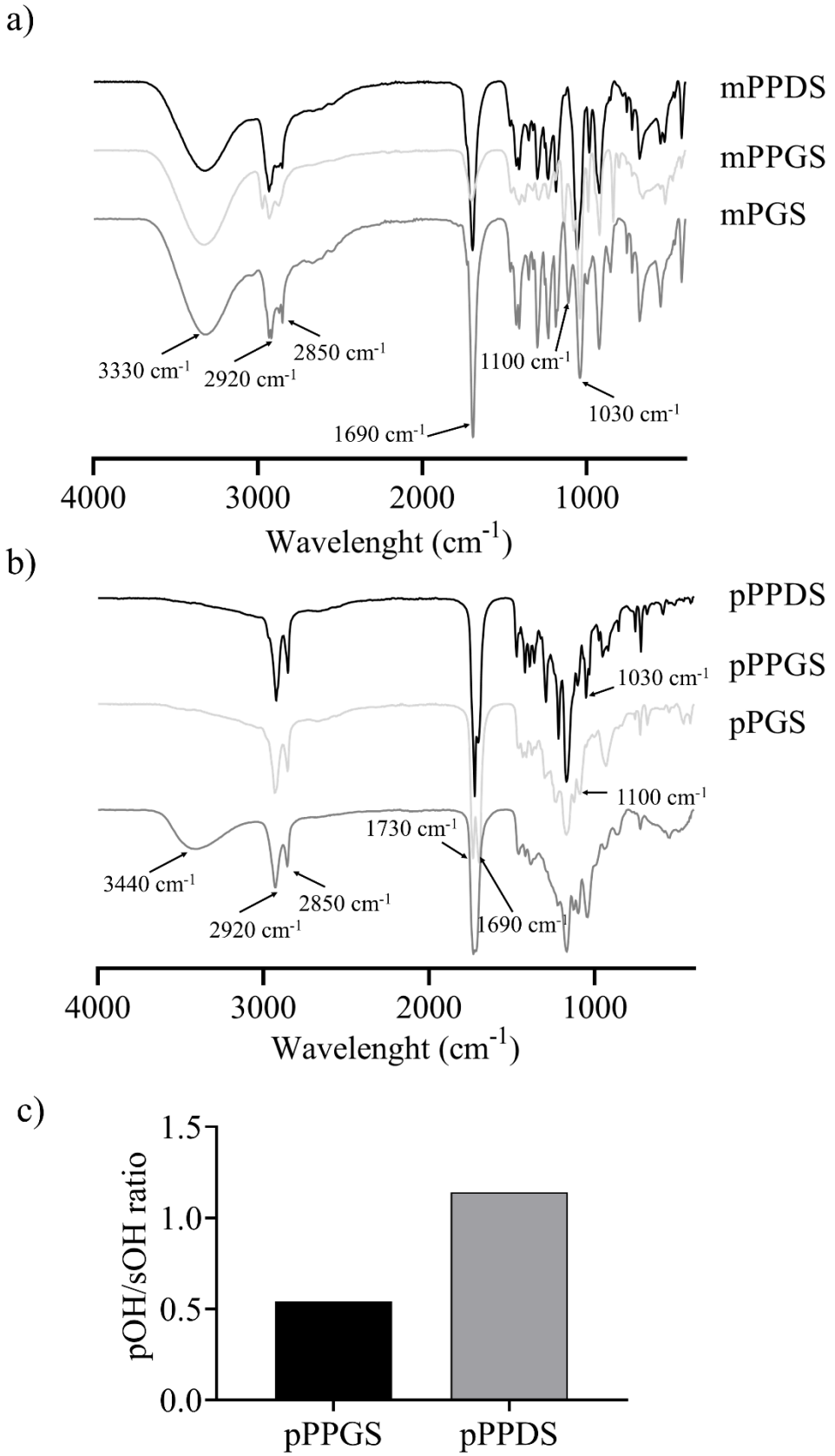

Figure 7. FTIR spectra (transmittance, a.u.) of different polyester mixtures (Scheme 1) prepolymerized under N_2 atmosphere conditions at 130°C and at (a) 0h (monomers) and after (b) 24h ("prepolymers"). (c) Ratio between primary hydroxyl groups (pOH) at 1030 cm^{-1} and secondary hydroxyl groups (sOH) at 1100 cm^{-1} of the pPPGS and pPGS FTIR sample spectra.

Glycerol and its asymmetrical hydroxyl reactivity during PGS synthesis

PGS FTIR spectra from Figure 8a present the evolution from mPGS (0h) to pPGS (24h) under N_2, and the final PGS HBP completely cured at 130 ºC for 48h more. The broad band maximum intensity of hydroxyl groups is displaced from 3335 cm^{-1} for mPGS at 0h, to 3438 cm^{-1} and 3453 cm^{-1} for pPGS and PGS respectively. The ratio of pOH/sOH represented in Figure 8b exhibits a decreasing trend on its value from around 2 for mPGS, 0.8 for pPGS and a final 0.6 for the final cured PGS HBP.

It can be interpreted that free carboxyl groups have more affinity for pOH of Gly, leading to more linear chemical macromers during the prepolymerization instead of interacting with sOH, which remains unaltered until the cured step starts and PGS structure becomes more crosslinked.

If compared ^1H NMR spectra of pPGS sample (24h) (Figure 9a), with the mPGS (Figure 9b), several differences may be observed. The five possible Gly reactant families are only represented after the 24h of prepolymerisation, thanks to each hydrogen proton signal which are located in between δ3.5-5.5 ppm, including the free OH- of unreacted Gly as a broad band around δ2.8 ppm. Thus, the pOH and sOH groups which reacted with the SA carboxyl groups were calculated according to the adapted equations from [7] and represented at Figure 9c.

The acyl glyceride chemical groups (δ3.5-5.5 ppm), identified thanks to the ^1H NMR spectra, tend to grow in intensity from mPGS to pPGS, with the time of prepolymerization. This fact has a direct correlation with the reaction affinity of different hydroxyl groups from Gly and de diacid from the SA. More particularly, from Figure 9c, can be confirmed how the pOH are the first ones which react by polycondensation, leading to more linear macromer formulation of the pPGS. The sOH has been demonstrated to be the main responsible of the polyester crosslinking, having less reactivity than the pOH.

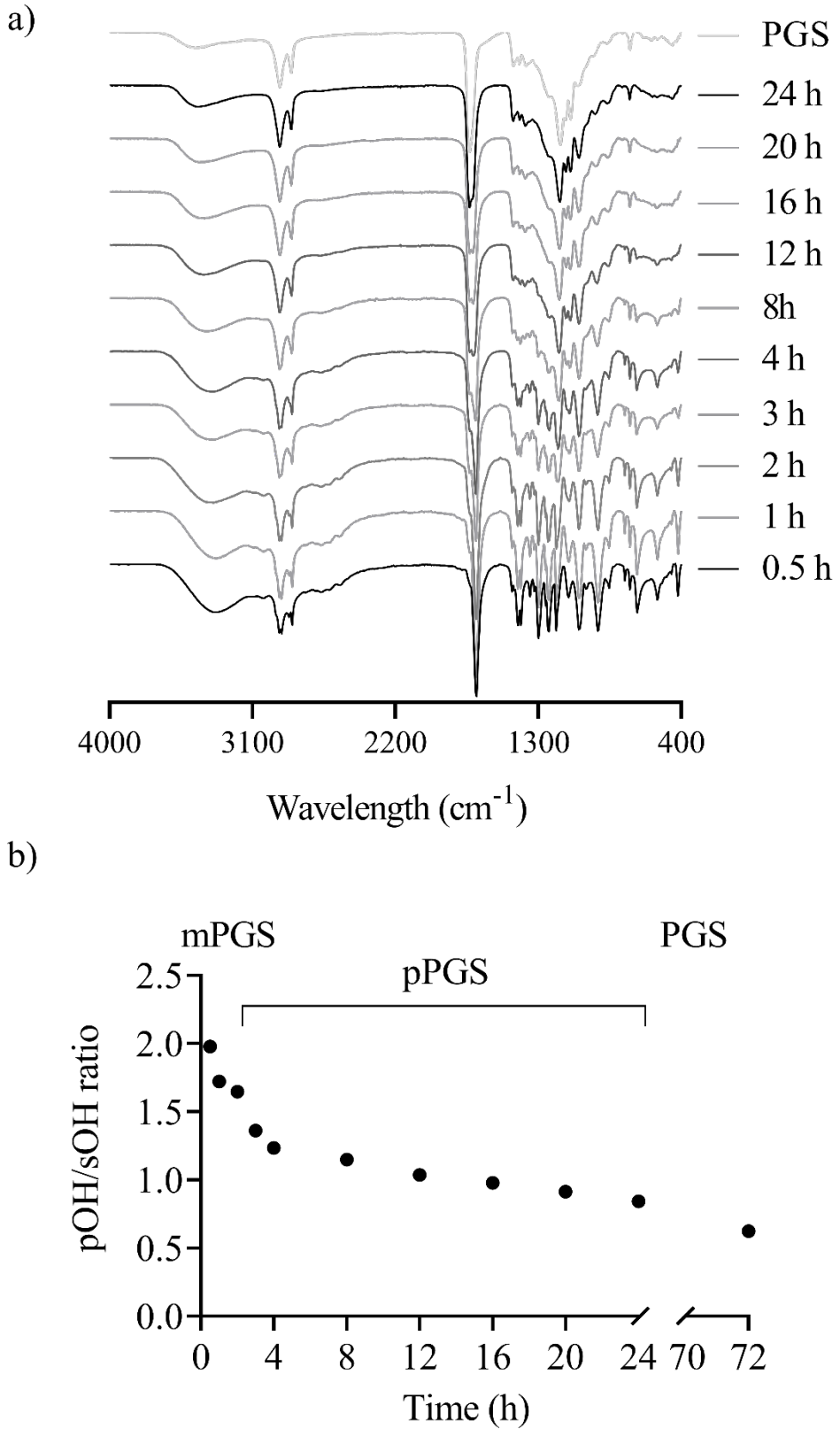

Figure 8. (a) FTIR spectra (transmittance, a.u.) of PGS synthesis steps: Step 1, mPGS prepolymerization under N_2 atmosphere conditions at 130 °C from 0h to 24h (pPGS). Step 2, cured process at 130 ºC for 48h more until the final polymer is achieved (PGS). (b) Ratio between primary hydroxyl groups (pOH) at 1030 cm^{-1} and secondary hydroxyl groups (sOH) at 1100 cm^{-1} for all the samples from FTIR spectra.

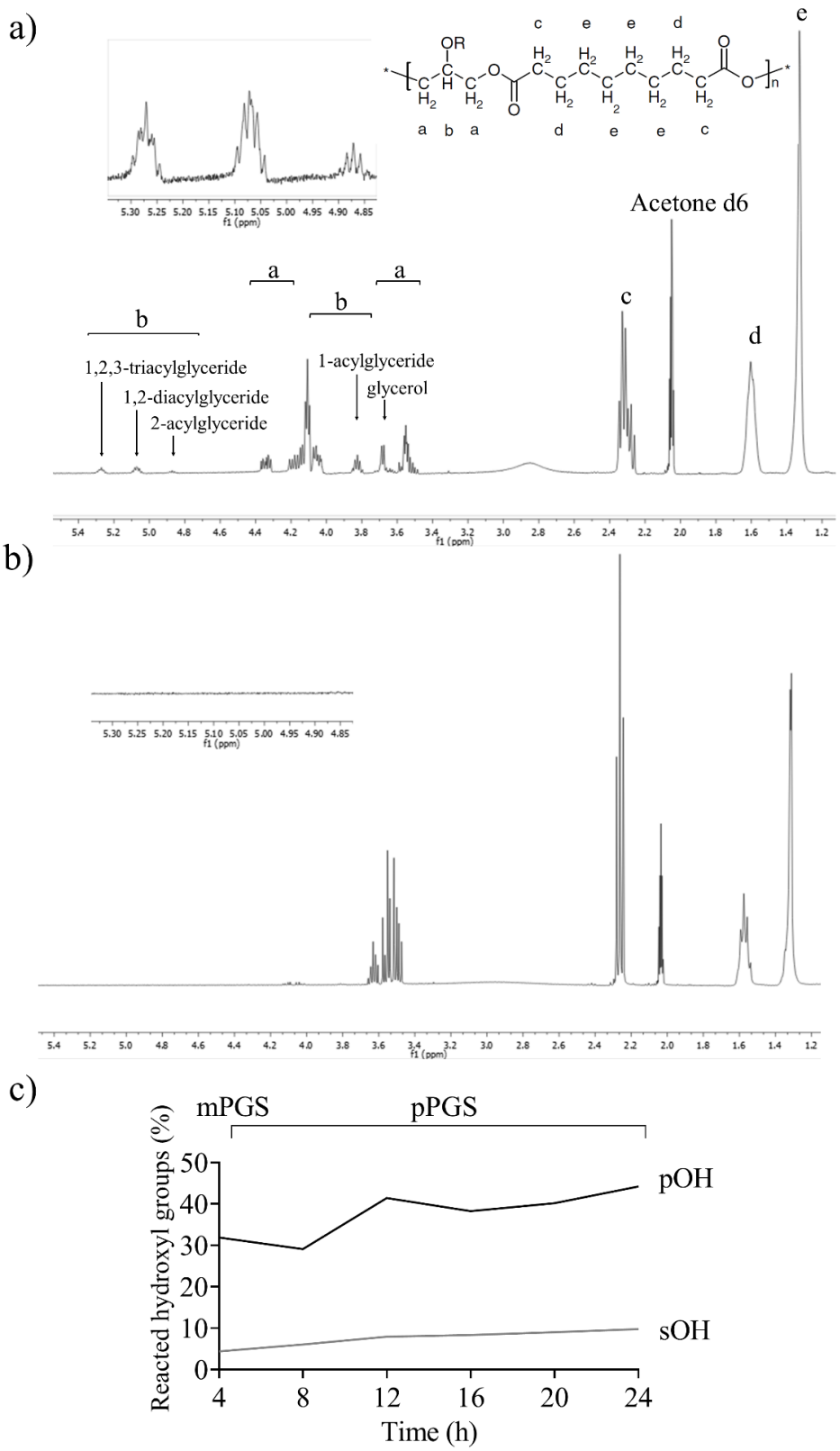

Figure 9. ^{1}H NMR spectrum, in acetone-d6 ($\delta_{Acetone\text{-}d6}$ at 2.05 ppm), of the (a) pPGS (24h) and (b) mPGS (0h) at 130 ºC under N_2. In the structure are the samples chemical assignments. (c) Percentage of pOH and sOH groups consumed by polycondensation during the prepolymerization reaction.

Glycerol influence on the kinetic of the PGS prepolymerization reaction

The thermogravimetric experiment (Figure 10a) was performed in order to simulate a fully PGS synthesis containing both steps of polymerization, step 1 from mPGS to pPGS and then the step 2 till PGS during 48h more. The conditions settled were the conventional ones but the environment, which was N_2 gas flow with constant renewal of the surroundings. The change of the conditions allows the free evaporation of Gly and the resulting water as a sub product of the polycondensation reaction due to the no containment area of the reaction surroundings. This enables the indirect understanding of the constant water and Gly loss effect (due to high synthesis temperature = 130 ºC) on the final PGS sample synthesis through the constant monitoring of its mass loss, with a final value of 55%.

At the beginning of the reaction is the moment of major percentage of weight loss (around 15% on the first 0.5h). This may be because of the hygroscopic nature of the mPGS which could absorb environmental water while the sample was placed onto the TGA equipment. The presence of water alters the kinetic response of the reaction due to the inhibition of the polycondensation reaction. Inhibition which stops, once the free water content is evaporated because of the temperature, when the most significant increase in conversion occurs (between 1-2h).Thus, the water present in the initial monomers, slightly delays the reaction, since being a polycondensation subproduct, it displaces the reaction equilibrium and, when the water absorbed by the monomers evaporates (around 0.5-1h), the reaction accelerates.

The final mass loss (55%) is significantly higher than the theorical possible assuming a 100% of the reaction among all the functional mPGS groups (OH and COOH), which may be around 30% (Figure 10a). Part of the final mass loss can be attributed to the excess of Gly when equimolar ratios where introduce for polymerizing. However, the amount of final mass loss recorded under the thermogravimetric simulation was significantly above the expected, clarifying the importance of Gly loss during the synthesis process of PGS.

Normalised power of mPGS and pPGS samples were obtained from DSC measurements which are displayed in Figure 10b. The pPGS T_m samples evolve across its melting point window range, which starts at mPGS major T_m around 118 ºC and ends around 10 ºC from pPGS prepolymerized during 24h. The only sample that present a clear T_g is the pPGS at 24h at -10 ºC once the full step 1 of the PGS polymerization has conclude. Thus, the last of the pPGS thermal scanning presents a more defined T_m instead of the less homogeneous thermal properties obtained from less prepolymerized samples.

As the synthesis time elapses, the occurrence of oligomers as they form and grow in the structure of the pPGS, was monitored. These different size oligomers still have the possibility to melt, generating a broad melting window showed in Figure 10b. The presence of a melting window determines a typical HBP prepolymerization [59]. This thermal effect highlights the heterogeneous kinetic trend of PGS prepolymerization, while reducing the material crystalline content in

pursuit of a more amorphous structure when prepolymerization time increases. As exposed in previous work [6], this trend leads to a fully and homogeneous amorphous HBP once the second, and last, polymerization step has taken place, with no melting point and a T_g around -12 ºC.

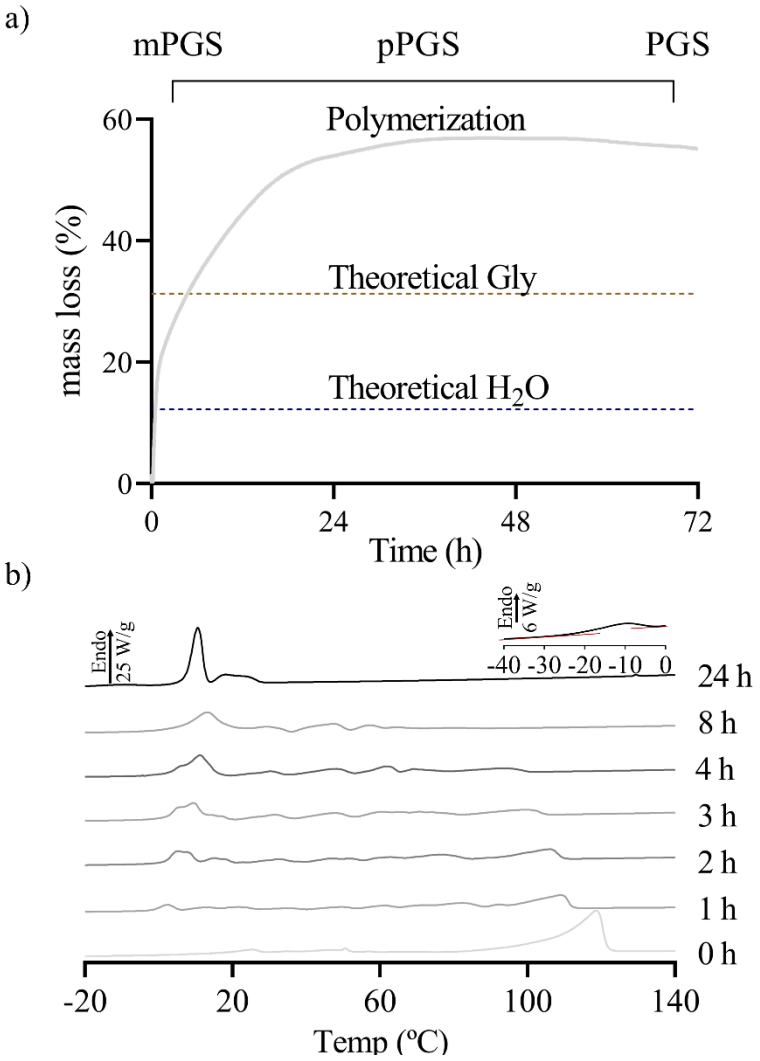

Figure 10. (a) TGA and (b) DSC curves representing the thermal characteristics of PGS pre- and polymerization under N_2 atmospheres for 24h at 130 ºC. (a) It is shown the time (h) vs weight loss (%). (b) The graph presents the temperature (ºC) vs normalized heat flow (W/g) of the mPGS at 0h and the different pPGS at different time of reaction (1h, 2h, 3h, 4h, 8h, and 24h). Insert of 24h sample T_g.

Figure 12a and b display the determination of the DE by mean of titration and ^{1}H-NMR values of mPGS and pPGS samples, respectively. For the ^{1}H-NMR DE calculation, adapted formulas from [7] were used. The DE have its maximum value at 80.65% for the titration results and around 54% for the ^{1}H-NMR approximation. Both have with its steepest DE increase during the first 4h of reaction but different numerical results. This is because the DE is defined based on the proportion of hydroxyl (or of hydroxyl-associated protons, since there is only 1 per hydroxyl), and hence the maximum degree of esterification of each species cannot reach 100%, but stay in lower fractions. Parallel studies, by mean of the sample FTIR spectra, were conducted for measuring the ratio of unreacted

hydroxyl groups and the ester carbonyl (Figure 12c). A strong downturn of the OH/COO^- ratio during the same first 4h of polymerization, is shown.

From all the data presented in Figure 12, can be confirmed how the early stages of the prepolymerization are key factors for the understanding of the PGS HBP synthesis. These first 4h of the prepolymerization process, are the moment where most of the polycondensation process take place, leading to the randomly distributed PGS HBP first oligomers.

Data extracted from GPC experiments are illustrated in Figure 11 and Table 1 presenting a linear trend of M_n and M_w, from 200 g/mol at mPGS, to around 3000 g/mol with the final pPGS. PDI values are around 1.5, except mPGS which, due to the Gly and SA individual peak presence, is higher (PDI = 3.1).

Table 1 Molecular weights from GPC measurements of mPGS and pPGS samples

Time (h)	**0.0**	**4.0**	**8.0**	**12.0**	**16.0**	**20.0**	**24.0**
M_n (g/mol)	113.9	757.3	858.9	1464.0	1580.0	1906.0	2204.0
M_w (g/mol)	355.3	925.4	1224.0	2190.0	2118.0	2717.0	3510.0
PDI	3.1	1.2	1.4	1.5	1.3	1.4	1.6

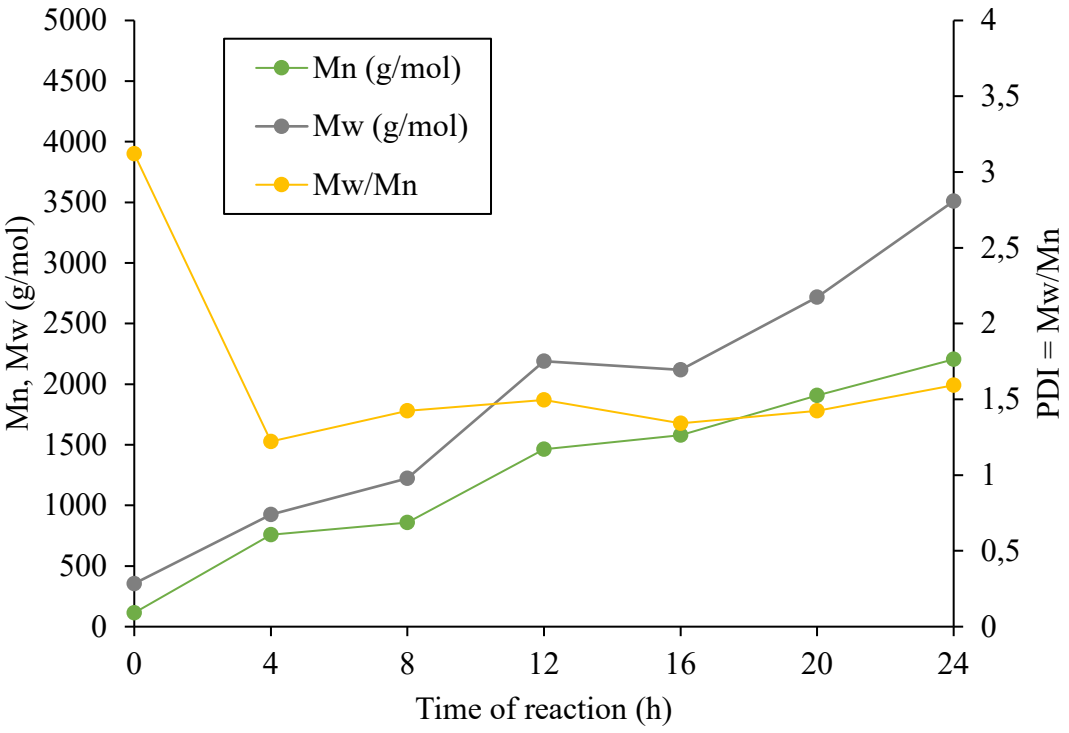

Figure 11. GPC results of M_w, M_n, and its ratio evolution from 0h to 24h

Different molecular weight distribution determines how the chain growth of the PGS HPB has a very regular trend, nearly linear with time and values of PDI which determine how the polyester behaviour is the typical HBP [60]. Other authors have proved how the melting peak of semi-crystalline polymer samples are directly related to its branching, the more the branching the less the melting

peak [59]. Thus, from Figure 10b and previous works with fully cured PGS [6], can be concluded how the prepolymerization process influences on branching degree by modifying its polyester thermal properties. The first semi-crystalline structure (mPGS) evolves to more amorphous oligomer chains due to the raising on its polycondensation process which leads to more branching degree. This fact is supported by the range of melting temperatures instead of single peak distribution during its DSC thermal analysis, indicative of how the ability of chains to crystalize is reduced with the more branched structure content. Once the polymerization of the polymer has concluded (after 24h of prepolymerization and 48h more of curing) the maximum degree of branching is achieved leading to a fully amorphous crosslinked PGS HBP with no crystalline content.

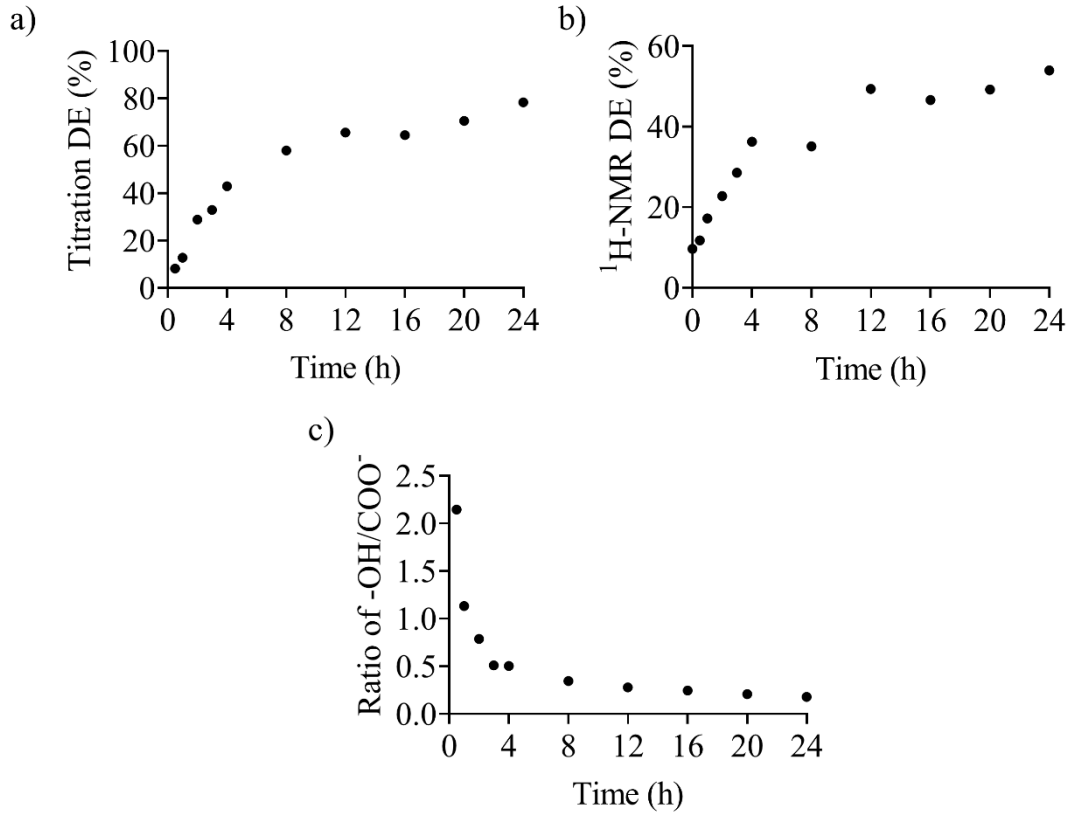

Figure 12. DE calculated by mean of (a) titration and (b) ^{1}H-NMR of mPGS and pPGS samples, respectively. (c) Ratio of -OH/COO- from FTIR spectra peaks at 1730 cm^{-1} for COO- groups and the maximum value of-OH from 3300 to 3400 cm^{-1}.

CONCLUSIONS

Monomeric mixtures of three alcohols (PPD, PPG and Gly) were prepolymerized together with SA during 24h under N_2 atmosphere at 130 ºC. Different time samples were collected from standard mPGS prepolymerization in other to unveil the chemical evolution over time. To this effect, the process parameters during synthesis were controlled by applying a confined environment that allows Gly and water by products to remain into the system, avoiding Gly loss while a constant flux of N_2 was applied.

When comparing, the three alcoholic monomers prepolymerized with SA, Gly was the only one with a defined increment of its viscosity through its synthesis time when rheological measurements were performed. On the other hand, prepolymers from PPD and PPG present a constant viscosity value under same rheometric conditions as Gly but differences on FTIR spectra unveil the first of the key synthesis parameters. The chemical hydroxyl distribution, and final prepolymer bonding structure (from FTIR and ^{1}H-NMR results), define how the reaction tends the polycondensation of pOH rather than sOH, leading to a linear and less crosslinked polyester during its early stages (first 4h). This determines why synthesis of PGS need of two-step synthesis to obtain a fully crosslinked PGS HBP.

TGA mass loss analysis clarifies the hygroscopic behaviour of mPGS and specify how water act as an inhibitor of the polycondensation reaction and the irretrievable loss of Gly unless we control the pPGS synthesis environment. These data highlight the importance of confinement of the prepolymerization reaction in order to control its final PGS HBP synthesis controlling its monomer ratio to remain equimolar. Data obtained from DSC analysis of mPGS and pPGS at different time points (0h, 1h, 2h, 3h, 4h, 8h, and 24h) illustrate a melting window from T_m at 118 ºC to 10 ºC. The melting point window becomes sharper and more defined once the prepolymerization ends and its branching degree raises, together with its amorphous state for the shake of crystalline distribution.

DE calculated thanks to titration, ^{1}H-NMR and FTIR determines a similar trend with values around 40% for both, titration and ^{1}H-NMR at 4h when, as expected, most of the polycondensation reaction take place establishing the polyester backbone structure. Afterwards, the DE value grows until different values of 80% and 60% (titration and ^{1}H-NMR respectively) due to its different quantification method.

From GPC M_w and M_n values, a linear tendency can be elucidated on its molecular weight evolution, from 200 g/mol to values around 3000 g/mol with PDI around 1.5, which indicates how the prepolymer is prone to growth as an HBP once its linear reactivity through primary hydroxyl groups is reduced (after 4h). In total, early stages of the PGS HBP synthesis procedure and understanding its synthesis parameters, such as hydroxyl affinity, water and Gly loss effect together with the DE, are crucial for the scalability and reproducibility of its final product. The first 4 hours of the process determine the final state of the polymer linear chain growth. After this time, the prepolymerization tends to create more branching chemical structures which may lead to a more crosslinked polymer.

CHAPTER 2: Influence of pre-polymerisation atmosphere on the properties of pre- and poly(glycerol sebacate)

ABSTRACT

Poly(glycerol sebacate) (PGS) is a versatile biodegradable biomaterial on account of its adjustable mechanical properties as an elastomeric polyester. Nevertheless, it has shown dissimilar results when synthesised by different research groups under equivalent synthesis conditions. This lack of reproducibility proves how crucial it is to understand the effect of the parameters involved on its manufacturing and characterise the polymer networks obtained. Several studies have been conducted in recent years to understand the role of temperature, time, and the molar ratio of its monomers, while the influence of the atmosphere applied during its pre-polymerisation remained unknown. The results obtained here allow for a better understanding about the effect of inert (Ar and N_2) and oxidative (oxygen, dry air, and humid air) atmospheres on the extent of the reaction. The molecular pattern of intermediate pre-polymers and the gelation time and morphology of their corresponding cured PGS networks were studied as well. Overall, inert atmospheres promote a rather linear growth of macromers, with scarce branches, resulting in loose elastomers with long chains mainly crosslinked. Conversely, oxygen in the latter atmospheres promotes branching through secondary hydroxyl groups, leading to less-crosslinked ‘defective’ networks. In this way, the pre-polymerisation atmosphere could be used advantageously to adjust the reactivity of secondary hydroxyls, in order to modulate branching in the elastomeric PGS networks obtained to suit the properties required in a particular application.

Keywords: poly(glycerol sebacate); polymerisation atmosphere; glycerol; polycondensation; pre-polymerisation; curing

INTRODUCTION

Poly(glycerol sebacate) (PGS) is an elastomeric polyester with suitable properties for biomedical and tissue engineering applications, such as biodegradability and biocompatibility [32,61–63]. First reported as a biomaterial by Wang *et al.* in 2002 [3], PGS can be manufactured in a wide range of consistencies, from soft to hard [64], enhancing tissue regeneration and/or substitution [62]. Its versatility enables mimicking the mechanical and structural features of several tissues, such as cornea [65,66], adipose [67], blood, cartilage, nerve [68], cardiac muscle [17,69] and bone [35,70,71].

PGS synthesis is typically based on a two-stage polycondensation, starting with the pre-polymerisation of its reagents glycerol (Gly) and sebacic acid (SA). Carboxylic groups of the diacid condense with hydroxyl groups of the triol leading to ester groups (and a water molecule), eventually yielding oligo- or macromers, most of which are presumably linear, while they might be branched due to the tri-functionality of the alcohol. This pre-polymerisation process is conventionally carried out at constant temperature around 120 ºC-130 ºC, for 24h under an inert atmosphere such as nitrogen or argon to prevent oxidation of reagents [1,3]. The pre-polymer (pPGS) is a wax-like mixture of species that can still be dissolved. The different species eventually start curing into a solid elastomer, when the condensation of terminal groups of branched chains causes the gelation of a percolated network. This second stage of the process goes on for 48h under vacuum conditions at the same temperature, leading to a flexible polymer (PGS) [6,15,33–37].

In the last two decades, some studies have revealed the need for an optimised, simple and reproducible synthesis procedure, to avoid variability in the final properties of the polymer, and reduce manufacturing costs [5,15]. On the one hand, some authors have addressed the influence of synthesis parameters for a better understanding of the synthesis process and clarify how they alter the final polymer properties. Temperature stands as the most studied parameter during pre-polymerisation and curing of PGS, ranging between 110 ºC and 150 ºC [6,36]. Furthermore, curing time has also been investigated, as well as the ratio between monomers [5]. On the other hand, to further reduce the synthesis time, the use of a microwave oven has been proposed, for example. The drawback of this method is that the synthesis rate is faster at the expense of glycerol loss because of the high temperatures reached, thereby distorting the molar ratio between monomers [5,11]. Other authors performing a microwave-assisted synthesis showed that, by using a water-based reagent mixture, the reaction temperature remained more homogenous and kinetics decelerated. This is due to the fact that water is a by-product of the esterification between Gly and SA, thanks to the solvent diffusion effect, leading to a more reproducible reaction [10].

Notwithstanding the foregoing, the PGS synthesis is conventionally conducted under an inert atmosphere to replicate the condition set when it was synthesised for the first time by Nagata *et al*. in 1998 under the name of Yg10, using a nitrogen atmosphere [1]. Although the polymerisation temperatures are milder than those reported in this foremost work (215 ºC-250 ºC), no studies have reported to date

the real need for an inert atmosphere, and its effect on the resulting viscous pre-polymer remains undetermined.

To unveil the potential influence of this parameter, pre-polymerisation was tested in different atmosphere compositions over 24h at 130 ºC as described in [6]. The environments selected were: argon (Ar) and nitrogen (N_2) as inert gases; oxygen (O_2), which may produce oxidative reactions due to its interaction with glycerol hydroxyls [72,73]; dry (compressed) air (DA), as a combination of inert and oxidative atmospheres; and humid air (HA) to study the additional effect of environmental water vapour. Next, the obtained pre-polymers were cured conventionally, to correlate properties of pPGS (and their corresponding PGS elastomer) with the synthesis atmosphere. This approach will enable monitoring the performance of pre-polymerisation as required, to then manipulate the viscous mixture and shape the cured PGS as a scaffold or porous membrane, for example. Thus, PGS networks would be obtained matching the properties demanded by a particular biomedical application.

MATERIALS AND METHODS

Preparation of pPGS pastes and PGS films

PGS pre-polymers (pPGS) were synthesised by condensation of glycerol (Gly; 99%, Sigma-Aldrich) and sebacic acid (SA; 99% Sigma-Aldrich), as reported in detail in a previous work [6]. An equimolar Gly:SA mixture (*i.e.* 3:2 ratio of OH:COOH functional groups) was heated up briefly to 140 ºC (above the SA melting point) to ensure homogeneity, and then kept at 130 ºC. The gas flow circulating through the reactor during pre-polymerisation was selected from N_2, Ar, O_2, dry air (DA) and humid air (HA; 33% relative humidity). The pre-polymerisation reaction was prolonged in each case to several time points up to 24h. Next, the viscous pPGS was withdrawn and cured in Teflon® open moulds in a forced ventilation oven, at 130 ºC for 48h, to obtain 1-mm thick PGS films.

After curing, the films were rinsed in tetrahydrofuran (THF, Scharlau) for two days in an orbital shaker with a solvent renewal, to remove unreacted monomer residues and non-crosslinked chains. Next, THF was progressively replaced with ethanol (EtOH; absolute ethanol, Scharlau) over two additional days to avoid the fracture of swollen networks, concluding with the gradual change to Ultra-pure MilliQ water for the last two days. Finally, PGS samples were dried overnight at room conditions, and then in a vacuum for 24h. Unless otherwise specified, the films were cut into 6 mm diameter samples.

Characterization of pPGS pastes under different atmospheres

Degree of esterification of pPGSs

The degree of esterification (DE) of pPGSs obtained under each atmosphere after 24h of synthesis was determined by titration method, adapted from [5]. The DE of the starting Gly:SA monomer mixture (mPGS) was also obtained for comparison. To this effect, 100 mg of viscous pPGS were poured into an Erlenmeyer flask with 50 mL of a 25:75% wt EtOH:THF solution and placed on a stirrer at 500 rpm until completely dissolved. Then, 5 drops of 0.5% phenol red solution (Sigma-Aldrich) were added for pH-monitoring, and the Erlenmeyer flask was sealed with parafilm to prevent atmospheric CO_2 to form K_2CO_3. A 0.1 M solution of potassium hydroxide (KOH; Sigma-Aldrich) in EtOH was added drop-by-drop to perform the titration, until the colour of the solution changed from transparent to pinkish-purple, indicating a pH value of 10.7. The final degree of esterification was calculated using the following equation, adapted from [5]:

$$DE = 1 - {(V_1 - V_0)}\Big/{(V_{mon} - V_0)} \quad (1)$$

where V_1 is the volume of KOH solution used to titrate each pre-polymer sample, and V_0 and V_{mon} are the volumes used for the blank test and consumed by mPGS, respectively.

Fourier-Transform Infrared Spectroscopy

Fourier-Transform Infrared Spectroscopy (FTIR) spectra of pPGS samples obtained at different reaction time points up to 24h were collected to follow the progress of hydroxyl, carboxylic and ester bonds under different synthesis

atmospheres. A Platinum ATR spectrometer (ALPHA II, Bruker) was used for this purpose. The spectra resulted from averages of 24 scans at a resolution of 4 cm^{-1}, between 400 and 4000 cm^{-1}.

Differential Scanning Calorimetry measurements

Differential Scanning Calorimetry (DSC) measurements of pPGSs (pre-polymerised for 24h) and mPGS were performed in a Perkin Elmer DSC 8000. Samples were cooled to -80 ºC, and scanned up to 60 ºC at 20 ºC·min^{-1} under a constant N_2 flow of 50 ml/min. The melting point was determined for each sample from its calorimetric curve as the maximum of the endothermic peak.

Thermogravimetric analysis

Thermal degradation tests of pPGS samples (polymerised for 24h) were performed to determine the effect of the atmosphere composition on the thermal decomposition profile of the pastes. A SDTQ600 thermogravimetric analyser (TGA, TA Instruments) was used to register the mass loss from 30 °C to 600 °C at a heating rate of 10 °C min^{-1} under a N_2 flow of 50 ml/min. The monomer mixture (mPGS) was measured for comparison.

Characterization of PGS cured after pre-polymerisation at different atmospheres

FTIR, TGA and DSC measurements were also performed on PGS samples as previously described. Additionally, the following experiments were conducted:

Viscosity tests

A Discovery HR-2 hybrid rheometer (TA Instruments) was used to scan the viscosity of pPGS samples during gelation until the rupture of the formed elastomer. pPGS pastes were placed between aluminium, 25 mm-diameter, parallel plates, separated by a gap of 1000 µm. The viscosity was recorded throughout the curing process at constant temperature (130 ºC) at 1.5 rad·s^{-1} of rotational speed.

Wettability tests

Dry PGS samples were analysed using a Dataphysics OCA 25 (DataPhysics Instruments GmbH), to determine their wettability. Water contact angles (WCAs) were obtained from at least ten 3 ul-drops of Ultra-pure MilliQ water for each sample, by the sessile drop technique. In order to unveil the presence of surface-hidden polar groups in the elastomers, as observed in [6], the WCAs of analogous wet samples were obtained. To this end, PGS samples were immersed for 24h in Ultra-pure MilliQ water. The excess of water on the surfaces was carefully removed before measurements.

Swelling at equilibrium

An XS105 Dual Range balance (Mettler Toledo) was used for weighing dry PGS samples and later immersed in Ultra-pure MilliQ water at 37 ºC over different time lengths until constant weight. The equilibrium water content (EWC) was defined as follows:

$$EWC = {}^{m_w}/_{m} \quad (2)$$

where m_w is the mass of water in the swollen sample at equilibrium, and m is the mass of dry sample. In parallel, PGS networks were swollen in EtOH, a more affine solvent than water. These measurements might broaden differences between samples that remain subtle when swelling in water. An equation analogous to (2) was used to calculate the equilibrium EtOH content (EEC) in each case. Triplicate measurements were taken for each sample and solvent.

Density measurements

A Mettler ME 33360 density kit, accessory to the balance was used to determine the density of dry PGS samples through Archimedes' principle. The samples were weighed open-air and immersed in n-octane (98 %, Sigma-Aldrich, $\rho_{\text{n-octane}}$ = 0.703 g·cm^{-3}) at room temperature. It has been reported that PGS does not swell significantly in n-octane [6] and can thus be safely used in these tests. The density (ρ) was determined as the ratio of the weight of the dry sample (m) through the volume of n-octane displaced (V):

$$\rho = {}^{m}/_{v} = {}^{m}/_{(m\_\ m_{n-octane})/\rho_{n-octane}} \quad (3)$$

where $m_{n\text{-}octane}$ is the measured weight of the sample immersed in n-octane. Three samples were taken from every batch condition registered to carry out measurements.

Mechanical compression tests

In order to determine the compressive elastic modulus (E) of the dry PGS samples, a Thermomechanical Analysis device TMA/SS6000 Seiko Instruments Inc was used. Five replicates per PGS type were scanned. The experiments were conducted at room temperature between 0.5 and 1500 mN at 100 mN·min^{-1} to obtain the stress-strain curves. The elastic moduli were obtained from the slopes in the initial ramp, from 0 to 5 kPa, and in the second linear zone, in the range between 70 and 120 kPa.

Dynamic Mechanical Spectroscopy

Dynamic mechanical thermal analyses were performed to characterize the main relaxation process associated to the glass transition of dry PGS samples under different atmospheric synthesis conditions by means of a Dynamic Mechanical Analyser DMA 8000 (PerkinElmer). Rectangular shaped specimens, approximately 100 mm^2, were tested from -80°C to 180°C at 3°C min^{-1} at 1 Hz of frequency in the single cantilever mode. The evolutions of the storage modulus (E') and $\tan\delta$ (the ratio between loss and storage moduli of viscoelastic materials) with temperature were recorded. To compare the different PGS samples, the temperature at the $\tan\delta$ peak was determined.

RESULTS AND DISCUSSION

Influence of the pre-polymerisation atmosphere on the pPGS degree of esterification

In order to identify the chemical bonds and degree of esterification (DE) of pPGS viscous mixtures, FTIR and titration techniques were used. The FTIR spectra (

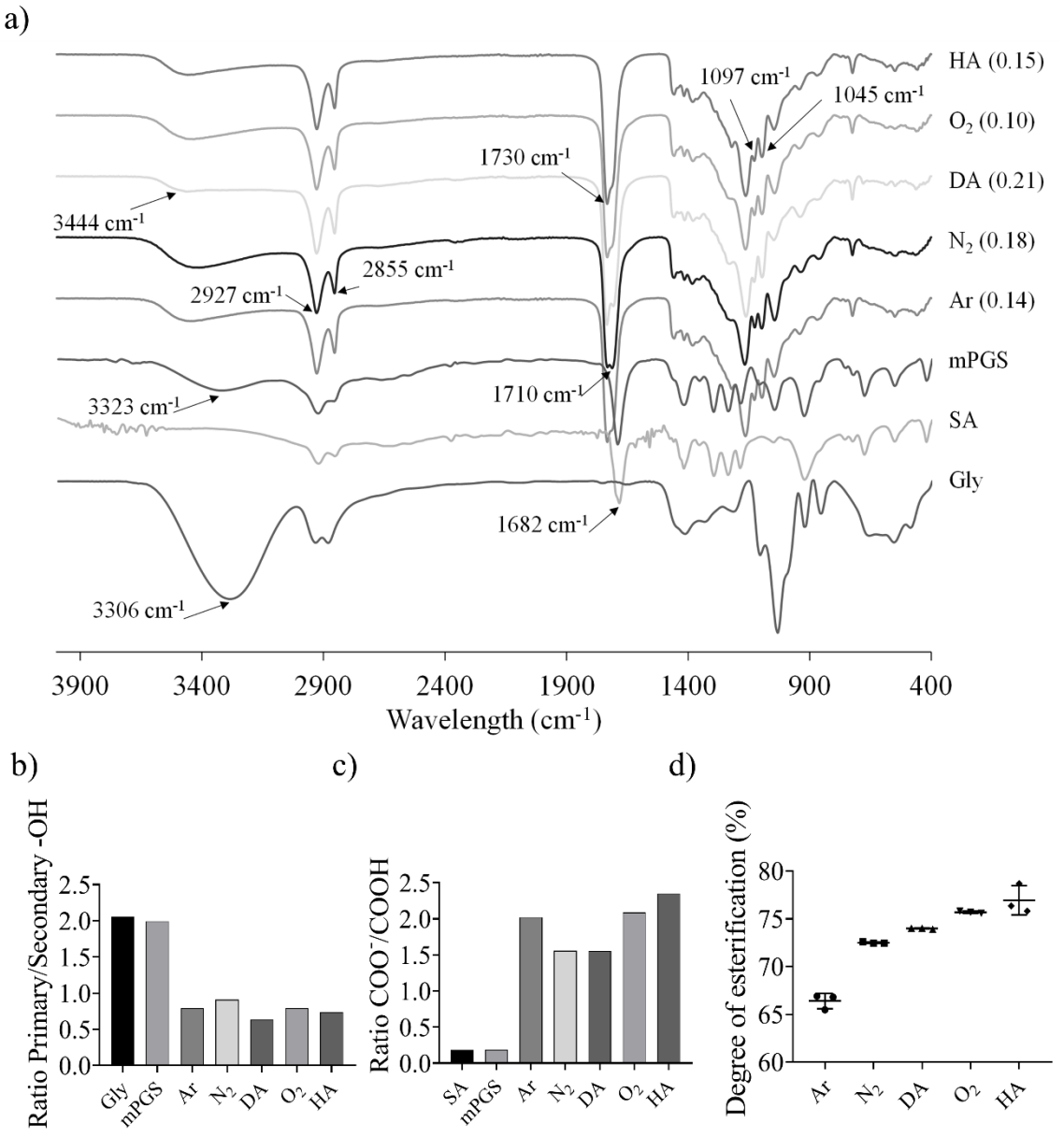

Figure 13a) of all pPGS, mPGS and SA show a main peak at 1731 cm^{-1} assigned to the C=O stretching vibrations. The alkane groups (C-H) of the polymer backbone appear as two characteristic sharp peaks at 2855 cm^{-1} and 2927 cm^{-1}. mPGS and SA peak also at 1682 cm^{-1} representative of the carbonyl stretching of the free carboxylic acid groups (-COOH). The peaks at 1045 cm^{-1} and 1097 cm^{-1} are indicative of the co-existence of primary and secondary saturated alcohol groups (C-O and O-H stretching) and evolve differently, same as the broad, unspecific band around 3440 cm^{-1}.

Generally speaking, during the pre-polymerisation of PGS, Gly alcohol groups react with free carboxyl groups of SA by means of condensation reactions to form ester groups. Several interesting findings can be inferred from the comparison between the FTIR spectra of pPGS mixtures obtained under different atmospheric conditions (Ar, N_2, DA, O_2 and HA) and Gly, SA and the monomeric mixture. Initially, primary hydroxyl groups are twice more frequent than secondary groups in the precursor Gly, as expected (Figure 13c). This ratio decreases below 1 when the pre-polymerisation with SA takes place, for all atmospheres tested, which suggests that, in an early stage, PGS synthesis yields mainly linear structures because of the superior reactivity of primary hydroxyl groups of Gly.

Simultaneously, as shown in Figure 13a, the sharp peak at 1682 cm^{-1} (free -COOH groups) from SA and mPGS shifts to 1710 cm^{-1} and then to 1730 cm^{-1} at the time ester groups ($-COO^-$) are formed. A similar trend is found in the hydroxyl broad band: the increase in transmittance of this band shifting from 3300 cm^{-1} to 3580 cm^{-1} and its area becoming smaller are indicative of esterification taking place by consuming hydroxyl groups. The high $-COO^-$/-COOH (Figure 13b) and low -OH/$-COO^-$ (Figure 13a, between brackets) ratios observed after 24h of pre-polymerisation when it is performed under HA suggest that this atmosphere allows this reaction to take place most efficiently. N_2 apparently has the opposite effect.

The DE values obtained from the titration experiments with the pPGS samples are shown in Figure 13d. An increasing trend is observed when oxidative atmospheres are used (DA and O_2) and water vapour is present in the environment (HA). DE values around 72.5% and 66.40% for N_2 and Ar, respectively, are indicative of a lower interaction between -OH and free -COOH groups during these pre-polymerisations. The DE values in oxidative atmospheres are higher than in inert environments, around 76%. It can be confirmed that synthesis under atmospheres containing O_2 increases the ratio of initiation of the reaction, which is in accordance with [74]. Taken together, the FTIR and titration results suggest that oxidative atmospheres enhance the pre-polymerisation rate. Water vapour, for its part, may hinder the evaporation reactant Gly (that it is well known to occur [5]), bringing this reaction to a higher extent.

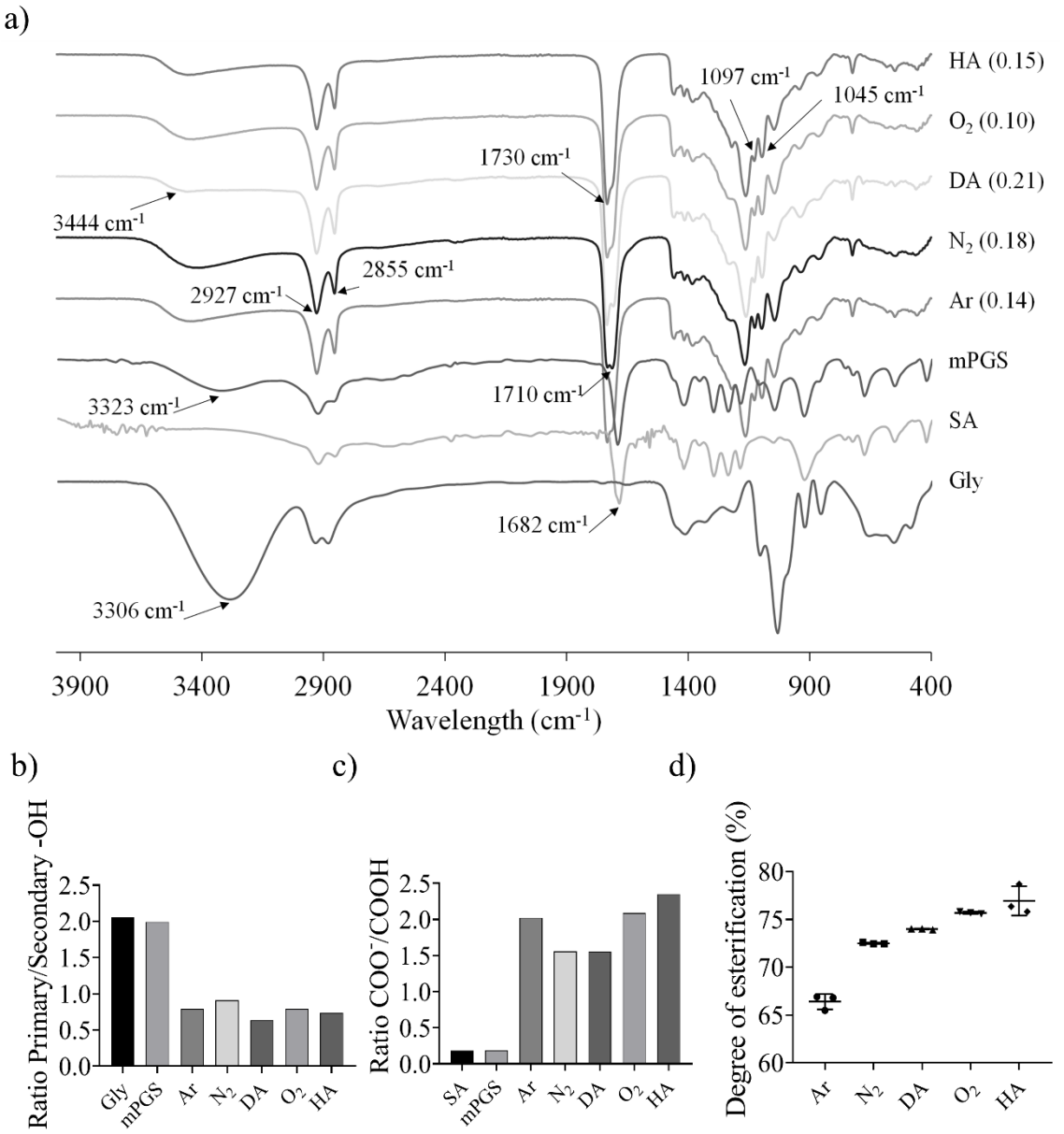

Figure 13. (a) FTIR spectra (transmittance) of pPGS mixtures pre-polymerised under different atmospheres for 24h at 130 °C. The spectra of SA, Gly and mPGS mixture are represented as control values. The values between brackets show the transmittance ratio between 3480 cm^{-1} and 1730 cm^{-1} (-OH/-COO^-). (b) Ratio between ester and free carboxylic acid obtained as the transmittance ratio between 1731 cm^{-1} and 1682 cm^{-1}, respectively. (c) Ratio between primary and secondary hydroxyl groups obtained as the transmittance ratio between 1045 cm^{-1} and 1097 cm^{-1}. (d) Degree of esterification (DE) values of pPGS after pre-polymerisation under different atmospheres during 24h at 130 ºC.

Influence of the pPGS degree of esterification on its thermal properties

Figure 14a shows the normalised power during the heating scan of the DSC measurements of pPGS samples, together with their melting point (T_m) values taken as the maximum of the melting endothermic peak. The monomers mixture displays two different T_m: one around 26 ºC (less intense), and another at 118.68 ºC (strong endothermic peak, shown in the insert at another scale), as expected

given the different T_m of its constituents Gly (18.2 ºC) and SA (130.2 ºC). The melting peaks of the mixture unify as pre-polymerisation occurs and the result gradually shifts to values around 10 ºC for inert atmospheres (12.24 ºC for Ar and 9.89 ºC for N_2) or lower when O_2 and/or environmental water are present (around 6 ºC for O_2 and HA samples). All these pre-polymers are, thus, still semicrystalline, whereas crosslinked PGS networks turned out to be fully amorphous after curing [6].

Although O_2 and HA have shown to esterify to a greater extent, the presence of oxidative species from Gly seems to facilitate chain mobility in the pPGS paste, lowering their T_m values. In the case of HA, diffusion of water vapour throughout the mixture taking place in the reactor could hinder the evaporation of Gly, as previously mentioned, thus acting synergistically with the oxidative ambient to this effect.

The thermogravimetric profiles of pPGSs and the monomer mixture are plotted in Figure 14b. For comparison purposes, the thermal degradation temperature has been tabulated as the inflection point of the main weight loss (T_d in the insert). Again, mPGS shows the behaviour of its components, with two weight loss stages, that of Gly (T_d = 213.93 ºC) and SA (T_d = 435.19 ºC). The pre-polymers display a mild weight loss between 175 and 275 ºC, attributed to free Gly (in excess in the monomer mixture), which is less evident as the reaction proceeds and it is further consumed, in oxidative environments. In accordance with this observation, T_d (calculated in the main weight loss stage, between 400 and 500 ºC) for pPGS obtained under Ar, N_2 and DA appears at around 425 ºC, while higher values are obtained under O_2 and HA atmospheres (428.59 ºC and 434.9 ºC, respectively).

Notwithstanding, it is worth mentioning that the profile of HA pPGS paste differs greatly from the rest, with a significant intermediate weight loss between 275 ºC and 400 ºC (around 20%), indicative of a wider variety of species in this pre-polymer, some more sensitive to thermal degradation.

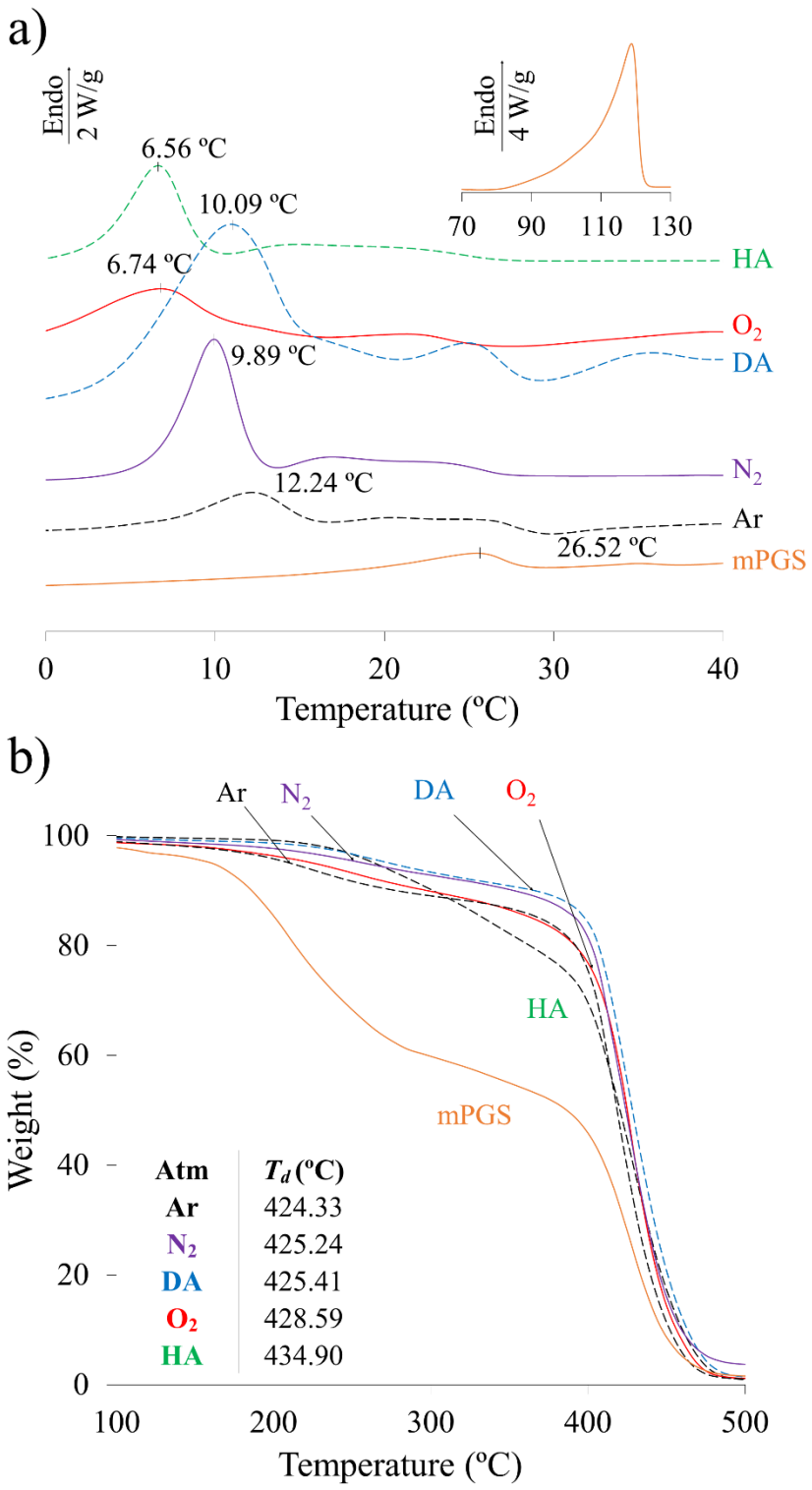

Figure 14. (a) DSC and (b) TGA thermograms plotting the normalised power and weight as a function of temperature, respectively, for mPGS and pPGS pastes obtained under different atmospheres after 24h at 130 ºC. Values displayed in (a) are the melting temperatures (T_m) indicating the maximum value of the endothermic melting peak. The mPGS profile is shown as control, displaying in the insert the characteristic melting point of SA. Data in table on (b) lists the inflection point (T_d) of the main degradation stage, obtained from derivative curves. Colours included for the shake of clarity.

Effect of the pre-polymerisation atmosphere on pPGS gelation

The viscosity rate over time was monitored simulating the conventional curing step conditions of a PGS pre-polymer, typically in a force-ventilated oven at 130 ºC during 48h [18]. Gelation and subsequent polymerisation in the solid state (curing) were monitored until the PGS networks broke under the stress exerted by the plates (Scheme 3).

Scheme 3. Synthesis procedure of pPGS from mPGS for the rheometric characterisations.

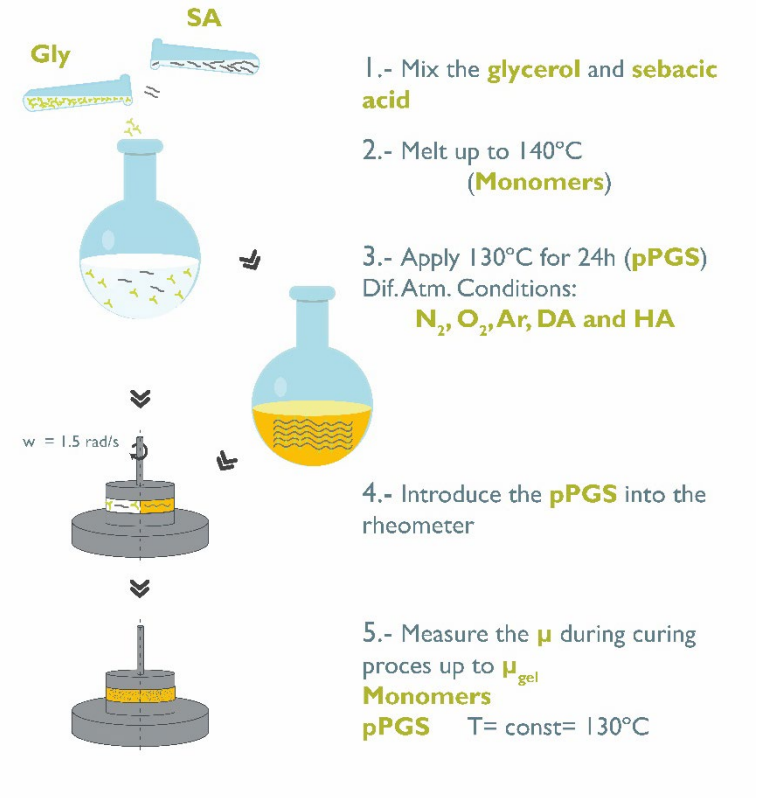

The viscosity profiles of pPGS pastes, previously pre-polymerised (as polymer melt) under different atmospheric conditions, are presented in Figure 15. It is worth indicating that origin of x-axis (0h) corresponds to the start of the second polymerisation stage, carried out in the rheometer. Table 2 lists the value of initial viscosity (η_0), gelation time (located at the intersection point of the extrapolated liquid and solid polymerisation trends), and the ultimate viscosity and time for it, obtained at the end of the experiment (breaking point). These results allow for a better understanding about the effect of each atmosphere on the resulting pPGS and the corresponding cured PGS network final morphology.

Initial viscosity values are higher for pastes obtained under HA, O_2 and DA atmospheres (higher degree of conversion at 0h), which gel after few hours. This trend correlates with the amount of oxygen and water vapour in the tested environment. It has been proven that O_2 rich atmospheres applied during polymer synthesis may increase the viscosity of the solution, because of its high electron affinity which leads to an increase of reactivity by removing electrons from monomers [75]. In the case of HA, if one assumes that water vapour hinders the evaporation of Gly from the reacting mixture, as suggested before, its excess would enhance the formation of branched chains during the pre-polymerisation

process, which explains its greater viscosity. Indeed, in [6] it was found that an excess of Gly in the reacting mixture promoted the activation of secondary hydroxyls and led (after pre-polymerisation under N_2 and curing) to highly-branched oligomers, poorly crosslinked to each other. Such samples lost, after rinsing, more than 70% of its weight, resulting in very sticky polymers, really difficult to handle. Besides, water has been found to thermally stabilize the reacting mixture by facilitating heat transfer [10], which could contribute to this effect.

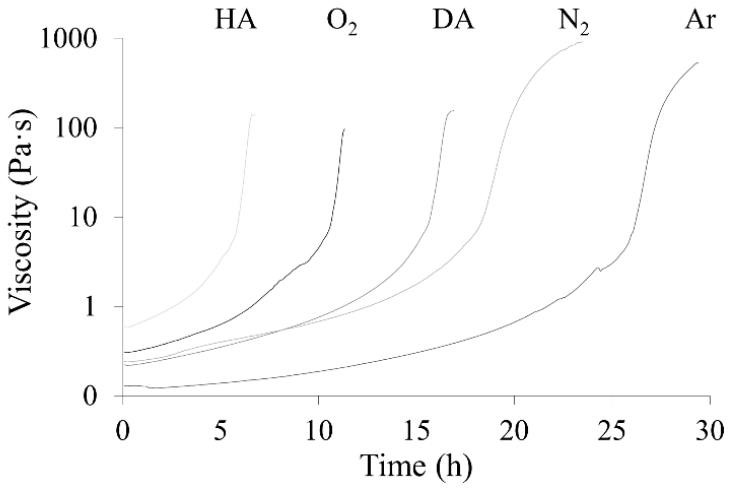

Figure 15. Viscosity monitoring of pPGS (pre-polymerised under different atmospheres) vs. time, at 130 ºC.

Inert atmospheres yield less viscous pastes that require longer times for the percolation of a crosslinked polymer, following a gradual and prolonged increase of viscosity. When compared, N_2 seems to favour the production of more viscous macromers (and probably slightly more branched) than Ar during the pre-polymerisation stage.

Table 2 Representative parameters of the curing process: initial (pPGS) viscosity (η_0), gelation time (t_{gel}), and ultimate (maximum, i.e. that of PGS) viscosity (η_{max}) attained in the rheometer at the breaking point (t_{max}) under the stress of its plates.

Atm	η_0 (Pa·s)	t_{gel} (h)	η_{max} (Pa·s)	t_{max} (h)
Ar	0.13	24.86	535.45	29.25
N_2	0.24	17.17	920.99	23.67
DA	0.22	15.08	155.66	16.92
O_2	0.31	10.25	96.63	11.33
HA	0.59	5.58	141.15	6.75

The final viscosity, obtained at the breaking point, correlates with the gelation time of the different pre-polymers: on those pre-polymerised under inert atmospheres the polymeric chains contribute more effectively to the elastomeric behaviour, while those obtained under oxidative atmospheres have a more branched morphology, being softer. All in all, the rheometry results point out that by setting the atmospheric conditions in the first polymerisation stage, not only the pre-polymers but also the PGS networks obtained greatly differ from each other.

Effect of the pre-polymerisation atmosphere on the physicochemical properties of cured PGS

The -OH/-COO^- ratio of PGS, obtained from their FTIR spectra (Figure 16a) does not differ significantly between samples, being close to 0.11 for all conditions. This indicates that the final cured PGS network achieves, insofar this experimental technique can provide chemical information about the polymeric matrix, equivalent endpoints following each pre-polymerisation atmosphere. If compared to Figure 13a, the pre-polymer obtained in presence of N_2 is, therefore, the resulting material with the lowest rate of terminal -OH during curing.

As for the primary/secondary -OH ratio, it does not vary significantly during the curing process (Figure 16b), unlike during pre-polymerisation of mPGS (Figure 13b). Apparently, the consumption of primary hydroxyls is favoured, as opposed to secondary ones, during the whole process. Notwithstanding, networks pre-polymerised under oxidative atmospheres show slightly higher ratios, which agrees with branching through secondary hydroxyls described in the previous section. As for the ester/free carboxylic acid ratio (Figure 16c), it increased significantly from the values reached after pre-polymerisation (Figure 13c), especially for those obtained under inert atmospheres.

The density of the PGS networks, Figure 16d, slightly decreases after pre-polymerisation in oxidative and humid atmospheres. This finding, though subtle, supports the hypothesis that these conditions yield defective (less crosslinked) branched networks, and are aligned with the observations in [6,9] for PGS cured at mild temperatures.

The water contact angles of the surfaces are shown in Figure 16e, together with those obtained on wet analogous surfaces. The purpose of equilibrating the samples in water was to remove the potential effect of hydrogen-bonding interactions between polar terminal groups in the dry state for PGS samples [6] and other rubbers [76]. Still, an aspect worth noting is that oxygen in the reacting atmosphere presumably produces alcohol-oxidised species, namely aldehydes and/or carboxylic acids from primary hydroxyls or ketones from secondary ones, which slightly increase the wettability of these samples compared to those obtained under inert atmospheres. Indeed, up to eleven oxidation compounds of glycerol have been isolated and identified under distinct conditions (presence of salts, catalysts, free oxygen or sunlight, to name a few) [74].

Table 3 Equilibrium water (EWC) and EtOH (EEC) contents of cured PGS samples starting from different pPGS.

	EWC (%)	EEC (%)
Ar	4.49 ± 1.36	86.60 ± 0.97
N_2	4.51 ± 1.89	91.14 ± 1.36
DA	4.99 ± 1.74	82.70 ± 3.31
O_2	5.70 ± 1.05	97.58 ± 3.69
HA	2.97 ± 1.53	84.69 ± 8.95

Although water is not as good as EtOH as a swelling solvent of PGS (20-fold higher content at equilibrium, according to Table 3), it can be argued that oxygen in the pre-polymerisation atmosphere slightly improves this feature in the resulting hydrophobic networks.

Effect of the pre-polymerisation atmosphere on thermal and mechanical properties of cured PGS

Figure 17a and b present the normalised power in the DSC heating scan of PGS samples along with their melting points (T_m), when still detectable, and glass transition temperatures (T_g). The latter were located as an increase in the normalised power (positive shift in the trend). The endothermic melting peaks vanish while the melting temperatures decrease compared to those of the pre-polymers and get closer to the glass transition. This effect is more evident for those samples pre-polymerised under the presence of oxygen, probably because branching hinders folding of polymer segments into crystallites. Indeed, in PGS pre-polymerised with HA, the melting peak of the crystalline phase is no longer discernible, which is characteristic of an amorphous elastomer. As for the glass transition temperatures, they range between -15 ºC to -25 ºC, being higher when crosslinking of macromers are more extensive and chain stiffness increases, i.e. under inert atmospheres.

Weight loss curves from Figure 17b illustrate that PGS samples are stable up to 250 ºC, which coincides with the literature [77]. They show a single weight loss step in all cases, located between 350 ºC and 475 ºC, which overlaps in all samples except for HA PGS, which again shows weight loss at lower temperatures. This is, once more, indicative of its branched morphology, which, as observed during our monitorisation, leads to the presence of oligomers that decompose in the polymer matrix. Figure 17c and d, show the dynamic-mechanical spectra of the samples, in terms of the storage moduli (E') and (b) loss tangent ($tan\ \delta$).

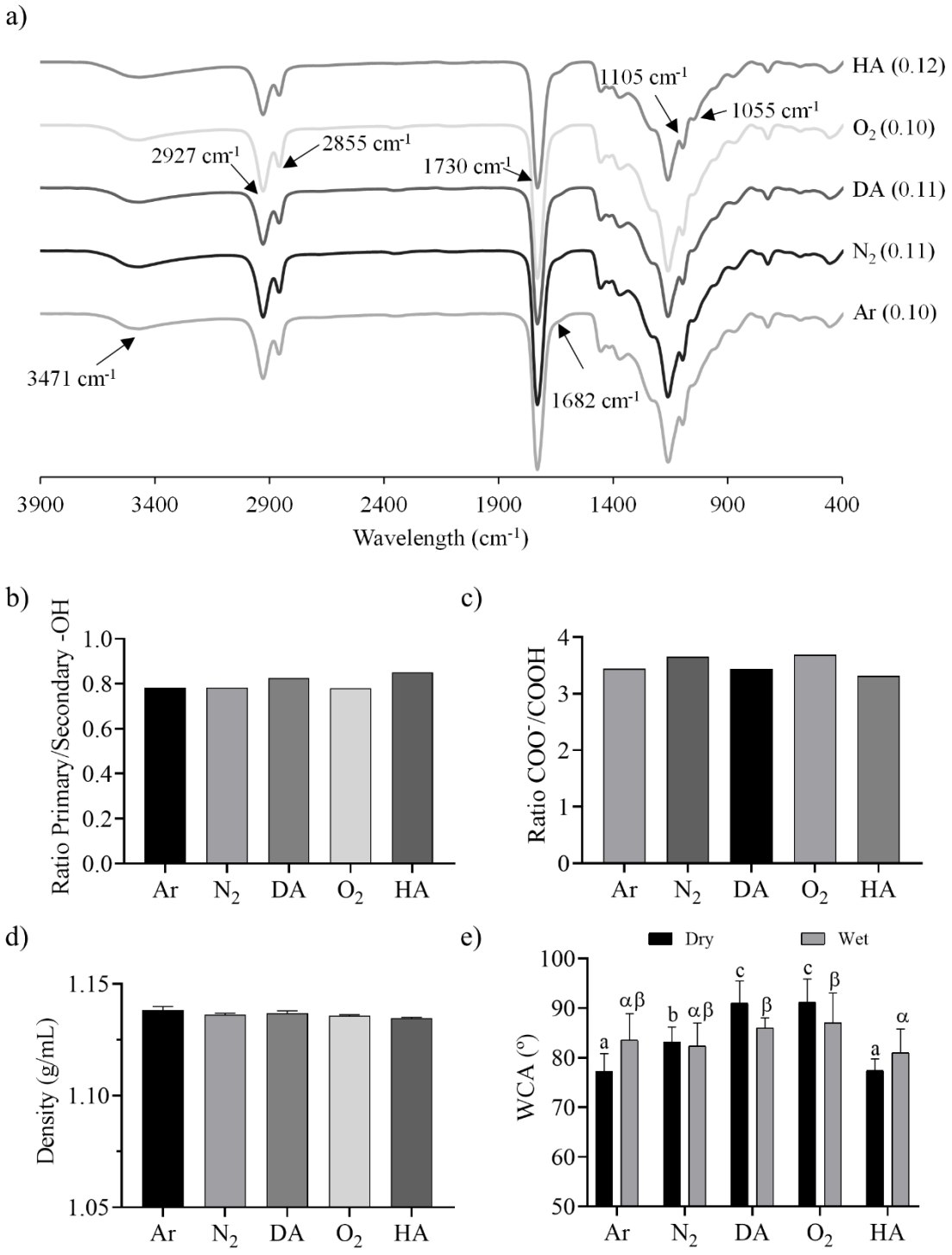

Figure 16. (a) FTIR spectra (transmittance, a.u.) of cured PGS networks previously pre-polymerised under different atmospheres. The values between brackets show the transmittance ratio between 3480 cm^{-1} and 1730 cm^{-1} (-OH/-COO-).(b) Ratio between primary and secondary hydroxyl groups obtained as the transmittance ratio between 1045 cm^{-1} and 1097 cm^{-1}. (c) Ratio between ester and free carboxylic acid obtained as the transmittance ratio between 1731 cm^{-1} and 1682 cm^{-1}, respectively. (d) PGS density measurements. (e) Water contact angles (WCA) on cured samples, in their dry (black, Latin letters) state and after stabilisation in water (wet, grey, Greek letters). Sample data distributions were analysed through a one-way ANOVA and a post-hoc Games-Howell multiple mean comparison test, with a p-value of 0.05. Matching letters indicate homogeneous groups.

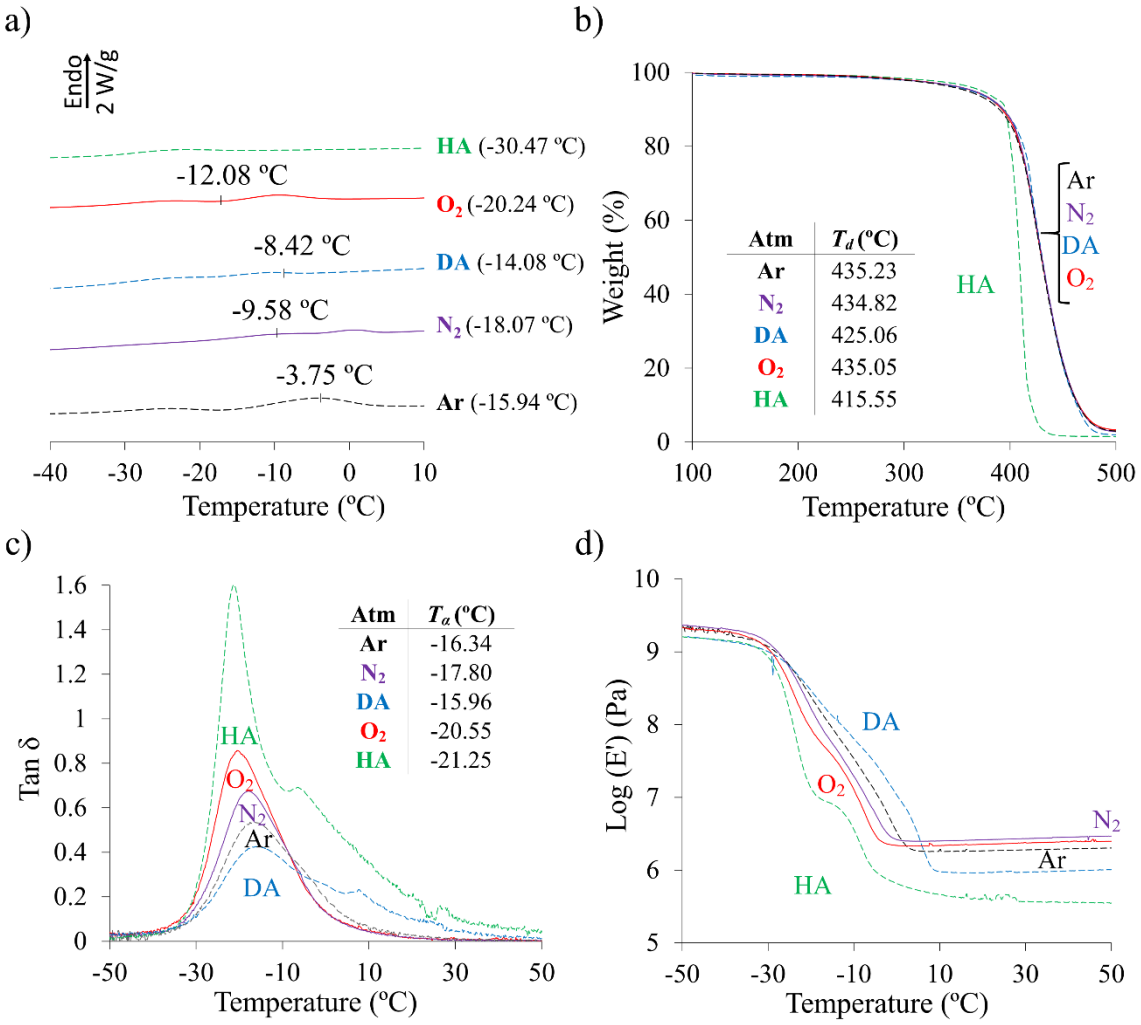

Figure 17. (a) DSC normalised power of PGS networks synthesised under different atmospheres, as a function of temperature. The melting temperatures (T_m) have been located at the maximum of the endothermic melting peak. Glass transition temperatures (T_g) between brackets. (b) TGA thermograms. Insert: inflection point (T_d) of the main degradation stage, obtained from derivative curves. (c) Temperature dependence of loss tangent (*tan δ*) and (d) the storage moduli (E') of PGS networks pre-treated under different atmospheres. The insert in (c) lists the temperature of the maximum values of the main peak in *tan δ* (T_α) characterising the main relaxation process associated to the glass transition of PGS simples. Colours included for the shake of clarity.

The main relaxation appears between -30 ºC and 0 ºC for samples pre-polymerised under inert atmospheres and narrows to show an abrupt drop ending up at -20 ºC for those samples obtained under O_2 and HA. These results are consistent with the observations on the calorimetric profiles.

The temperature at the maximum of the associated peak in *tan δ*, T_α, shifts accordingly to lower temperatures, around -20 ºC. Interestingly, this peak displays a shoulder at higher temperatures, between -5 ºC and 10 ºC, for these samples, not so distinctively showing in the networks obtained under inert atmospheres. This indicates that the mobility of certain segments in these PGS networks is hindered up to these temperatures, probably due to branching that hinders rotations over the main chain bonds and decrease the flexibility of the polymer chain.

Additionally, the rubbery plateau modulus decreases following pre-polymerisations under oxidative and humid atmospheres, which matches the results obtained from the compressive measurements. The compressive elastic moduli, E_1 and E_2, were taken from the stress-strain curves (Figure 18) at their two linear zones: the first slope from 0 to 5 KPa and the second from 70 to 120 KPa, and are listed in Table 4. Aligned with previous findings, the elastic moduli, which is in all cases in the typical range of elastomers, are higher when networks are pre-polymerised under inert atmospheres. N_2. Moreover, Ar seems to promote a linear growing of macromers, with scarce branching, that eventually crosslink while curing to a high degree. O_2 and water vapour in the atmosphere boost reactivity of secondary hydroxyls of Gly to react more readily, leading to more branched and eventually defective networks with lower mechanical properties.

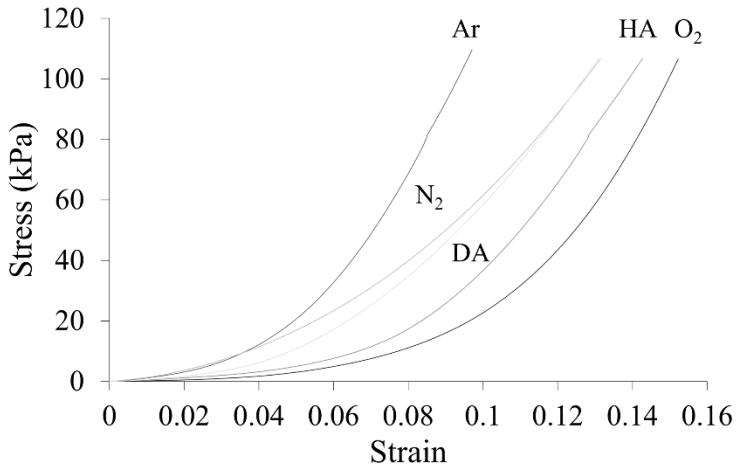

Figure 18. Stress-unitary strain average curves obtained from five compressive replicates of each PGS sample pre-treated under different atmospheres.

Table 4 Young moduli (*E*) evaluated in the two linear regions of the curves.

	E_1 (kPa)	E_2 (kPa)
Ar	380 ± 300	1750 ± 380
N_2	230 ± 80	1580 ± 360
DA	170 ± 100	1920 ± 430
O_2	110 ± 60	2470 ± 490
HA	230 ± 150	1690 ± 130

CONCLUSIONS

It is widely accepted that PGS synthesis by condensation yields mainly linear structures in an early stage, because of the enhanced reactivity of primary hydroxyl groups of glycerol. Indeed, secondary hydroxyl groups appear to remain less reactive until primary -OH have been partially consumed. This work has shown that this can be easily strengthened, if it is of interest, by the synthesis atmosphere, leading to PGS networks with significantly different properties.

Thus, the results here presented reveal that, in the outlining of a PGS network, temperature, time, or the ratio between reactants Gly:SA aren't the only crucial variables to be taken into consideration, as it was previously considered, but also the reacting atmosphere during polymerisation in the liquid state, before gelation.

This so-called pre-polymerisation proceeds at a greater extent if carried out under oxidative atmospheres (DA, O_2 and HA), but in a branched fashion because of the simultaneous formation of oxidised species that boost the reactivity of secondary hydroxyls from Gly. Water vapour contributes to this effect, likely by hindering glycerol evaporation from the reacting mixture. Inert atmospheres, on the other hand (Ar even more than N_2), promote a rather linear growth of macromers, with scarce branching.

The pre-polymers obtained under inert atmospheres are less viscous. Nonetheless, the presence of glycerol and by-products thereof decrease the melting point of pastes obtained under oxidative and humid environments, which can also be an interesting feature when manufacturing PGS-based structures. The increase in viscosity is more gradual in pPGS obtained under inert atmospheres, thus gelation takes longer. The resulting networks are loose elastomers with long chains, overall effectively crosslinked. Conversely, the branched, less-crosslinked networks obtained after curing pre-polymers obtained in the presence of oxygen are less elastic and softer, and their main mechanical relaxation splits, as branching prevents the free rotation of the main chain.

Each of these pre-polymers, having singular properties and yielding different polymer morphologies, could find particular applications as biomaterials, particularly when processed to obtain microporous structures in the tissue engineering field.

CHAPTER 3: Role of curing temperature of poly(glycerol sebacate) substrates on protein cell interaction and early cell adhesion

ABSTRACT

A new, simplified method for preparing model surfaces of PGS coatings is introduced in this study. The development of a novel procedure to obtain very smooth continuous polymeric surfaces from PGS was performed to study the material influence with protein cell interactions. The PGS substrates cured under different temperatures, lead to different chemical properties and topographies determining its fate as a biomaterial. The physicochemical characterization of the surfaces obtained confirms that there are differences in the networks formed by spin-coating when different temperatures are used in the curing stage. Higher synthesis temperatures lead to denser networks with fewer polar groups available on the surface.

Moreover, material-protein interactions were studied and characterised, by using different extracellular matrix proteins such as fibronectin (Fn) and collagen type I (Col I), to reveal the biological behaviour of different PGS substrates. For that, Atomic Force Microscopy (AFM) images and quantification of protein adsorbed in single protein, sequential and competitive incubations were used for this purpose. These protein coating experiments reveal that Fn is adsorbed in form of clusters while Col I form a characteristic fibrillar network. Fn present an inhibitory effect when is firstly incubated under Col I network. Human umbilical endothelial cells (HUVECs) were cultured on PGS surfaces to study the effect of synthesis temperature. To this effect, early focal adhesions (FA) were analysed by immunofluorescence techniques. This highlighted the contrasts between PGS samples showing variations on biological characterisation studies.

Keywords: Poly (glycerol sebacate), focal adhesion, protein adsorption, polymer protein interaction

INTRODUCTION

Biodegradable elastomers are becoming fundamental in the field of materials for medical applications[78–80]. Particularly, poly(glycerol sebacate), PGS, which is an elastomeric hyperbranched polyester named firstly by Wang et al. as a potential biomaterial in 2002, is nowadays one of the most studied polymers [3,81,82]. This is because PGS possesses good biocompatibility and biodegradability together with suitable chemical and mechanical properties [32,61,62,64]. All this together allows PGS usage as a scaffolding material in biomedical and tissue engineering applications, such as drug delivery [27,63] and tissue regeneration of cartilage, nerve, cardiac muscle and bone [13]–[20], among others.

Some of the most common techniques for understanding polymer characterization and polymer-tissue interaction, are chemical and biological polymer functionalisation [83,84]. Proteins such as fibronectin (Fn), collagen, laminin and vitronectin, all of them components of extra cellular matrix (ECM) are commonly used for biological characterization of biomaterials [85]. Each tissue has a specific ECM composition tailored to their specific physiological needs. This specificity is built thanks to the cross talking between several biochemical and biophysical cellular constituents, and its microenvironment. The ECM proteins functions are to provide an adequate attachment structure for tissue morphogenesis, differentiation and homeostasis [86]. Particularly, collagen family comprises 28 different species and have structural function contributing to cell mechanical properties. Collagen type I (Col I) happens to be the utmost of its collagen family representative due to its large presence across several body tissues, specifically, on the endothelial wall of the blood vessels [87,88]. The typical Col I structure has form of fibrils with a diameter around 50 to 200 nm. In order to build this fibrillar structure, many three -stranded Col I molecules packed conjointly are needed. There is a space between their adjacent fibrils of 67 nm, which define a characteristic Col I pattern of bands [89]. Fibronectin on the other hand, is a glycoprotein present in blood, connective tissues, extracellular fluids and as a part of cell surfaces. Fn structure is formed by two subunits of 220 kDa that play a central role in cell adhesion [90,91].

These two proteins, Col I and Fn, are directly related to the adhesive cell interactions with their substrates and local microenvironments, which are fundamental for the understanding of biomaterial-cells interactions [88,92]. The main class of cell adhesion receptor protein is called integrin, which binds to extracellular matrix ligands by providing anchor points for the cytoskeleton organization of the cells, called focal adhesion (FA). Integrins play an important role not only in early adhesion by the formation of FA, but regarding cell migration and its fate, acting as a major fibronectin receptor on most cells and are usually studied for biomaterial characterisation [92–94].

Moreover, it has been proved how Col I and Fn incubated together on polymer surfaces generates a synergic effect leading to better support for endothelialization [95]. The understanding of cell-protein-material signalling behaviour is one of the reasons of this study. This main aim could be achieved

thanks to the development of a PGS coating technique for studying the PGS-protein-cell surface interaction without any other interference.

For doing that, a novel PGS spin coating synthesis technique was performed with different curing temperatures (130 ºC, 150 ºC and 170 ºC) to achieve a thin film that provides no surface external interaction and facilitate the proper PGS substrate interaction with proteins and cells. Thus, the characterization among different PGS synthesis conditions were produced because of its own chemical and mechanical properties instead of its defective and non-homogeneous surface. Chemical and surface characterization were performed onto the PGS substrates, with and without the presence of different combination of Col I and Fn as major representative proteins of ECM. For further PGS surface determination, biocompatibility and protein-cell interaction studies with human umbilical endothelial cells (HUVECs) were performed. Immunofluorescence techniques highlighted the effect of different PGS curing temperature on HUVECs early FA.

MATERIALS AND METHODS

Materials

A stoichiometric amount of sebacic acid and glycerol (3:2) (99%, Sigma-Aldrich) was placed in a sealed reactor under a constant flow of N_2 atmosphere, which allows water and evaporated glycerol to recirculate avoiding glycerol loss during its polycondensation reaction. Thus, the prepolymerization reaction took place at 130 ºC for 24h under constant stirring to get the PGS pre-polymer (pPGS). Subsequently, thin PGS films on a scale of just a few nanometers thick were obtained by spin coating (WS-650MZ-23, Laurell Technologies). A 0.01% w/v solution of pPGS in ethanol (Ethyl alcohol, pure, Sigma-Aldrich) was poured onto 12 mm diameter glass coverslips and then accelerated for 30 seconds at 10000 rpm under N_2 in the spin-coater equipment. For the complete reaction of pPGS wax like paste into a fully cured PGS polymeric film, three different curing temperatures were applied for 48h in an oven (130 ºC, 150 ºC and 170 ºC). After cooling down to eliminate unreacted monomers and impurities, the three sets of PGS substrates were three times washed in a diluted ethanol/water solution (5% v/v) and next dried overnight under vacuum conditions at room temperature.

Fourier-Transform Infrared Spectroscopy

Fourier-Transform Infrared Spectroscopy (FTIR) spectra of PGS substrates cured at different temperatures were collected by using a Platinum ATR from ALPHA II spectrometer under an attenuated total reflection mode (ATR). To obtain the different spectra the parameters used were: 24 scans at 4 cm^{-1} resolution, between 600 and 4000 cm^{-1}.

Wettability and surface tension tests

Wettability of PGS substrates once cured was determined by water contact angle (WCA) measurements. Data were collected in sessile drop mode by a Dataphysics OCA25 Instruments GmbH, from 3 µl Ultra-pure MilliQ water drops and at least ten measurements per type of elastomer.

PGS substrates surface energy (σ_{Total}) were calculated following Owens, Wendt, Rabel and Kaelble model [96] and Young equations. In this model, two surface energy components, polar (σ_p), and dispersive (σ_d), determine the intermolecular surface interactions. To obtain the, five different solvents (diethylenglycol, ethanol, diiodomethane, glycerol and formamide (Sigma-Aldrich)) together with the previous values of water angles (WCA), were used repeating the procedure explained above.

Substrate adsorption and protein quantification

Series of PGS samples cured at different temperatures were UV sterilised for 15 min each side prior to adsorption. Solutions of fibronectin from human plasma (Fn; Sigma-Aldrich, Spain) and/or Collagen type I (Col I; PureCol® Type I Collagen Solution, 3 mg/ml (Bovine), Advanced BioMatrix) in Phosphate Buffered Saline (PBS; Sigma-Aldrich, Spain) were adsorbed on the PGS substrates. A total of 100 µL of protein solution was added for an incubation period of 10 min onto each substrate and next the remnant was collected for further analysis. After

the protein incubation, the disks were washed twice with PBS and next dried under argon gas flow. Different protein concentrations were considered: 400 µg/mL, 80 µg/mL, and 40 µg/mL for Col I, and 100 µg/mL, 20 µg/mL, and 10 µg/mL for Fn. In order to analyse the effect of different protein combination onto the substrates, sequential and competition of both proteins were performed. For sequential protein adsorption study, Fn and Col I were incubated: Fn 100 µg/mL first and then Col I 80 µg/mL (Fn/Col I) and in the opposite way, Col I 400 µg/mL and then Fn 20 µg/mL (Col I/Fn).The protein concentrations were chosen in this way to create a firstly saturated protein adsorbed layer, so it can be observed the effect of protein-material affinity and try to observe the protein-protein interaction taking into account Vroman effect. Furthermore, proteins were mixed at different volumetric proportions (Fn 10 µg/mL:Col I 40 µg/mL, 75:25, 50:50 and 25:75) for protein competition analysis, and then incubated onto the PGS substrates. The amount of total protein adsorbed was quantified by means of the bicinchoninic acid method using the Micro BCA™ Protein Assay Kit (Thermo Scientific™, Spain) and bovine serum albumin (BSA) as the standard provided by the same kit. Glass coverslip was used as a control and 4 replicas of each protein condition were performed for each substrate.

Atomic Force Microscopy

An atomic force microscope (AFM) (Bruker Multimode 8 model) operating in tapping mode was used for evaluating the topography and composition of PGS substrates. A Bruker RFESPA model silicon tip was used with resonant frequency of 75 kHz, constant spring of 3 N/m, and a linear speed set at 2 µm/s. The oscillation-free amplitude of 700 mV was applied by modifying the drive amplitude. A ratio between the amplitude set-point and the free amplitude of 0.85 was kept. Images of 5x5 μm^2, 2x2 μm^2, 1x1 μm^2 and 500x500 nm^2 were taken for PGS substrates and the non-treated glass coverslip with and without protein coatings. For AFM image analysis the NanoScope Analysis v1.50 (Bruker) software was used.

Cell culture

Human umbilical vein endothelial cells (HUVECs, Cellworks) were cultured in endothelial cell medium (Innoprot) supplemented as recommended by its supplier specifications and maintained in an incubator at 37 ºC and 5% of CO_2. Cell culture medium was replaced every 2 days until reaching confluence and passaging of the cells was required. Cells with passage below 10 were used for all experiments.

HUVECs were plated at a density of 4000 cells·cm^{-2} on both coated and non-coated PGS substrates cured at different temperatures, and glass coverslip as controls. For cell adhesion experiments, HUVECs were placed for 3 h in endothelial cell medium in absence of serum and then fixed in 4% paraformaldehyde (Panreac) for 20 min at room temperature (RT). After fixation samples were rinsed with PBS and stored at 4 ºC.

Fluorescence staining and imaging

Fixed HUVECs were first permeabilized with DPBS and 0.5% Triton X-100 (Sigma Aldrich) at RT for 5 min. Samples were blocked using DPBS and 2% BSA (Sigma-Aldrich) for 2 h at room temperature (RT) and next incubated with monoclonal antivinculin, clone hVIN-1 (1:400, Sigma Aldrich) as first antibody for 2 h at RT. After three rinses in DPBS and 0.1% Triton X-100, samples were incubated for 1 h at RT with secondary antibody Alexa Fluor 555 Goat anti-Mouse IgG (1:700, Thermo fisher) and Alexa Fluor™ 488 Phalloidin (1:100, Thermo fisher). Finally, after washing twice with DPBS and 0.1% Triton X-100, samples were mounted with Vectashield with 4',6-diamidino-2-phenylindole dihydrochloride (DAPI, Vector Laboratories) and fluorescence images were taken in a Nikon Eclipse 80i microscope.

Cell viability assay

AlamarBlue™ viability assays (Thermo Fisher Scientific) were performed after 1, 3, 5 and 7 days of HUVEC culture onto the non-coated PGS substrates and glass cover slides, to verify its good biocompatibility. Four replicates per sample type were used. Shortly, 20 µL of endothelial cell medium was withdrawn from each sample well and then replaced by AlamarBlue reagent and incubated for 3 h at 37 ºC. Supernatants were placed in a 96 well plate for reading its absorbance signal at wavelengths of 570 and 600 nm. Cell death control was needed, and for that, a 10% of dimethyl sulfoxide (DMSO, Sigma Aldrich) was added to four glass cover slides cultured as previously described. Acellular glass cover slides were used as blank reagent solution for the subtraction of background absorbance.

Data analysis

Image analysis for HUVEC focal adhesion (FA) was performed using the software ImageJ (NIH, Springfield, VA) Trainable Weka Segmentation plugin to obtain a binary mask. By using the same software from the binary masks, FA size, and cell surface area from cytoskeleton images were quantified and analysed. A minimum of ten pictures were analysed, with at least one cell per image, and means and standard deviations were calculated. GraphPad Prism8 software was used for statistical analysis. Either unpaired two-tailed t-test or one-way ANOVA with Tukey post-hoc test were performed where applicable.

RESULTS AND DISCUSSION

Effect of the curing temperature on the chemical and surface properties of PGS films

In other to characterise the presence of PGS onto the circular glass cover slips and confirm the full evaporation of the solvent, FTIR techniques were carried out. The FTIR spectra for each of the PGS curing conditions and glass coverslips as a control are represented in Figure 19. The spectra show a broad band around 3460 cm^{-1} from hydroxyl groups (O-H elongation) together with the aliphatic backbone of C-H absorption, which is located at 2850-2950 cm^{-1} (Figure 19b left). The characteristic peak of the ester carbonyl ($-COO^-$) resulting from the polycondensation reaction among hydroxyl groups and free carboxyl groups of glycerol and sebacic acid, respectively, is located at 1740 cm^{-1} (Figure 19b right). Figure 19c presents the ratio of free hydroxyl groups and reacted carbonyl ester groups, showing a downward trend when a higher curing temperature was applied. None of the previous characteristic peaks are present in the spectrum of neat glass, as expected.

All this together confirms the presence of PGS cured under the three temperature curing conditions (130 ºC, 150 ºC and 170 ºC). The higher the curing temperature, the more the reactivity of PGS monomers and the more crosslinked elastomer was achieved, as exposed in Figure 19c. These results are in accordance with literature for PGS non spin-coated films [2,6].

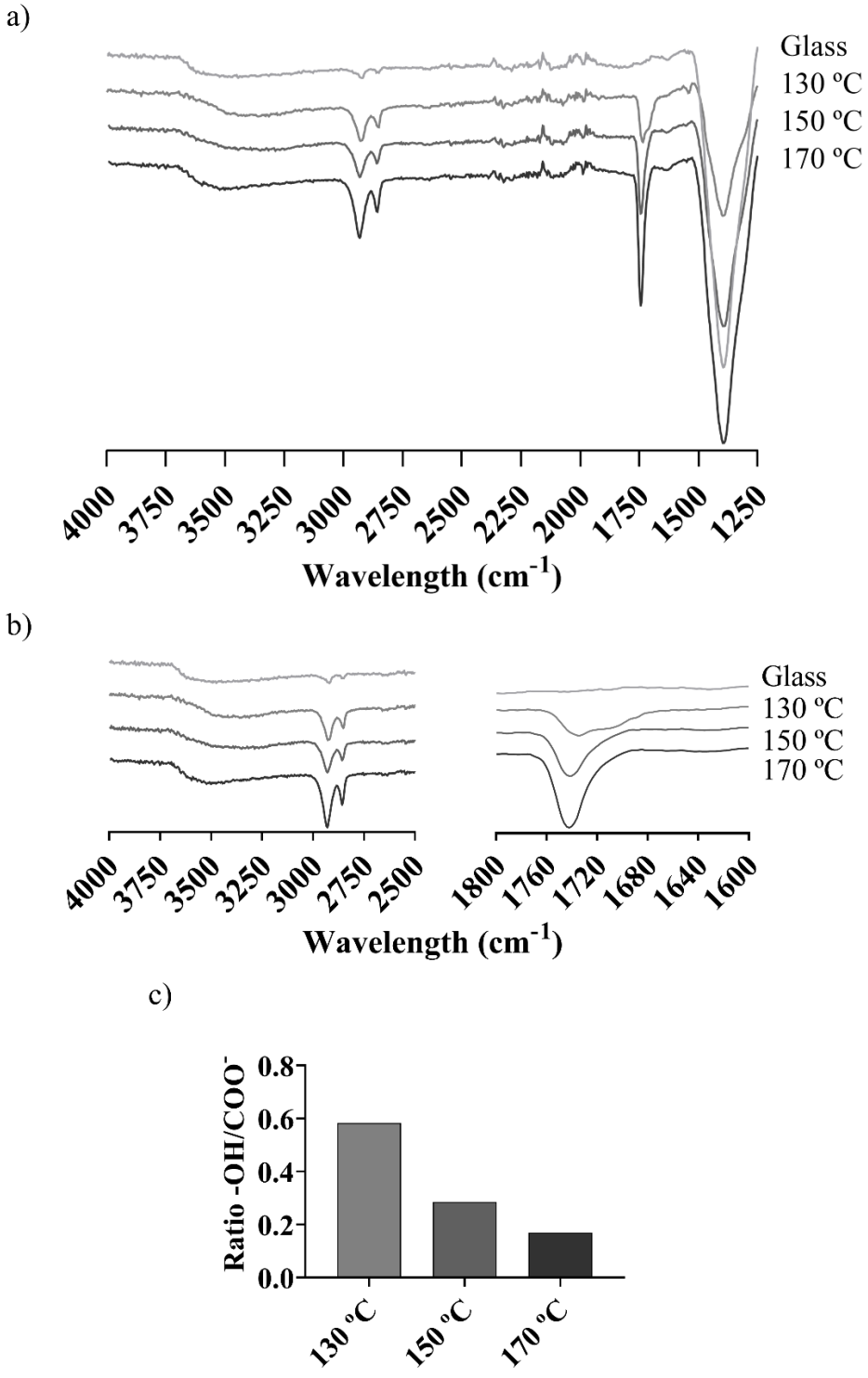

Figure 19. FTIR general spectra (transmittance) of PGS coatings obtained at different cured temperatures (130 ºC, 150 ºC and 170 ºC) and glass cover slides. (b) Detailed FTIR spectra at the PGS characteristic chemical peaks wavelengths: 1600-1800 cm^{-1} for COO^- peak on the right and 2500-4000 cm^{-1} for free ^-OH groups and $-CH_2$ bonding on the left. (c)-OH/COO^- ratio obtained from transmittances at 3350 cm^{-1} and 2927 cm^{-1}

There is a generalized trend about how hydrophobic surfaces adsorb a greater amount of proteins in coating experiments [97]. To confirm this hypothesis, the characterisation of PGS substrates was necessary. Therefore, Table 5 compiles the WCA and surface tensions (σ_{total}) of the three sets of substrates, the latter split into their two components, polar (σ_p) and dispersive (σ_d) together with their

surface polarity (σ_p/σ_{total}). WCA values of PGS substrates are higher than the ones from glass coverslips, as expected from a relatively hydrophobic polymer [6]. The polar component of the polymeric films is significantly lower than the polymer-free coverslip. This is indicative of how glass have a more hydrophilic surface behaviour when compared with PGS substrates. It can also be observed that the surface tension of PGS 150 ºC and 170 ºC, are slightly higher than that of PGS 130 ºC, due to an increase in the dispersive component and a slightly increase in the polar component in the case of PGS 170 ºC, while the polar component of PGS 150 ºC decreases (Table 5). In any case, these results from polymer structures cured under different temperatures present slightly different WCA and surface energy values. Anyway, differences in WCA values are only significant, with a p value below 0.0001, when you compare Glass with the rest of the PGS substrates.

Table 5 Surface energy components and WCAs of glass and PGS samples cured at different temperatures, calculated from contact angle data and using the OWRKs equation.

Material	σ_d (mN/m)	σ_p (mN/m)	σ_{total} (mN/m)	WCA (º)	σ_p/σ_{total}
Glass	16.43	34.03	50.47	45.30 ± 4.82	0.67
130 ºC	14.48	18.48	32.96	71.16 ± 1.43	0.56
150 ºC	17.72	18.08	35.80	68.07 ± 3.94	0.51
170 ºC	15.50	19.84	35.34	67.46 ± 3.94	0.56

Characterization and quantification of poly (glycerol sebacate) protein adsorption.

Figure 20a shows the AFM images obtained after protein coating experiments with sequential coating and monoproteins, in order to determine the effect of PGS substrates cured at different temperatures. Protein adsorption quantification was performed thanks to the colorimetry test microBCA (Figure 20b).

Results from AFM Col I protein coating (Figure 20a, Col I column) throw a fibre diameter of 20 ± 5 nm for each of the substrates, which act as a building block of an homogeneous compact network generated from Col I protein-protein interactions. This behaviour results particularly outstanding with PGS samples cured at high temperatures (Figure 20b).

There is no significant difference derived from Fn adsorption AFM results, where protein conformation remains globular throughout all the PGS surfaces tested (Figure 20a Fn column). Protein quantification does not reveal major differences in Fn adsorption, where similar Fn protein outputs were obtained for all PGS samples and glass coverslips.

AFM images from sequential coating highlighted the influence of the order of protein deposition. On the one hand, when Fn is the first layer of protein coating, the second layer of Col I is not able to form its typical fibrillar structures that are formed when Col I is adsorbed in a single step. This may be because the Col I-

Col I shift to Col I-Fn interactions, with Fn already adsorbed onto the surface [95]. And then there is not enough amount of Col I for the formation of its single protein network. This behaviour is alike no matter the temperature set to cure the PGS substrates (Figure 20a column Fn/Col I). In line with the above, Figure 20b shows that Fn/Col I proteins adsorbed on the material surface is negligible when compared with the rest of the protein coating scenarios.

On the contrary, when Col I is the first protein layer which is adsorbed by PGS material substrate, Col I fibrillar network is formed and remains stable after Fn (Figure 20a Col I/Fn column). The amount of protein adsorbed is similar to the values obtained when Col I is using as a single protein coating in all substrates. In the case of higher temperatures (150 ºC and 170 ºC), PGS substrates appear to influence the Fn coating which seems to partially desorb the Col I adsorbed in the first stage. This effect would be because of a partial desorption of Col I, by forming soluble Fn-Col I structures instead of PGS-Col I. Fn-Col I protein interaction effect produces an additive absorption between Col I fibrillar structure and Fn because of its protein molecular size, which make Fn fits between the Col I protein interspaces. However, Col I is not able to adsorb in the empty spaces left between Fn proteins, leading to a mix between single protein adsorption and layer by layer coating [98,99].

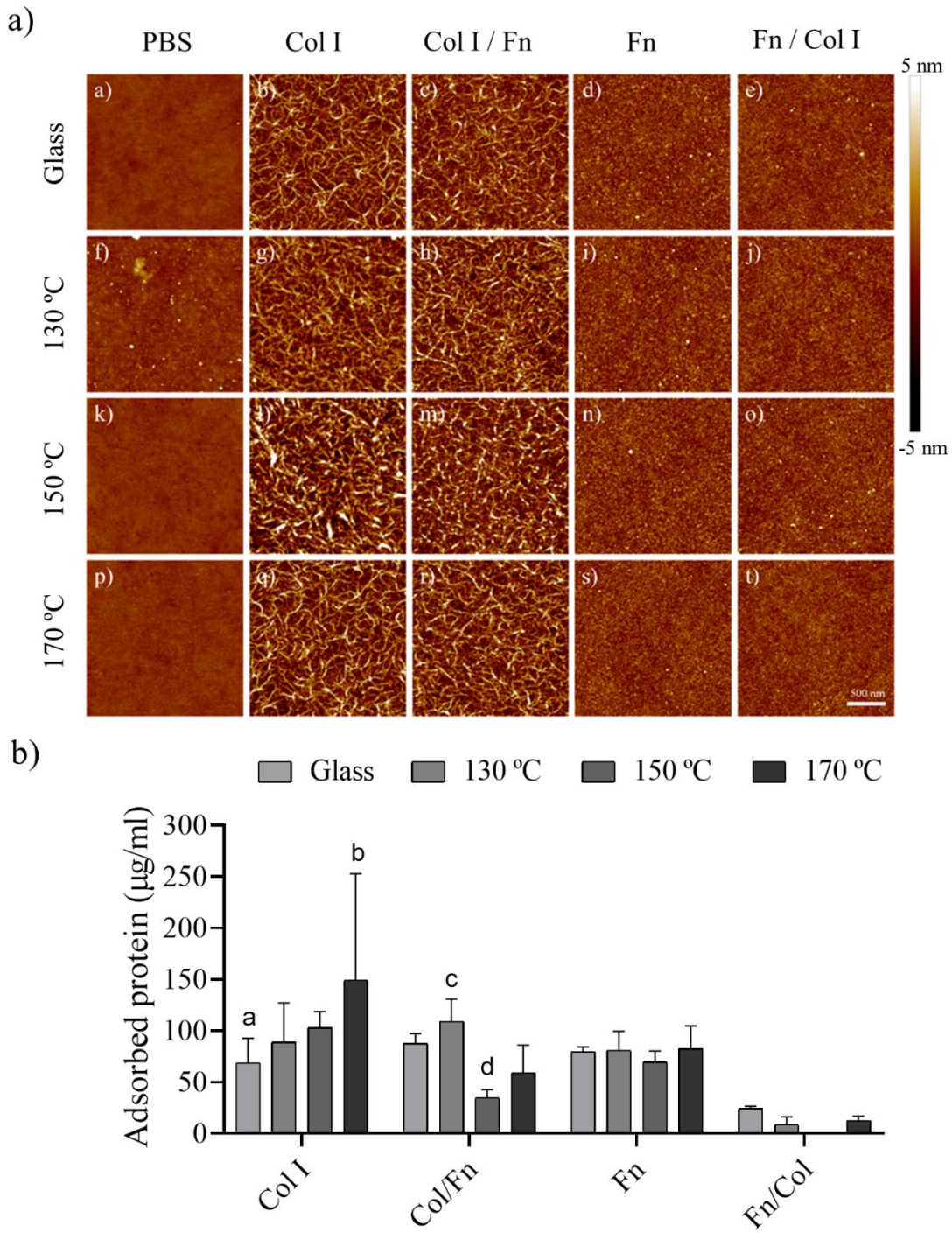

Figure 20. (a) AFM height images of 2x2 µm^2 and (b) protein adsorption quantification (mean and SD) from microBCA colorimetric technique with single protein (Fn 100 µg/ml or Col I 400 µg/ml) and sequential adsorption assays of Fn and Col I (Fn 100 µg/ml+ Col I 80 µg/ml), and vice versa (Col I 400 µg/ml + Fn 20 µg/ml) on PGS cured at different temperatures. The first column in (a) shows as a reference the PGS substrates before protein adsorption. All images share the 500 nm scale bar. Glass covers without spin-coated PGS are shown in (b) as control. Sample data distributions were analysed through two-way ANOVA and a Bonferroni post hoc multiple mean comparison test, with a p-value of 0.01.

Different volumetric proportions of Col I and Fn were incubated onto PGS substrates and glass to study the effect of protein competition. The chosen concentrations were Col I at 40 μg/ml and Fn at 10 μg/ml at 75:25, 50:50 and 25:75 of Col I:Fn with concentrations of 32.5 μg/ml, 25 μg/ml and 17.5 μg/ml respectively. These concentrations were selected to have equal concentration of binding sites and similar surface coverage efficiency according to each protein supplier recommendations. AFM images after adsorption assays are represented in Figure 21a together with their corresponding protein quantification in Figure 21b.

Protein quantification results show how PGS substrates present different values of protein adsorption once 25:75 and 50:50 dilutions were incubated (values around 50 μg/ml and 30 μg/ml respectively), but no significant differences were appreciated between substrates (Figure 21b).

If 75:25 protein dilution is incubated onto the substrates, not enough amount of protein is adsorbed to be measured by the colorimetric technique used. This is because Col I fibres are no longer formed because of the interaction with Fn within the dilution and onto the surface of the material. Thus, proteins lead to Fn-Col I interaction instead of Col I-Col I avoiding its adsorption throughout the surface of each material [99].

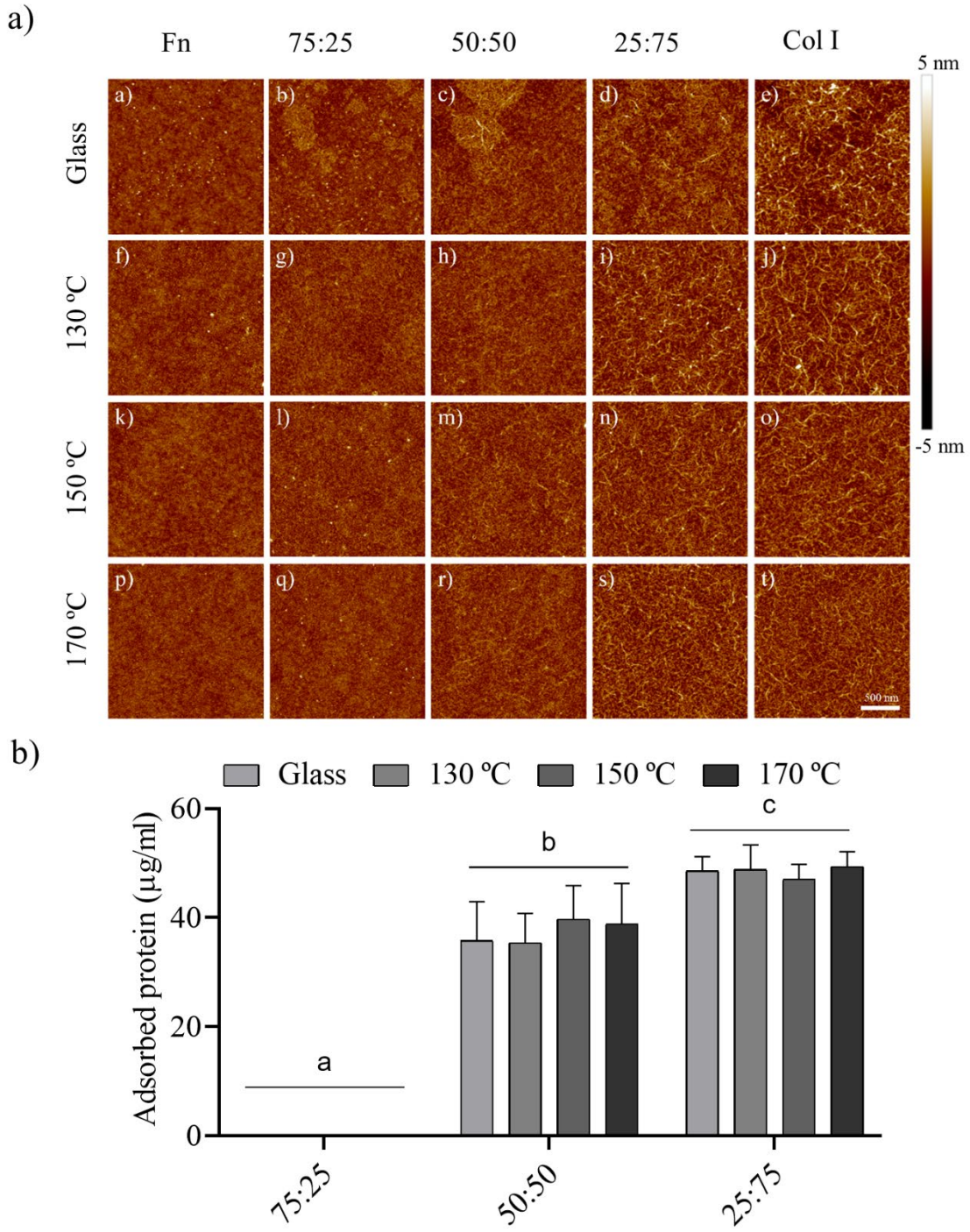

Figure 21. (a) AFM height images of 2x2 µm^2 and (b) protein adsorption quantification (mean and SD) from microBCA colorimetric experiments after competition adsorption assays with Fn and Col I on glass and PGS cured at different temperatures. The indicated percentages of intermediate protein mixtures are volumetric ratios of Fn 10 µg/ml over Col I 40 µg/ml. All images share the scale bar of 500 nm. Sample data distributions were analysed through a two-way ANOVA and Bonferroni post hoc multiple mean comparison test, with a p-value<0.05 (all letters (a, b, c, d, e, f, g and h mean significant differences: p< 0,0001). Matching letters indicate homogeneous groups.

Effect of PGS with HUVECs culture on early cell adhesion

Before investigating the role of PGS-proteins-HUVECs early adhesion and their different substrate effect on FA formation, viability experiments of free protein PGS substrates, cured at different temperatures, were performed. For that, HUVECs were cultured for 7 days onto the polymer substrates and then analysed by means of AlamarBlue™ colorimetry assays (Figure 22). PGS samples presented good biocompatibility, as happen with glass coverslips, with no significant differences between them. This effect could be thanks to PGS biocompatibility reported by literature [3,32], although in this case spin-coated samples are being used, which due to their manufacture, may not correspond in their morphology (crosslinks) or physical state (less crystallinity, for example) with the equivalent films (cured at the same temperature) [6].

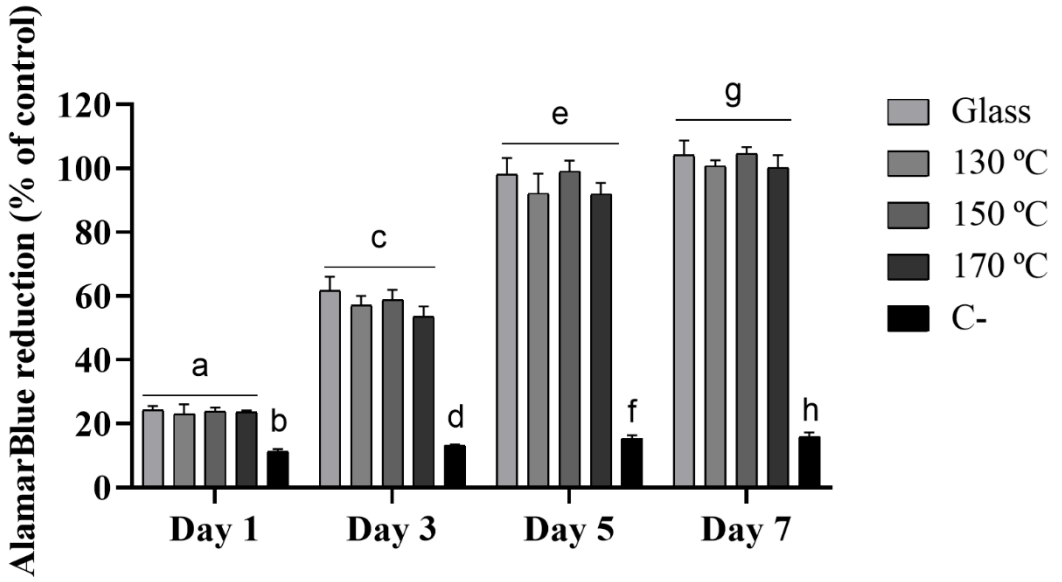

Figure 22. HUVECs viability results from AlamarBlue™ colorimetric technique. Glass was used as a control of good cell viability, and a 10% DMSO solution was added acting as cytotoxic control (C-). Sample data distributions were analysed through a two-way ANOVA and Bonferroni post hoc multiple mean comparison test, with a p-value<0.05 (all letters (a, b, c, d, e, f, g and h mean significant differences: p< 0,0001). Matching letters indicate homogeneous groups.

After viability assays, to investigate the role of different PGS temperatures of curing on HUVECs early adhesion and their effects on FA formation, immunofluorescence quantification was performed onto the same protein free PGS substrates. From Figure 23a can be determined how HUVECs FA expression is mostly exhibited in cytoskeleton periphery and nucleus. The number of FAs increases with curing temperature (Figure 23b). This temperature-dependent trend is also observed with FA percentage of cell area (cytoskeleton surface) (c) and (d) relative area of FA compared to the total cell area, by actin quantification. While PGS 170 ºC does not correlate with the previously exposed with relative FA area of 4.4 % similar to PGS 130 ºC with 4.7%. It also presents a significantly smaller average FA size values of 1.7 μm^2 in contrast with the 4.55 μm^2 of PGS 150ºC. All this together, highlight 150 ºC as the temperature yielding the most remarkable FA results.

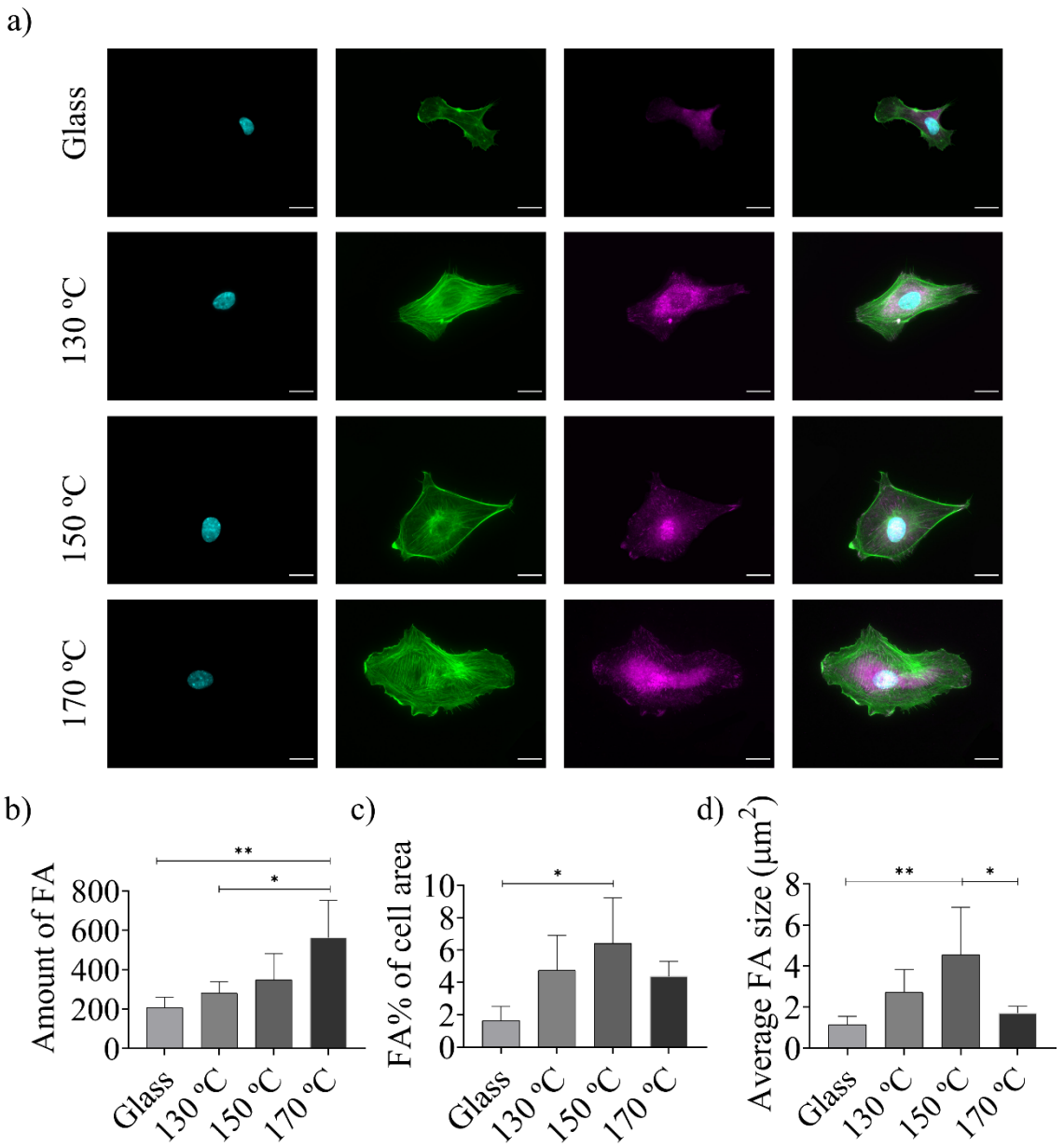

Figure 23. (a) Immunofluorescence images of HUVEC nuclei (Cyan), actin cytoskeleton (green), and vinculin (magenta) as a focal adhesion (FA) marker cultured on Glass and different PGS cured materials. Quantification of the size, (b) amount and (c) areas and (d) size of FA. FA area was calculated as the percentage of the total cell area. All immunofluorescence images share its scale bar (20 µm). Sample data distributions were analysed through a one-way ANOVA and Bonferroni post hoc multiple mean comparison test, with a p-value<0.05. *p<0.05 and **p<0.01.

Effect of Col I and Fn sequential and competitive adsorption on HUVECs focal adhesion

To investigate the role of PGS-proteins-HUVECs early adhesion and their different substrate effect on FA formation immunofluorescence quantification was done as exposed in Figure 24. All PGS conditions have better FA results if compared with Glass. Particularly. when Fn and Fn/Col I are incubated onto the PGS samples, FA parameters increase with PGS curing temperature. Since in Figure 20, Fn and Fn/Col I present homogeneous single amount of protein and none significant protein adsorption values respectively, this effect is produced because of the PGS substrate cured at different temperature conditions (PGS

condition in Figure 24). Thus, the results obtained with Fn/Col I condition coincides with the Fn and Col I protein interaction where Fn competes with Col I-Col I linkage avoiding its fibrillar structure to be formed [99].

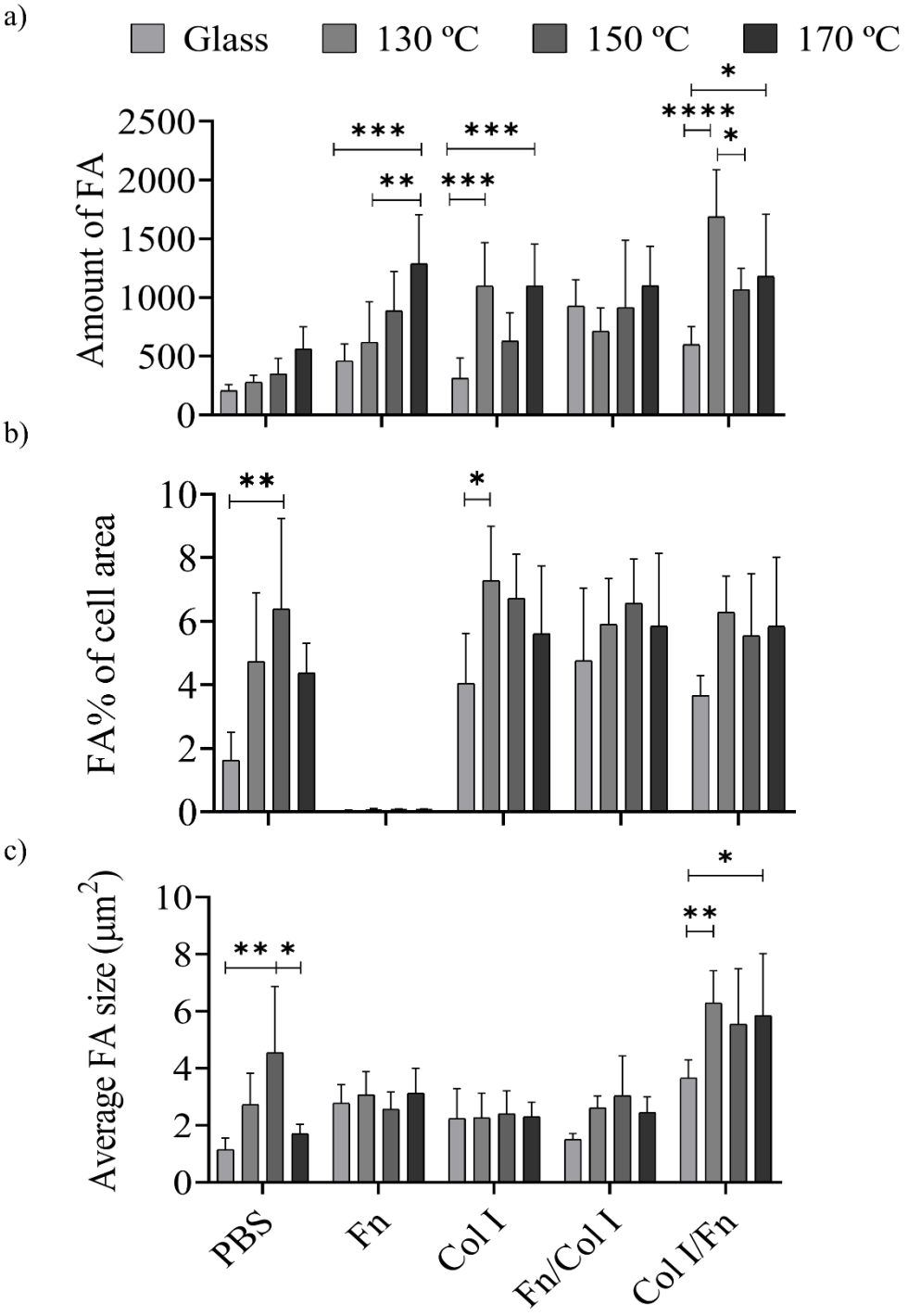

Figure 24. HUVECs fluorescence quantification of (a) number of FA, (b) relative surface of FA compared to the total cell area and (c) average size of FA, from protein sequencing adsorption assays on glass and PGS cured at different temperatures. FA area was calculated as a relation with the total cell area in percentage (%).Sample data distributions were analysed through a two-way ANOVA and Bonferroni post hoc multiple mean comparison test, with a p-value<0.05. *p<0.05, **p<0.01, ***p<0.001 and ****p<0.0001.

In concordance with Col I quantification (Figure 20) where more Col I is adsorbed if curing temperature increases, the amount of FA and the FA% of cell area (Figure 24a and b) become higher than glass substrates. This is because of the synergic effect of PGS substrates and the Col I adsorption onto the surface which produces better cell-material interactions.

Furthermore, Col I/Fn produces a join effect, particularly with 130 ºC condition, where cell response increases its FA. When Col I is incubated before Fn, Fn is able to fit the free spaces between Col I-Col I fibres by bonding the PGS substrate and generating Col I-Fn interactions, which may increase the amount of binding sites for cell adhesion.

The influence of PGS substrates cured under different temperatures onto competitive incubation of Fn and Col I proteins (Fn 10 μg/ml and Col I 40 μg/ml) can be determined from immunofluorescence FA quantification (Figure 25). Each of the PGS substrates coated with Fn:Col I mixtures dilutions present significant and better FA outcomes if compared with Glass. All PGS substrates incubated with protein mixture dilutions, present an increasing trend with the amount of FA and its relative cell surface. Particularly 150 ºC material condition has significantly more amount of FA on 75:25 dilution, although no protein was able to be detected by the colorimetric techniques used (Figure 21). Thanks to AFM images,75:25 dilution proteins are clearly present onto the polymer surfaces. In this case, the increase on the amount of FA is produced because of the low-density protein coating, which allows cells to interact with the PGS substrate which promotes cell adhesion as well. Furthermore, 25:75 dilution, with more content of Col I, present an increasing significant trend of FA number, directly related to the increase of PGS curing temperature. The protein quantification values together with AFM images from Figure 21 show the same amount of protein adsorbed. All this together indicates that significant FA increment effect is produced since HUVECs interact, not only with the proteins adsorbed, but with PGS substrate material by producing a rising synergic effect with curing temperature.

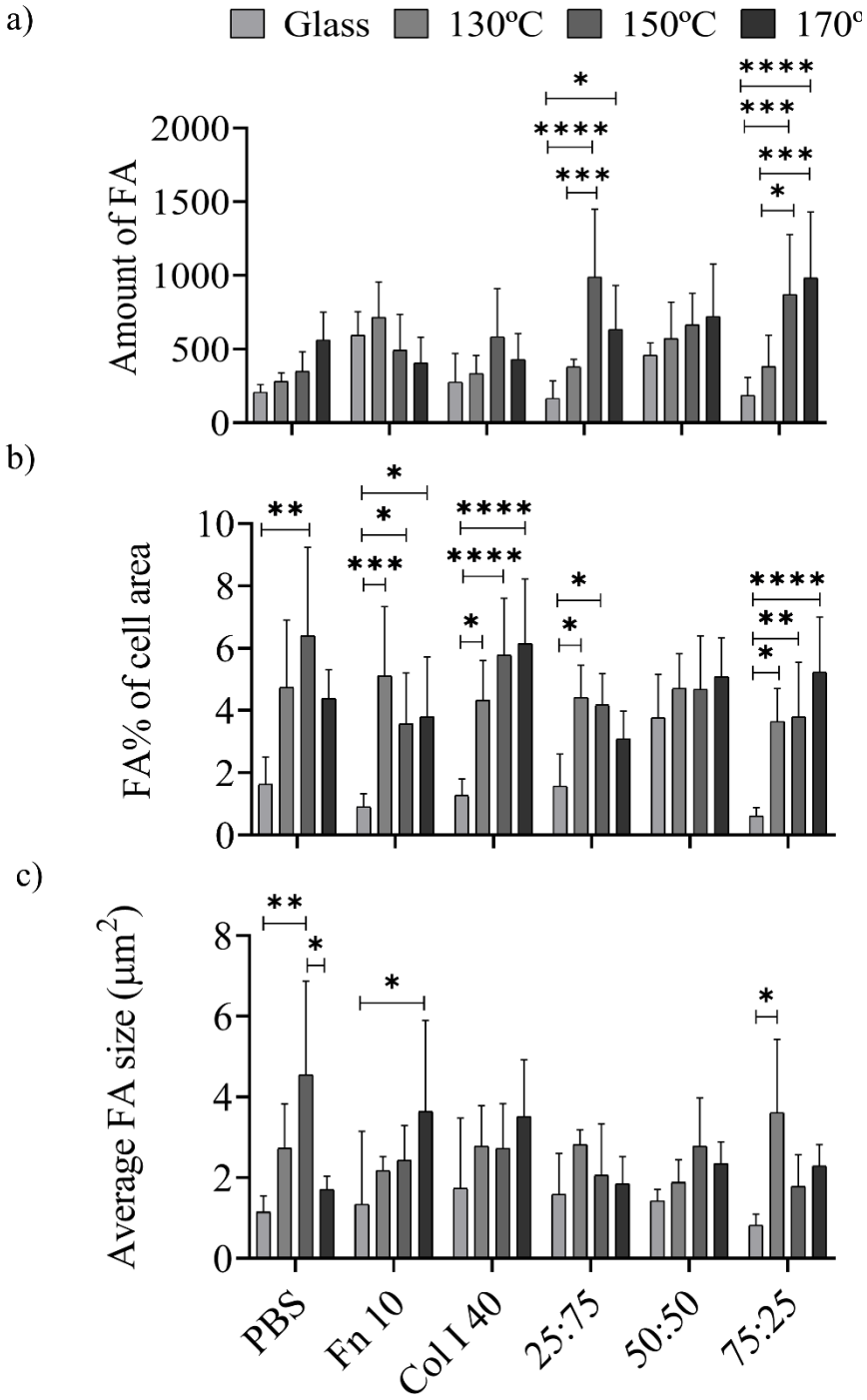

Figure 25. HUVECs fluorescence quantification of (a) number of FA, (b) relative surface of FA compared to the total cell area and (c) average size of FA, from competition adsorption assays of Fn and Col I from low concentrated solutions on glass and PGS cured at different temperatures. FA area was calculated as a relation with the total cell area in percentage (%).Sample data distributions were analysed through a two-way ANOVA and Bonferroni post hoc multiple mean comparison test, with a p-value<0.05. *p<0,05, **p<0.01, ***p<0.001 and ****p<0.0001.

CONCLUSIONS

A novel PGS synthesis technique was developed and optimized by performing polymer coatings at a nanometric scale to reveal the different PGS properties. PGS coatings were cured under different temperature conditions (130 ºC, 150 ºC and 170 ºC) and next were chemically and biologically characterized. The FTIR spectra present a direct correlation between PGS curing temperature and its reaction kinetics. When higher temperatures were applied during PGS second synthesis step, more polycondensation is produced. WCA present a non-significant common behaviour on its values, while curing temperature raises, its value becomes slightly smaller. As happened with WCA values, σ_{total} of 150 ºC and 170 ºC have similar values while PGS 130 ºC σ_{total} decreases because of its lesser σ_d component.

AFM together with microBCA results, reveal protein material interactions and the amount of protein adsorbed by each surface. PGS substrates single protein adsorption present no major differences on the amount of Fn adsorbed, which displays cluster protein distribution. In the case of Col I, higher curing temperatures of PGS substrates, increase its protein adsorption. This favoured Col I-Col I interactions generating a homogeneous fibrillar Col I network. On the contrary, sequential adsorption of proteins reveal that Col I is not able to be absorbed if Fn the first layer applied due to its Fn-Col I interactions that form soluble complexes. If Col I is the main coating layer, particularly with 130 ºC condition, Fn interact with Col I thanks to Fn smaller size, which fit through the empty spaces within the network of Col I already formed. This scenario shows heterogeneous values distribution of protein adsorption among different PGS samples. Different PGS samples incubated with competition of proteins mixed in different volumetric proportions present no significant differences. When Col I dilution content increases, the total protein adsorption value becomes higher because of the inhibitory effect of Fn when incubated together with Col I and the major PGS substrates Col I affinity.

As regards PGS substrates-HUVECs biological characterisation, non-cytotoxicity results during 1, 3, 5 and 7 days by using the colorimetric AlamarBlue™ were observed. Immunofluorescence results reveal differences among PGS material regarding the presence of the total amount of FA, quantified by vinculin fluorescence expression. When PGS synthesis temperature increases, the number of HUVECs FA improves too. Once the protein coatings were applied, every PGS condition present better cell response when compared with glass. Col I/Fn present a synergic effect which increased cell FA values, particularly with 130 ºC. When dilutions of mixture protein were incubated, specifically, 25:75 dilution with more content of Col I, present an increasing significant trend of FA number, directly related to the increase of PGS curing temperature.

GENERAL DISCUSSION

The scope of this thesis was the determination of PGS material morphology and properties: on the hand the determination of PGS synthesis mechanism, and on the other hand the characterization of PGS final network properties after modifying its synthesis parameters (temperature and atmospheric conditions). Other groups had studied PGS synthesis and its different biomedical applications based on its properties [4–6,9]. Though none of them had stablished yet the exact impact of some of the early stages of PGS synthesis and the effect of parameters such as different atmospheric conditions as we propose in this thesis work.

The study of different PGS synthesis scenarios for the understanding of mPGS hydroxyl reactivity through prepolymerization time were performed, as exposed in **Chapter 1**. From other groups studies and after performing TGA mass loss analysis, it was clarified how the loss of water and the effect of Gly loss alters, in an uncontrolled manner the pPGS synthesis. To help prevent the loss of water subproduct and Gly in order to control and monitor the mPGS prepolymerization and obtain reproducible and scalable results, the reactor system was adapted (Scheme 1). After that, mixtures of three alcohols (PPD, PPG and Gly) were prepolymerized together with SA during 24h under N_2 atmosphere at 130 ºC. Subsequent to its sample characterization from 0h to 24h, the polycondensation mechanism by hydroxyl reaction were reveal. The chemical hydroxyl distribution, and final prepolymer bonding structure (from FTIR and ^{1}H-NMR results), define how the reaction tends the polycondensation of pOH rather than sOH, leading to a linear and less crosslinked polyester during its early stages (first 4h). DSC characterization illustrated a melting window from 0h to 24h with its T_m values at 118 ºC to 10 ºC. The evolution to sharper and more defined melting peaks defined how the branching degree of the prepolymer structure raised, which is directly related to its amorphous state increment for the shake of crystalline distribution [6,59]. The DE determined by FTIR, titration and ^{1}H-NMR presented a similar trend with values around 40% for both, titration and ^{1}H-NMR quantification after 4h reaction when most of the polycondensation reaction took place establishing the polyester backbone structure. GPC results indicated how the prepolymer is prone to growth as an HBP once its linear reactivity through primary hydroxyl groups is reduced (after 4h). After this time, the prepolymerization tends to create more branching chemical structures which may lead to a more crosslinked polymer.

Once the chemical characterization of the early stages of the prepolymerization was conducted, the study of different atmospheric conditions applied during pPGS and PGS synthesis were performed (**chapter 2**). Oxidative atmospheres (DA, O_2 and HA) induced to the simultaneous formation of oxidised species that boosted the reactivity of secondary hydroxyls from Gly. Water vapour contributes to this effect, likely by hindering glycerol evaporation from the reacting mixture. Inert atmospheres, on the other hand (Ar even more than N_2), promoted a rather linear growth of macromers, with scarce branching.

The pre-polymers obtained under inert atmospheres were less viscous. Nonetheless, DSC results highlighted how the presence of glycerol and by-

products decreased the melting point of pPGS mixtures obtained under oxidative and humid environments. The increase in viscosity was more gradual in pPGS obtained under inert atmospheres, thus gelation took longer. The resulting networks were loose elastomers with long chains, overall, effectively crosslinked. Conversely, the branched, less-crosslinked networks obtained after curing pre-polymers obtained in the presence of oxygen were less elastic and softer, and their main mechanical relaxation split, as branching prevents the free rotation of the main chain.

Each of these pre-polymers, having singular properties and yielding different polymer morphologies, could find applications as biomaterials.

To conclude, PGS coatings at a nanometric scale, to reveal the different polymer properties when cured under different temperature conditions (130 ºC, 150 ºC and 170 ºC) were synthetized as exposed in **chapter 3**. Its chemical characterization revealed how when higher temperatures were applied during PGS second synthesis step, more polycondensation is produced, as expected [5,6]. WCA presented a non-significant common behaviour on its values. Meanwhile, AFM images illustrated how when Fn is adsorbed onto the different PGS and glass surfaces, cluster protein distribution is displayed. If Col I is the protein of interest, the observed structure displays a homogeneous Col I-Col I fibrillar network which amount of protein adsorption increased with PGS curing temperature by increasing its protein affinity. On the other hand, with Fn as first protein incubated when sequential protein adsorption had been carried out, Col I is not able to be adsorbed. Protein-protein interactions produced soluble Fn-Col I complexes which cannot be adsorbed by PGS substrates. Besides, Col I cannot fit within the empty spaces between Fn clusters because of its size differences. When Col I was the main coating layer, the interaction among proteins and the material surfaces improved. In this case, thanks to Fn smaller size, its protein clusters can fit through Col I fibrillar network already formed. Different PGS samples incubated under competition of proteins, mixed in different volumetric proportions, presented no significant differences. While, when Col I dilution content increased, the join effect of Col I substrate affinity, together with the reduction of the Fn adsorption inhibitory effect, lead to higher values of protein adsorbed. The determination of PGS substrates viability confirmed its expected good biocompatibility by colorimetric AlamarBlue™ HUVECs biological characterisation after 1, 3, 5 and 7 days of cell culture. Lastly, determination of HUVECs FA by immunofluorescence techniques by vinculin fluorescence quantification, exhibited how the increment of curing temperature on protein free PGS substrates, improves the amount of HUVECs FA. Following PGS protein adsorption, every PGS condition present better cell response when compared with glass. Particularly, 130 ºC present a synergic effect which increased cell FA values when incubated with sequencing Col I/Fn proteins. When dilutions of mixture protein were incubated, specifically, 25:75 dilution with more content of Col I, present an increasing significant trend of FA number, directly related to the increase of PGS curing temperature.

Thus, the determination and characterization of the synthesis mechanism of PGS at the early stages of its synthesis and by modifying its parameters had been fully

achieved. Together with PGS biological characterisation and demonstration of its different polymeric networks once modifying its curing temperature. All of this probes how such a versatile polymer PGS is and how, by modifying its synthesis parameters, in a controlled manner, a broad band of polymeric networks with different properties can be obtained based on its future biomedical applications.

GLOBAL CONCLUSIONS

Based on the work done about the characteristics of the PGS synthesis based on its parameters along with its final properties, exposed throughout the previous chapters, especially in the section of conclusions of each one of them, the following general conclusions have been reached:

Chapter 1:

- During prepolymerization between glycerol and sebacic acid, the reaction tends to the polycondensation of primary hydroxyl groups rather than secondary hydroxyl groups.
- A linear and less crosslinked polyester is produced during pPGS at early stages (4h)
- Water act as an inhibitor of the polycondensation reaction but reduces glycerol loss.
- A successful confinement of the prepolymerization reaction was achieved avoiding glycerol loss.
- The prepolymer is prone to growth as an hyperbranched polyester with high degree of esterification.

Chapter 2:

- The atmosphere applied during PGS synthesis reaction plays a key role on poly(glycerol) sebacate morphology.
- Inert atmospheres promote linear growing of macromers from triol and diacid and gelation takes longer, but resulting elastomers are more effectively cross-linked
- Oxidative atmospheres boost reactivity of secondary hydroxyls and foster branching.
- Water vapour supports this effect arguably by hindering glycerol evaporation.

Chapter 3:

- PGS polymer coatings at a nanometric scale can be obtained by spin coating techniques.
- Fn is adsorbed onto each of the substrates exhibiting cluster protein distribution with no major differences among PGS substrates.
- The interaction between Col I proteins leads to a homogeneous fibrillar network which increases with PGS curing temperature.
- Viability studies present good biocompatibility with no significant differences between PGS substrates.
- HUVECs early adhesions increase with PGS substrates cured at higher temperatures.

WORK IN PROGRESS AND FUTURE OUTLOOK

Nowadays, several mechanical and biological characterization experiments are being carry out to complement the present work to be published.

Furthermore, this thesis is part of a collaborative project which challenge to advance towards the development of artificial lymph nodes for in vitro applications. PGS together with other biopolymers such as PLA and PCL will be used to develop a preliminary version of this node. This node should act as a functional segment of the lymph node, based on a semipermeable containment structure (with pores of subcellular size to allow the diffusion of gases and nutrients into static and dynamic cell cultures). For that purpose, an organized stratified cell microenvironment structure, in whose interior the coexistence of the variety of cell types involved is viable, is been synthetize.

CONTRIBUTIONS

The work carried out for the realization of this doctoral thesis has also given rise to the following technical and scientific publications:

International conferences:

Poster presentation: Development of a three-dimensional scaffold (3D scaffold) based on Poly(glycerol sebacate) (PGS) for in vitro model of renal pathologies

Authors: **R. Martín-Cabezuelo**, J. Tomás Chenoll, G. Vilariño Feltrer, J.A. Gómez Tejedor, and A. Vallés Lluch.

Name of the conference: III Congreso Nacional Jóvenes Investigadores en Biomedicina (CONBIOPREVAL 2017)

Poster presentation: Monitoring of polyglycerol sebacate synthesis and correlation with the resultant network parameters.

Authors: **Rubén Martín-Cabezuelo**, Raquel Sancho-Sanmartín, Guillermo Vilariño-Feltrer, Jose A. Gómez-Tejedor and Ana Vallés-Lluch.

Name of the conference: 29th European Conference on Biomaterials (ESB 2018)

Poster presentation: Development of a three-dimensional Poly(glycerol sebacate) scaffold (3D-scaffold) for an in vitro model of lymph node

Authors: **Rubén Martín-Cabezuelo**, Sancho-Sanmartín Raquel, Tomás-Chenoll Julia, Vilariño-Feltrer G, Gómez-Tejedor JA and Vallés-Lluch A.

Name of the conference: 45th European Society for Artificial Organs (ESAO 2018)

Oral presentation: Key effect of the Poly(glycerol sebacate) synthesis during early stages and its monitoring.

Authors: **R. Martín-Cabezuelo**, A. Naderpour-Peñalver, G. Vilariño-Feltrer, A. Vallés-Lluch.

Name of the conference: 30th European Conference on Biomaterials (ESB 2019)

Articles under revision:

Influence of pre-polymerisation atmosphere on the properties of pre- and poly(glycerol sebacate)

Authors: **Rubén Martín-Cabezuelo**, Guillermo Vilariño-Feltrer, Ana Vallés-Lluch

Scientific Journal: Materials Science & Engineering C (Submitted)

Articles under preparation:

Title: Role of Curing Temperature of Poly(Glycerol Sebacate) Substrates on Early Cell Adhesion

Authors: **Rubén Martín-Cabezuelo**, José Carlos Rodríguez Hernández, Guillermo Vilariño-Feltrer and Ana Vallés-Lluch

Under preparation

Title: Unveiling the key synthesis mechanism for optimal poly(glycerol sebacate) hyperbranched polymer synthesis

Authors: **Rubén Martín-Cabezuelo**, Guillermo Vilariño-Feltrer, Sigen A, Wenxin Wang and Ana Vallés-Lluch

Under preparation

REFERENCES

[1] M. Nagata, T. Machida, W. Sakai, N. Tsutsumi, Synthesis, characterization, and enzymatic degradation of network aliphatic copolyesters, J. Polym. Sci. Part A Polym. Chem. 37 (1999) 2005–2011. https://doi.org/10.1002/(SICI)1099-0518(19990701)37:13<2005::AID-POLA14>3.0.CO;2-H.

[2] M. Nagata, T. Kiyotsukuri, H. Ibuki, N. Tsutsumi, W. Sakai, Synthesis and enzymatic degradation of regular network aliphatic polyesters, React. Funct. Polym. 30 (1996) 165–171. https://doi.org/10.1016/1381-5148(95)00107-7.

[3] Y. Wang, G.A. Ameer, B.J. Sheppard, R. Langer, A tough biodegradable elastomer, Nat. Biotechnol. 20 (2002) 602–606. https://doi.org/10.1038/nbt0602-602.

[4] R. Rai, M. Tallawi, A. Grigore, A.R. Boccaccini, Synthesis, properties and biomedical applications of poly(glycerol sebacate) (PGS): A review, Prog. Polym. Sci. 37 (2012) 1051–1078. https://doi.org/10.1016/j.progpolymsci.2012.02.001.

[5] X. Li, A.T.L. Hong, N. Naskar, H.-J. Chung, Criteria for Quick and Consistent Synthesis of Poly(glycerol sebacate) for Tailored Mechanical Properties, Biomacromolecules. 16 (2015) 1525–1533. https://doi.org/10.1021/acs.biomac.5b00018.

[6] Á. Conejero-García, H.R. Gimeno, Y.M. Sáez, G. Vilariño-Feltrer, I. Ortuño-Lizarán, A. Vallés-Lluch, Correlating synthesis parameters with physicochemical properties of poly(glycerol sebacate), Eur. Polym. J. 87 (2017) 406–419. https://doi.org/10.1016/j.eurpolymj.2017.01.001.

[7] Q. Liu, M. Tian, T. Ding, R. Shi, Y. Feng, L. Zhang, D. Chen, W. Tian, Preparation and characterization of a thermoplastic poly(glycerol sebacate) elastomer by two-step method, J. Appl. Polym. Sci. 103 (2007) 1412–1419. https://doi.org/10.1002/app.24394.

[8] Z.J. Sun, C.W. Sun, B. Sun, X.L. Lu, D.L. Dong, The polycondensing temperature rather than time determines the degradation and drug release of poly(glycerol-sebacate) doped with 5-fluorouracil, J. Biomater. Sci. Polym. Ed. 23 (2012) 833–841. https://doi.org/10.1163/092050611X562157.

[9] Q.-Z. Chen, A. Bismarck, U. Hansen, S. Junaid, M.Q. Tran, S.E. Harding, N.N. Ali, A.R. Boccaccini, Characterisation of a soft elastomer poly(glycerol sebacate) designed to match the mechanical properties of myocardial tissue, Biomaterials. 29 (2008) 47–57. https://doi.org/10.1016/j.biomaterials.2007.09.010.

[10] C.C. Lau, M.K. Bayazit, J.C. Knowles, J. Tang, Tailoring degree of esterification and branching of poly(glycerol sebacate) by energy efficient microwave irradiation, Polym. Chem. 8 (2017) 3937–3947. https://doi.org/10.1039/C7PY00862G.

[11] H.M. Aydin, K. Salimi, Z.M.O. Rzayev, E. Pişkin, Microwave-assisted

rapid synthesis of poly(glycerol-sebacate) elastomers, Biomater. Sci. 1 (2013) 503–509. https://doi.org/10.1039/c3bm00157a.

[12] H. Ye, C. Owh, X.J. Loh, A thixotropic polyglycerol sebacate-based supramolecular hydrogel showing UCST behavior, RSC Adv. 5 (2015) 48720–48728. https://doi.org/10.1039/C5RA08222F.

[13] I. Pomerantseva, N. Krebs, A. Hart, C.M. Neville, A.Y. Huang, C.A. Sundback, Degradation behavior of poly(glycerol sebacate), J. Biomed. Mater. Res. - Part A. 91 (2009) 1038–1047. https://doi.org/10.1002/jbm.a.32327.

[14] Y. Li, W.D. Cook, C. Moorhoff, W.C. Huang, Q.Z. Chen, Synthesis, characterization and properties of biocompatible poly(glycerol sebacate) pre-polymer and gel, Polym. Int. 62 (2013) 534–547. https://doi.org/10.1002/pi.4419.

[15] J.M. Kemppainen, S.J. Hollister, Tailoring the mechanical properties of 3D-designed poly(glycerol sebacate) scaffolds for cartilage applications, J. Biomed. Mater. Res. Part A. 94A (2010) 9–18. https://doi.org/10.1002/jbm.a.32653.

[16] C. Zhu, A.E. Rodda, V.X. Truong, Y. Shi, K. Zhou, J.M. Haynes, B. Wang, W.D. Cook, J.S. Forsythe, Increased Cardiomyocyte Alignment and Intracellular Calcium Transients Using Micropatterned and Drug-Releasing Poly (Glycerol Sebacate) Elastomers, (2018). https://doi.org/10.1021/acsbiomaterials.8b00084.

[17] N. Masoumi, K.L. Johnson, M.C. Howell, G.C. Engelmayr, Valvular interstitial cell seeded poly(glycerol sebacate) scaffolds: Toward a biomimetic in vitro model for heart valve tissue engineering, Acta Biomater. 9 (2013) 5974–5988. https://doi.org/10.1016/j.actbio.2013.01.001.

[18] P.M. Crapo, J. Gao, Y. Wang, Seamless tubular poly(glycerol sebacate) scaffolds: High-yield fabrication and potential applications, J. Biomed. Mater. Res. - Part A. 86 (2008) 354–363. https://doi.org/10.1002/jbm.a.31598.

[19] K.-W. Lee, Y. Wang, Elastomeric PGS Scaffolds in Arterial Tissue Engineering, J. Vis. Exp. (2011) 1–6. https://doi.org/10.3791/2691.

[20] Y.W. Jin Gao, Ann E. Ensley, Robert M. Nerem, Poly(glycerol sebacate) supports the proliferation and phenotypic protein expression of primary baboon vascular cells, J Biomed Mater Res A. 83 (2007) 1070–5. https://pubmed.ncbi.nlm.nih.gov/17584900/.

[21] C.G. Jeong, S.J. Hollister, A Comparison of the Influence of Material on in Vitro Cartilage Tissue Engineering With PCL, PGS, and POC 3D Scaffold Architecture Seeded With Chondrocytes, Biomaterials. 31 (2010) 4304–4312. https://doi.org/10.1016/j.biomaterials.2010.01.145.

[22] S.H. Zaky, K.W. Lee, J. Gao, A. Jensen, K. Verdelis, Y. Wang, A.J. Almarza, C. Sfeir, Poly (glycerol sebacate) elastomer supports bone regeneration by its mechanical properties being closer to osteoid tissue

rather than to mature bone, Acta Biomater. 54 (2017) 95–106. https://doi.org/10.1016/j.actbio.2017.01.053.

[23] F. Ghosh, W.L. Neeley, K. Arnér, R. Langer, Selective removal of photoreceptor cells in vivo using the biodegradable elastomer poly(glycerol sebacate)., Tissue Eng. Part A. 17 (2011) 1675–82. https://doi.org/10.1089/ten.TEA.2008.0450.

[24] M. Trese, C. V. Regatieri, M.J. Young, Advances in retinal tissue engineering, Materials (Basel). 5 (2012) 108–120. https://doi.org/10.3390/ma5010108.

[25] Q. Pan, Y. Guo, F. Kong, Poly(glycerol sebacate) combined with chondroitinase ABC promotes spinal cord repair in rats, J. Biomed. Mater. Res. - Part B Appl. Biomater. (2017) 1770–1777. https://doi.org/10.1002/jbm.b.33984.

[26] C.A. Sundback, J.Y. Shyu, Y. Wang, W.C. Faquin, R.S. Langer, J.P. Vacanti, T.A. Hadlock, Biocompatibility analysis of poly(glycerol sebacate) as a nerve guide material, Biomaterials. 26 (2005) 5454–5464. https://doi.org/10.1016/j.biomaterials.2005.02.004.

[27] Z.J. Sun, C. Chen, M.Z. Sun, C.H. Ai, X.L. Lu, Y.F. Zheng, B.F. Yang, D.L. Dong, The application of poly (glycerol-sebacate) as biodegradable drug carrier, Biomaterials. 30 (2009) 5209–5214. https://doi.org/10.1016/j.biomaterials.2009.06.007.

[28] Q. Chen, Shuling Liang, G.A. Thouas, Synthesis and characterisation of poly(glycerol sebacate)-co-lactic acid as surgical sealants, Soft Matter. (2011) 6484–6492. https://doi.org/10.1039/c1sm05350g.

[29] X.J. Loh, A. Abdul Karim, C. Owh, Poly(glycerol sebacate) biomaterial: synthesis and biomedical applications, J. Mater. Chem. B. 3 (2015) 7641–7652. https://doi.org/10.1039/c5tb01048a.

[30] Q. Liu, L. Jiang, R. Shi, L. Zhang, Synthesis, preparation, in vitro degradation, and application of novel degradable bioelastomers - A review, Prog. Polym. Sci. 37 (2012) 715–765. https://doi.org/10.1016/j.progpolymsci.2011.11.001.

[31] H. Frey, R. Haag, Dendritic polyglycerol: a new versatile biocompatible material, Rev. Mol. Biotechnol. 90 (2002) 257–267. https://doi.org/10.1016/S1389-0352(01)00063-0.

[32] Y. Wang, Y.M. Kim, R. Langer, In vivo degradation characteristics of poly(glycerol sebacate), J. Biomed. Mater. Res. 66A (2003) 192–197. https://doi.org/10.1002/jbm.a.10534.

[33] R. Ravichandran, J.R. Venugopal, S. Mukherjee, S. Sundarrajan, S. Ramakrishna, Elastomeric Core/Shell Nanofibrous Cardiac Patch as a Biomimetic Support for Infarcted Porcine Myocardium, Tissue Eng. Part A. 21 (2015) 1288–1298. https://doi.org/10.1089/ten.tea.2014.0265.

[34] J. Gao, P.M. Crapo, Y. Wang, Macroporous Elastomeric Scaffolds with Extensive Micropores for Soft Tissue Engineering, Tissue Eng. 12 (2006)

917–925. https://doi.org/10.1089/ten.2006.12.917.

[35] M. Masoudi Rad, S. Nouri Khorasani, L. Ghasemi-Mobarakeh, M.P. Prabhakaran, M.R. Foroughi, M. Kharaziha, N. Saadatkish, S. Ramakrishna, Fabrication and characterization of two-layered nanofibrous membrane for guided bone and tissue regeneration application, Mater. Sci. Eng. C. 80 (2017) 75–87. https://doi.org/10.1016/j.msec.2017.05.125.

[36] A.G. Mitsak, A.M. Dunn, S.J. Hollister, Mechanical characterization and non-linear elastic modeling of poly(glycerol sebacate) for soft tissue engineering, J. Mech. Behav. Biomed. Mater. 11 (2012) 3–15. https://doi.org/10.1016/j.jmbbm.2011.11.003.

[37] C.-N. Hsu, P.-Y. Lee, H.-Y. Tuan-Mu, C.-Y. Li, J.-J. Hu, Fabrication of a mechanically anisotropic poly(glycerol sebacate) membrane for tissue engineering, J. Biomed. Mater. Res. Part B Appl. Biomater. 106 (2018) 760–770. https://doi.org/10.1002/jbm.b.33876.

[38] O. Valerio, T. Horvath, C. Pond, M. Misra, A. Mohanty, Improved utilization of crude glycerol from biodiesel industries: Synthesis and characterization of sustainable biobased polyesters, Ind. Crops Prod. 78 (2015) 141–147. https://doi.org/10.1016/j.indcrop.2015.10.019.

[39] M. Ayoub, A.Z. Abdullah, Critical review on the current scenario and significance of crude glycerol resulting from biodiesel industry towards more sustainable renewable energy industry, Renew. Sustain. Energy Rev. 16 (2012) 2671–2686. https://doi.org/10.1016/j.rser.2012.01.054.

[40] M. Haller, S. Ludig, N. Bauer, Bridging the scales: A conceptual model for coordinated expansion of renewable power generation, transmission and storage, Renew. Sustain. Energy Rev. 16 (2012) 2687–2695. https://doi.org/10.1016/j.rser.2012.01.080.

[41] T. Werpy, G. Petersen, Top Value Added Chemicals from Biomass: Volume I -- Results of Screening for Potential Candidates from Sugars and Synthesis Gas, Golden, CO (United States), 2004. https://doi.org/10.2172/15008859.

[42] T. Abudula, L. Gzara, G. Simonetti, A. Alshahrie, N. Salah, P. Morganti, A. Chianese, A. Fallahi, A. Tamayol, S.A. Bencherif, A. Memic, The effect of poly (glycerol sebacate) incorporation within hybrid chitin-lignin sol-gel nanofibrous scaffolds, Materials (Basel). 11 (2018). https://doi.org/10.3390/ma11030451.

[43] C. Gao, D. Yan, Hyperbranched polymers : from synthesis to applications, 29 (2004) 183–275. https://doi.org/10.1016/j.progpolymsci.2003.12.002.

[44] S. Matsumura, A.R. Hlil, C. Lepiller, J. Gaudet, D. Guay, Z. Shi, S. Holdcroft, A.S. Hay, Ionomers for proton exchange membrane fuel cells with sulfonic acid groups on the end-groups: Novel branched poly(ether-ketone)s, Am. Chem. Soc. Polym. Prepr. Div. Polym. Chem. 49 (2008) 511–512. https://doi.org/10.1002/pola.

[45] T. Zhang, B.A. Howell, A. Dumitrascu, S.J. Martin, P.B. Smith, Synthesis and characterization of glycerol-adipic acid hyperbranched polyesters,

Polymer (Guildf). 55 (2014) 5065–5072. https://doi.org/10.1016/j.polymer.2014.08.036.

[46] Y.H. Kim, O.W. Webster, Hyperbranched Polyphenylenes, Macromolecules. 25 (1992) 5561–5572. https://doi.org/https://doi.org/10.1021/ma00047a001.

[47] J.M.J. Fréchet, C.J. Hawker, Hyperbranched polyphenylene and hyperbranched polyesters: new soluble, three-dimensional, reactive polymers, React. Funct. Polym. 26 (1995) 127–136. https://doi.org/10.1016/1381-5148(95)00010-D.

[48] Y. Zheng, S. Li, C. Gao, Chem Soc Rev Hyperbranched polymers : advances from, Chem. Soc. Rev. (2015). https://doi.org/10.1039/C4CS00528G.

[49] D. Wang, T. Zhao, X. Zhu, D. Yan, W. Wang, Bioapplications of hyperbranched polymers, Chem. Soc. Rev. 44 (2015) 4023–4071. https://doi.org/10.1039/c4cs00229f.

[50] A. Douka, S. Vouyiouka, L.M. Papaspyridi, C.D. Papaspyrides, A review on enzymatic polymerization to produce polycondensation polymers: The case of aliphatic polyesters, polyamides and polyesteramides, Prog. Polym. Sci. 79 (2018) 1–25. https://doi.org/10.1016/j.progpolymsci.2017.10.001.

[51] G. Lisak, K. Wagner, P. Wagner, J.E. Barnsley, K.C. Gordon, J. Bobacka, G.G. Wallace, A. Ivaska, D.L. Officer, A novel modified terpyridine derivative as a model molecule to study kinetic-based optical spectroscopic ion determination methods, Synth. Met. 219 (2016) 101–108. https://doi.org/10.1016/j.synthmet.2016.05.016.

[52] S. Ordanini, F. Cellesi, Complex polymeric architectures self-assembling in unimolecular micelles: Preparation, characterization and drug nanoencapsulation, Pharmaceutics. 10 (2018). https://doi.org/10.3390/pharmaceutics10040209.

[53] Q. Zhu, F. Qiu, B. Zhu, X. Zhu, Hyperbranched polymers for bioimaging, RSC Adv. 3 (2013) 2071–2083. https://doi.org/10.1039/c2ra22210h.

[54] C.M. Paleos, D. Tsiourvas, Z. Sideratou, L.A. Tziveleka, Drug delivery using multifunctional dendrimers and hyperbranched polymers, Expert Opin. Drug Deliv. 7 (2010) 1387–1398. https://doi.org/10.1517/17425247.2010.534981.

[55] A. Jiménez, M.P.G. Armada, J. Losada, C. Villena, B. Alonso, C.M. Casado, Amperometric biosensors for NADH based on hyperbranched dendritic ferrocene polymers and Pt nanoparticles, Sensors Actuators, B Chem. 190 (2014) 111–119. https://doi.org/10.1016/j.snb.2013.08.072.

[56] C. Sun, X. Chen, Q. Han, M. Zhou, C. Mao, Q. Zhu, J. Shen, Fabrication of glucose biosensor for whole blood based on Au/hyperbranched polyester nanoparticles multilayers by antibiofouling and self-assembly technique, Anal. Chim. Acta. 776 (2013) 17–23. https://doi.org/10.1016/j.aca.2013.03.032.

[57] H. Zhang, L.P. Bré, T. Zhao, Y. Zheng, B. Newland, W. Wang, Mussel-inspired hyperbranched poly(amino ester) polymer as strong wet tissue adhesive, Biomaterials. 35 (2014) 711–719. https://doi.org/10.1016/j.biomaterials.2013.10.017.

[58] V.T. Wyatt, G.D. Strahan, Degree of Branching in Hyperbranched Poly(glycerol-co-diacid)s Synthesized in Toluene, (2012) 396–407. https://doi.org/10.3390/polym4010396.

[59] X. Luo, S. Xie, J. Liu, H. Hu, J. Jiang, W. Huang, H. Gao, D. Zhou, Z. Lü, D. Yan, The relationship between the degree of branching and glass transition temperature of branched polyethylene: Experiment and simulation, Polym. Chem. 5 (2014) 1305–1312. https://doi.org/10.1039/c3py00896g.

[60] W. Daniel, S.E. Stiriba, F. Holger, Hyperbranched polyglycerols: From the controlled synthesis of biocompatible polyether polyols to multipurpose applications, Acc. Chem. Res. 43 (2010) 129–141. https://doi.org/10.1021/ar900158p.

[61] R. Rai, M. Tallawi, A. Grigore, A.R. Boccaccini, Synthesis, properties and biomedical applications of poly(glycerol sebacate) (PGS): A review, Prog. Polym. Sci. 37 (2012) 1051–1078. https://doi.org/10.1016/j.progpolymsci.2012.02.001.

[62] I. Manavitehrani, A. Fathi, H. Badr, S. Daly, A. Negahi Shirazi, F. Dehghani, Biomedical Applications of Biodegradable Polyesters, Polymers (Basel). 8 (2016) 20. https://doi.org/10.3390/polym8010020.

[63] P. Shirazaki, J. Varshosaz, A. Kharazi, Electrospun Gelatin/poly(Glycerol Sebacate) Membrane with Controlled Release of Antibiotics for Wound Dressing, Adv. Biomed. Res. 6 (2017) 105. https://doi.org/10.4103/abr.abr_197_16.

[64] B.D. Ulery, L.S. Nair, C.T. Laurencin, Biomedical applications of biodegradable polymers, J. Polym. Sci. Part B Polym. Phys. 49 (2011) 832–864. https://doi.org/10.1002/polb.22259.

[65] P. Stafiej, F. Küng, D. Thieme, M. Czugala, F.E. Kruse, D.W. Schubert, T.A. Fuchsluger, Adhesion and metabolic activity of human corneal cells on PCL based nanofiber matrices, Mater. Sci. Eng. C. 71 (2017) 764–770. https://doi.org/10.1016/j.msec.2016.10.058.

[66] S. Salehi, M. Fathi, S. Javanmard, F. Barneh, M. Moshayedi, Fabrication and characterization of biodegradable polymeric films as a corneal stroma substitute, Adv. Biomed. Res. 4 (2015) 9. https://doi.org/10.4103/2277-9175.148291.

[67] M. Frydrych, S. Román, S. MacNeil, B. Chen, Biomimetic poly(glycerol sebacate)/poly(l-lactic acid) blend scaffolds for adipose tissue engineering, Acta Biomater. 18 (2015) 40–49. https://doi.org/10.1016/j.actbio.2015.03.004.

[68] J. Hu, D. Kai, H. Ye, L. Tian, X. Ding, S. Ramakrishna, X.J. Loh, Electrospinning of poly(glycerol sebacate)-based nanofibers for nerve

tissue engineering, Mater. Sci. Eng. C. 70 (2017) 1089–1094. https://doi.org/10.1016/j.msec.2016.03.035.

[69] R. Rai, M. Tallawi, N. Barbani, C. Frati, D. Madeddu, S. Cavalli, G. Graiani, F. Quaini, J.A. Roether, D.W. Schubert, E. Rosellini, A.R. Boccaccini, Biomimetic poly(glycerol sebacate) (PGS) membranes for cardiac patch application, Mater. Sci. Eng. C. 33 (2013) 3677–3687. https://doi.org/10.1016/j.msec.2013.04.058.

[70] D. Lin, K. Yang, W. Tang, Y. Liu, Y. Yuan, C. Liu, A poly(glycerol sebacate)-coated mesoporous bioactive glass scaffold with adjustable mechanical strength, degradation rate, controlled-release and cell behavior for bone tissue engineering, Colloids Surfaces B Biointerfaces. 131 (2015) 1–11. https://doi.org/10.1016/j.colsurfb.2015.04.031.

[71] A. Tevlek, P. Hosseinian, C. Ogutcu, M. Turk, H.M. Aydin, Bi-layered constructs of poly(glycerol-sebacate)-β-tricalcium phosphate for bone-soft tissue interface applications, Mater. Sci. Eng. C. 72 (2017) 316–324. https://doi.org/10.1016/j.msec.2016.11.082.

[72] V.A. Bhanu, K. Kishore, Role of oxygen in polymerization reactions, Chem. Rev. 91 (1991) 99–117. https://doi.org/10.1021/cr00002a001.

[73] R.T. Conley, Studies of the Stability of Condensation Polymers in Oxygen-Containing Atmospheres, J. Macromol. Sci. Part A - Chem. 1 (1967) 81–106. https://doi.org/10.1080/10601326708053918.

[74] J. Langer, Chemical Properties and Derivatives of Glycerol, Ann. Phys. (N. Y). (1969). https://www.aciscience.org/docs/Chemical_Properties_and_Derivatives_of_Glycerol.pdf.

[75] M. SZWARC, 'Living' Polymers, Nature. 178 (1956) 1168–1169. https://doi.org/10.1038/1781168a0.

[76] A. Vallés-Lluch, G. Gallego Ferrer, M. Monleón Pradas, Effect of the silica content on the physico-chemical and relaxation properties of hybrid polymer/silica nanocomposites of P(EMA-co-HEA), Eur. Polym. J. 46 (2010) 910–917. https://doi.org/10.1016/j.eurpolymj.2010.02.004.

[77] A.K. Gaharwar, A. Patel, A. Dolatshahi-Pirouz, H. Zhang, K. Rangarajan, G. Iviglia, S.-R. Shin, M.A. Hussain, A. Khademhosseini, Elastomeric nanocomposite scaffolds made from poly(glycerol sebacate) chemically crosslinked with carbon nanotubes, Biomater. Sci. 3 (2015) 46–58. https://doi.org/10.1039/C4BM00222A.

[78] M.C. Serrano, E.J. Chung, G.A. Ameer, Advances and Applications of Biodegradable Elastomers in Regenerative Medicine, Adv. Funct. Mater. 20 (2010) 192–208. https://doi.org/10.1002/adfm.200901040.

[79] B. Amsden, Curable, biodegradable elastomers: emerging biomaterials for drug delivery and tissue engineering, Soft Matter. 3 (2007) 1335. https://doi.org/10.1039/b707472g.

[80] E. Bat, Z. Zhang, J. Feijen, D.W. Grijpma, A.A. Poot, Biodegradable

elastomers for biomedical applications and regenerative medicine, Regen. Med. 9 (2014) 385–398. https://doi.org/10.2217/rme.14.4.

[81] O. Valerio, M. Misra, A.K. Mohanty, Poly(glycerol- co-diacids) Polyesters: From Glycerol Biorefinery to Sustainable Engineering Applications, A Review, ACS Sustain. Chem. Eng. 6 (2018) 5681–5693. https://doi.org/10.1021/acssuschemeng.7b04837.

[82] A. Zamboulis, E.A. Nakiou, E. Christodoulou, D.N. Bikiaris, E. Kontonasaki, L. Liverani, A.R. Boccaccini, Polyglycerol Hyperbranched Polyesters: Synthesis, Properties and Pharmaceutical and Biomedical Applications, Int. J. Mol. Sci. 20 (2019) 6210. https://doi.org/10.3390/ijms20246210.

[83] H. Schliephake, D. Scharnweber, M. Dard, A. Sewing, A. Aref, S. Roessler, Functionalization of dental implant surfaces using adhesion molecules, J. Biomed. Mater. Res. - Part B Appl. Biomater. 73 (2005) 88–96. https://doi.org/10.1002/jbm.b.30183.

[84] Q. Liu, T. Tan, J. Weng, L. Zhang, Study on the control of the compositions and properties of a biodegradable polyester elastomer, Biomed. Mater. 4 (2009). https://doi.org/10.1088/1748-6041/4/2/025015.

[85] S. Amin Yavari, M. Croes, B. Akhavan, F. Jahanmard, C.C. Eigenhuis, S. Dadbakhsh, H.C. Vogely, M.M. Bilek, A.C. Fluit, C.H.E. Boel, B.C.H. van der Wal, T. Vermonden, H. Weinans, A.A. Zadpoor, Layer by layer coating for bio-functionalization of additively manufactured meta-biomaterials, Addit. Manuf. 32 (2020) 100991. https://doi.org/10.1016/j.addma.2019.100991.

[86] C. Frantz, K.M. Stewart, V.M. Weaver, The extracellular matrix at a glance, J. Cell Sci. 123 (2010) 4195–4200. https://doi.org/10.1242/jcs.023820.

[87] S. Ricard-Blum, The Collagen Family, Cold Spring Harb. Perspect. Biol. 3 (2011) a004978–a004978. https://doi.org/10.1101/cshperspect.a004978.

[88] L. Cen, W. Liu, L. Cui, W. Zhang, Y. Cao, Collagen Tissue Engineering: Development of Novel Biomaterials and Applications, Pediatr. Res. 63 (2008) 492–496. https://doi.org/10.1203/PDR.0b013e31816c5bc3.

[89] and J.D. Harvey Lodish, Arnold Berk, S Lawrence Zipursky, Paul Matsudaira, David Baltimore, Molecular Cell Biology, 4th editio, 2000. https://www.ncbi.nlm.nih.gov/books/NBK21582/.

[90] H.P. Erickson, N. Carrell, J.A.N. Mcdonagh, Fibronectin Molecule Visualized in Electron Microscopy : A Long , Thin , Flexible Strand, (n.d.) 0–5.

[91] D.J. Romberger, Fibronectin, Int. J. Biochem. Cell Biol. 29 (1997) 939–943. https://doi.org/10.1016/S1357-2725(96)00172-0.

[92] C.H. Streuli, Integrins and cell-fate determination, J. Cell Sci. 122 (2009) 171–177. https://doi.org/10.1242/jcs.018945.

[93] Y. Takada, X. Ye, S. Simon, Protein family review The integrins, (2007).

https://doi.org/10.1186/gb-2007-8-5-215.

[94] M.J. Dalby, A.J. García, M. Salmeron-Sanchez, Receptor control in mesenchymal stem cell engineering, Nat. Rev. Mater. 3 (2018). https://doi.org/10.1038/natrevmats.2017.91.

[95] M. Sgarioto, P. Vigneron, J. Patterson, F. Malherbe, M.D. Nagel, C. Egles, Collagen type I together with fibronectin provide a better support for endothelialization, Comptes Rendus - Biol. 335 (2012) 520–528. https://doi.org/10.1016/j.crvi.2012.07.003.

[96] D.K. Owens, R.C. Wendt, Estimation of the surface free energy of polymers, J. Appl. Polym. Sci. 13 (1969) 1741–1747. https://doi.org/10.1002/app.1969.070130815.

[97] J. Wei, T. Igarashi, N. Okumori, T. Igarashi, T. Maetani, B. Liu, M. Yoshinari, Influence of surface wettability on competitive protein adsorption and initial attachment of osteoblasts, Biomed. Mater. 4 (2009). https://doi.org/10.1088/1748-6041/4/4/045002.

[98] M.E. Lacouture, J.L. Schaffer, L.B. Klickstein, A Comparison of Type I Collagen, Fibronectin, and Vitronectin in Supporting Adhesion of Mechanically Strained Osteoblasts, J. Bone Miner. Res. 17 (2002) 481–492. https://doi.org/10.1359/jbmr.2002.17.3.481.

[99] S. Mauquoy, C. Dupont-Gillain, Combination of collagen and fibronectin to design biomimetic interfaces: Do these proteins form layer-by-layer assemblies?, Colloids Surfaces B Biointerfaces. 147 (2016) 54–64. https://doi.org/10.1016/j.colsurfb.2016.07.038.